

The Institute of Paper Chemistry

Appleton, Wisconsin

Doctor's Dissertation

Effects of pH and Oxidizing Agents on the Rate
of Absorption of Hydrogen Sulfide
into Aqueous Media

C. Neal Carter

January, 1966

EFFECTS OF pH AND OXIDIZING AGENTS ON THE RATE OF
ABSORPTION OF HYDROGEN SULFIDE INTO AQUEOUS MEDIA

A thesis submitted by

C. Neal Carter

B.S. 1961, North Carolina State University
M.S. 1963, Lawrence College

in partial fulfillment of the requirements
of The Institute of Paper Chemistry,
for the degree of Doctor of Philosophy
from Lawrence University,
Appleton, Wisconsin

Publication Rights Reserved by
The Institute of Paper Chemistry

January, 1966

TABLE OF CONTENTS

	Page
SUMMARY	1
INTRODUCTION	3
BACKGROUND OF THE THESIS PROBLEM	5
The Aqueous Hydrogen Sulfide System	5
Thermodynamic Considerations	5
Physical Equilibrium	5
Chemical Equilibrium	10
Reaction Considerations	10
Hypochlorite Oxidation	11
Kinetic Considerations	17
Rate of Dissociation	17
Rate of Reaction with Hydroxyl Ion	18
Rate of Oxidation	18
The Penetration Theory of Gas Absorption	19
The Mathematical Model	19
Physical Absorption	20
Absorption with Chemical Reaction	21
Penetration Theory as Applied to Hydrogen Sulfide Absorption	24
Previous Work	24
Information from Gas Absorption Measurements	24
APPARATUS AND PROCEDURES	25
The Secondary Experiments	25
Physical Properties of Absorbents	25
Solubility Measurements	25
Static Method	25
Dynamic Method	26

Diffusivity Measurements	26
Free Boundary Techniques	27
Electrophoresis-Diffusion Apparatus Procedure	27
Ultracentrifuge Apparatus Procedures	27
Gas Absorption Technique	28
Oxidation Reactions	29
Iodometric Technique	29
Product Analysis	30
Absorption Experiments	31
Absorption Apparatus	31
Liquid Supply System	31
The Jet Nozzle and Take-Off Tube	33
Liquid Take-Off System	33
The Gas Supply and Exhaust System	34
Procedure for the Absorption Runs	34
Preparation of Solutions	34
Starting a Run	34
Continuing and Ending a Run	35
RESULTS AND DISCUSSION	38
The Secondary Experiments	38
Physical Properties of Absorbents	38
Solubility Measurements	41
Solubility in Acidic and Salt Solutions	41
Comparison of Results with Other Work	42
Solubility in Basic and Oxidizing Solutions	43
Diffusivity Measurements	44
Diffusion Coefficients by Free Boundary Techniques	45

Diffusion Coefficient by Gas Absorption Measurements	46
Comparison of Results with Previous Work	50
Oxidation Reactions	52
Oxidation Products	52
Oxidation of Hydrogen Sulfide	54
Comparison with Other Work	56
Oxidation of Sodium Sulfide	56
Comparison with Other Work	58
Mechanism of Oxidation	59
Revised Reaction Sequence	59
Oxidation on Basis of Revised Mechanism	63
Effect of Oxidizing Agent	63
Effect of pH	64
Further Supporting Evidence	68
Oxidation of Hydrogen Sulfide by Miscellaneous Oxidants	69
The Absorption Experiments	70
Effect of pH on Absorption	70
Summary of Results	70
Absorption Without Chemical Reaction	75
Absorption with Irreversible Reaction	75
Absorption with Reversible Reaction	77
Absorption with "Infinitely Fast" Reaction	79
Reasons for Disagreement with Theory	81
Comparison with Previous Work	85
Effect of Oxidizing Agents	90
Summary of Results	90
Effect of Oxidation Reaction Upon Absorption	93

Rate of Oxidation	98
Combined Effect of Oxidation and Neutralization Reactions	100
SUMMARY AND CONCLUSIONS	104
FUTURE WORK	108
ACKNOWLEDGMENTS	109
NOMENCLATURE	110
LITERATURE CITED	113
APPENDIX I. MATHEMATICAL DETAILS OF THE PENETRATION THEORY	117
Physical Absorption	117
Absorption with Simultaneous, First-Order, Irreversible Chemical Reaction	120
Absorption with Simultaneous, Second-Order, "Infinitely Fast," Irreversible Reaction	123
Absorption Accompanied by a Reversible Reaction	127
APPENDIX II. DETAILS OF THE LAMINAR JET	132
Laminar Flow	132
Gravitational Acceleration of the Jet	132
Boundary Layer Considerations	133
Flow Within the Nozzle	134
Flow Within the Jet	135
Other Considerations	138
Effect of Finite Media and Curved Surfaces	138
Other Sources of Error	139
APPENDIX III. DESCRIPTION OF ABSORPTION APPARATUS AND AUXILIARY EQUIPMENT	140
Absorption Apparatus	140
The Absorbent Supply System	140
The Gas Supply and Exhaust System	141

The Absorption Chamber, Jet Nozzle, Take-Off Tube, and Aligning Mechanism	142
The Liquid Take-Off System	144
The Constant-Temperature Bath	144
The Degassing Unit	147
APPENDIX IV. ANALYTICAL PROCEDURES AND PREPARATION OF SOLUTIONS	149
Preparation and Standardization of Solutions	149
Sodium Thiosulfate, 0.1 and 0.025 Normal	149
Silver Nitrate, 0.1 Normal	150
Sodium Hydroxide, 0.1 Normal	150
Hydrochloric Acid, 0.1 Normal	151
Preparation and Initial Analysis of Absorbent Solutions	151
Preparation of Solutions	151
Analysis of Distilled Water	152
Concentration of Basic Absorbent Solutions	153
Concentration of Acidic Absorbent Solutions	153
Concentration of the Oxidizing Absorbent Solutions	153
Determination of Hydrogen Sulfide Pickup	154
The Potassium Iodate-Iodide Technique	155
The Silver Nitrate Technique	157
The Sodium Hypochlorite Technique	158
APPENDIX V. EQUILIBRIUM SOLUBILITY OF HYDROGEN SULFIDE IN AQUEOUS SOLUTIONS	160
Experimental Procedures	160
Static Method	160
Dynamic Method	161
Equilibrium Solubility in Acidic and Salt Solutions	162
Solubility in Basic and Oxidizing Solutions	164

APPENDIX VI. RESULTS OF STUDIES ON THE OXIDATION OF SODIUM AND HYDROGEN SULFIDE BY HYPOHALITE SOLUTIONS	167
Present Work	167
Previous Work	168
Work of Willard and Cake	168
Work of Choppin and Faulkenberry	169
Work of Dunicz and Rosenqvist	170
Work of Murthy and Rao	170
APPENDIX VII. PERMANGANATE OXIDATION OF HYDROGEN SULFIDE	172
Results of Volumetric Techniques	172
Results of Gravimetric Techniques	174
Comparison with Previous Work	175
Summary and Conclusions	175
APPENDIX VIII. SAMPLE CALCULATION AND SUMMARY OF ABSORPTION RUNS	177
Calculation of Experimental Absorption Rate	177
Run No. 155 Data	177
Calculations	177
Calculation of Exposure Time	178
Calculation of Rate of Absorption Without Chemical Reaction and Φ	180
Calculation of First-Order Rate Constant	180
Calculation of Theoretical Φ with "Infinitely Fast" Reaction	181
Summary of Absorption Runs at 25°C. and a Partial Pressure of Hydrogen Sulfide of 760 mm. Hg	182

SUMMARY

The rate of absorption of hydrogen sulfide into aqueous solutions of hydrogen chloride, sodium hydroxide, and sodium hypochlorite was measured by the laminar liquid jet technique. The absorption rates were analyzed in terms of the penetration theory in order to determine the effect of various reactions involving hydrogen sulfide - ionization, neutralization, and oxidation.

In order to apply the penetration theory to the absorption data, it was first necessary to determine the solubility and diffusivity of hydrogen sulfide in sodium chloride solutions of various concentrations. These data, together with a modified form of the Debye-McAulay equation, relating solubility to ionic size and concentration, and the Stokes-Einstein equation, relating diffusivity to viscosity, were used to estimate the solubility and diffusivity of hydrogen sulfide in the various absorbents.

Since one must also know what reactions are occurring in the absorbent before applying the penetration theory to absorption data, it was necessary to determine the effect of pH and ionic strength on the stoichiometry of the hypochlorite oxidation of hydrogen sulfide. The results obtained could not be explained on the basis of a previously proposed reaction sequence which used sulfur as the key intermediate. A revised reaction sequence based upon an intermediate called dihydrogen sulfoxide (DHSO) was then proposed. The initial step in the revised sequence was the oxidation of hydrogen sulfide to DHSO which could then either react with more sodium hypochlorite to end up in a sulfate form or decompose to form sulfur. It was found that the effect of pH on the hypochlorite oxidation of sodium sulfide could also be explained on the basis of the DHSO intermediate.

The effect of pH upon the rate of absorption of hydrogen sulfide into solutions which contained no oxidizing agent was then determined. It was found that

the pH effect could be divided into three zones. When the initial pH of the absorbent was below 3, no chemical reaction affected absorption. For an initial pH between 3-11.8, the first-order forward and second-order reverse ionization reaction influenced absorption. The two rate constants were estimated to be 8.4 sec.^{-1} and $7.3 \times 10^7 \text{ liters/mole sec.}$, respectively. Above an initial pH of 11.8, the "infinitely fast" neutralization reaction between hydrogen sulfide molecules and hydroxide ions was found to be the rate-controlling reaction. The data also indicated the strong possibility that the laminar liquid jet and wetted-wall column might not give comparable results under conditions of absorption accompanied by an "infinitely fast" reaction.

Analysis of the combined effect of pH, exposure time, and oxidizing strength on the rate of absorption indicated that a very complex set of reactions were occurring in the absorbing liquid. In the initial pH range 7-11.8, the data indicated - in agreement with the previous hypothesis - that the initial oxidation product was DHSO which would then react with hydrogen sulfide molecules to form metastable complexes by sulfur-sulfur linkages. Above pH 11.8, both the neutralization and the oxidation reactions were found to affect absorption. The data also indicated that the production of hydroxide ions by the decomposition of DHSO between the liquid-gas interface and the hydrogen sulfide-hydroxide ion reaction plane influenced absorption.

While many of the conclusions reached in this study are speculative and need further verification, the data are consistent and can always be explained by the same basic reaction sequence.

INTRODUCTION

Hydrogen sulfide is an odorous gas, only slightly soluble in water. Being mildly acidic and highly reducing in chemical nature, it can be readily absorbed into aqueous media containing basic or oxidizing agents. This study was made in order to determine the effects of such reagents on the rate of absorption of hydrogen sulfide.

The penetration theory, which treats the unsteady diffusion of an absorbed gas into a liquid (1), was the mathematical model used in this study. The laminar liquid jet was the absorption apparatus used in determining the experimental rates of absorption. This technique, which involves the establishment of a liquid jet of a known geometry in an atmosphere containing a soluble gas, has been shown to meet the experimental requirements of the penetration theory.

The rate of physical absorption is governed by the equilibrium concentration of the gas at the interface, the diffusivity of the gas in the liquid, and the exposure time. Any chemical reaction of the gas occurring in the absorbent will increase the rate of absorption, the extent of increase being dependent on the rate of the reaction. In this respect, the penetration theory may be used to analyze experimental absorption data for the effect of various types of reactions on the rate of absorption.

The results of this study will provide pertinent information for practical systems used for scrubbing hydrogen sulfide, clarify ionization, neutralization, and oxidation kinetics involving hydrogen sulfide, and possibly throw new light on the complex chemistry of sulfur compounds. The ionization and neutralization reactions were studied using aqueous solutions of hydrochloric acid and sodium hydroxide at various concentrations. In the study of the oxidation reactions,

sodium hypochlorite and hypobromite were used for their experimental simplicity and practical applicability.

The complete work included measurement of the solubilities and diffusivities of hydrogen sulfide in various solutions, the stoichiometric relations of probable reactions involved, and the rates of absorption by various absorbents. In the analysis of data, certain thermodynamic and kinetic considerations were often needed to reach intelligent conclusions. Therefore, these considerations will be discussed first.

BACKGROUND OF THE THESIS PROBLEM

THE AQUEOUS HYDROGEN SULFIDE SYSTEM

THERMODYNAMIC CONSIDERATIONS

When hydrogen sulfide gas is brought into contact with pure water and is allowed to reach equilibrium, the three equations which represent this equilibrium may be written



Physical Equilibrium

In acidic solutions the equilibrium of Reactions (2) and (3) is shifted far to the left and only the equilibrium between the gaseous and aqueous hydrogen sulfide is important.

Wright and Maass (2) investigated the effect of pressure on the solubility of hydrogen sulfide and found that the solubility (see Fig. 1) followed Henry's law - the partial pressure of a gas is directly proportional to its mole fraction, \underline{X}_i , in solution:

$$p_i = K_i \underline{X}_i \quad (4)$$

where \underline{K}_i , the proportionality constant, is a function of temperature, solvent, and total pressure. If the solutions are dilute, the mole fraction of hydrogen sulfide is directly proportional to its molar concentration, \underline{C}_i . Equation (4) can then be rewritten

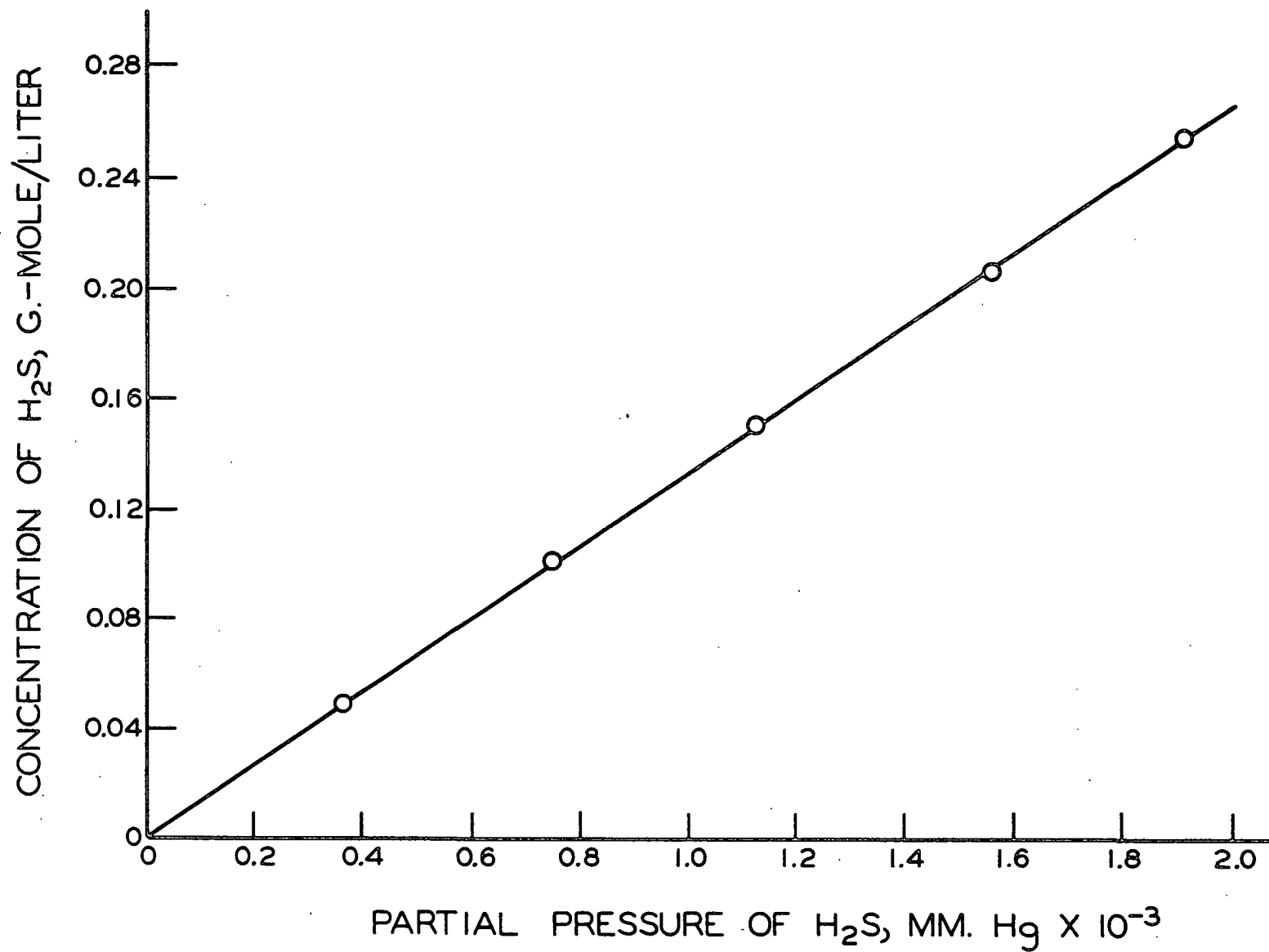


Figure 1. Solubility of Hydrogen Sulfide in Water at 25°C. (2)

$$p_i = H_i C_i \quad (5)$$

where \underline{H}_i is Henry's law constant based on concentration.

Since the solubility of hydrogen sulfide in pure water follows Henry's law, the ionization constants for Reactions (2) and (3) must be very small. This will be discussed later.

The basic criterion for the equilibrium of a substance distributed between two phases is that the chemical potential of the species be the same in both phases;

$$\mu_i^V = \mu_i^L \quad (6)$$

The chemical potential of an ideal gas can be written

$$\mu_i^V = \mu_i^{o,V} + RT \ln p_i \quad (7)$$

where $\mu_i^{o,V}$ is the standard chemical potential of the species. The standard state is customarily chosen to be the pure gas at unit atmosphere and is a function of temperature only. Similarly, the chemical potential of a species in a dilute solution can be written

$$\mu_i^L = \mu_i^{o,L} + RT \ln C_i \quad (8)$$

where $\mu_i^{o,L}$ is a function of both temperature and pressure. \underline{C}_i is chosen to have units of moles/liter in this work. Obviously, from Equations (6)-(8), Henry's law results.

When systems deviate from the ideal behavior, the pressure, \underline{p}_i , in Equation (7) and the concentration, \underline{C}_i , in Equation (8) can be replaced by the fugacity, \underline{f}_i , and activity, \underline{a}_i , respectively. Equation (7) can then be written

$$\mu_1^V = \mu_1^{O,V} + RT \ln f_1 \quad (9)$$

under the condition that

$$f_1 \rightarrow p_1 \text{ as } p_1 \rightarrow 0 \quad (10).$$

Equation (8) can be written

$$\mu_1^L = \mu_1^{O,L} + RT \ln a_1 \quad (11)$$

where

$$a_1 \rightarrow C_1 \text{ as } C_1 \rightarrow 0 \quad (12).$$

At low pressures and at 25°C., hydrogen sulfide (3) has been shown to closely follow the ideal gas law. Thus, it will be assumed that

$$f_1 = p_1 \quad (13)$$

throughout this work.

In a dilute solution one can define an activity coefficient as

$$\gamma_1 = a_1/C_1 \quad (14).$$

From Equation (12) it follows that

$$\gamma_1 \rightarrow 1 \text{ as } C_1 \rightarrow 0 \quad (15).$$

Because hydrogen sulfide is only slightly soluble in aqueous solutions - approximately 0.1 mole/liter in pure water - it will be assumed that its activity coefficient will be independent of the hydrogen sulfide concentration.

The activity coefficients of hydrogen sulfide can be varied by addition of a neutral salt. If both a pure water solution and a salt solution are in equilibrium with the same vapor phase,

$$\mu_i^v = \mu_{i,o}^L = \mu_{i,s}^L \quad (16).$$

This can then be rewritten in terms of activity coefficient by combining Equations (10) and (13):

$$\mu_{i,o}^{o,L} + RT \ln \gamma_{i,o} C_{i,o} = \mu_{i,s}^{o,L} + RT \ln \gamma_{i,s} C_{i,s} \quad (17).$$

The subscript s denotes hydrogen sulfide in the salt solution, and o denotes hydrogen sulfide in pure water. If the standard states are chosen such that

$$\mu_{i,o}^{o,L} = \mu_{i,s}^{o,L} \quad (18),$$

then

$$\gamma_{i,o} C_{i,o} = \gamma_{i,s} C_{i,s} \quad (19)$$

or

$$\gamma_{i,s} = \gamma_{i,o} (C_{i,o} / C_{i,s}) \quad (20).$$

Since $\gamma_{i,o}$ has already been assumed to be unity for all hydrogen sulfide concentrations, the additional condition for the salt solutions is

$$\gamma_{i,s} \rightarrow 1 \text{ as } C_{i,s} \rightarrow 0 \text{ and } C_{\text{salt}} \rightarrow 0 \quad (21).$$

Thus

$$\gamma_{i,s} = C_{i,o} / C_{i,s} \quad (22).$$

In summary, the solubility of hydrogen sulfide can be expressed by

$p_i = H_i \gamma_i C_i$. For pure water, γ_i was chosen to be unity, and for solutions containing an inert salt, γ_i was independent of the hydrogen sulfide concentration at any given temperature, the effect of pressure being neglected.

Chemical Equilibrium

Earlier it was stated that the equilibrium constants for Reaction (2), K_1 , and for Reaction (3), K_2 , are probably very small. A review of the literature indicated that while the value of K_1 was fairly well established at about 1×10^{-7} , the value of K_2 was not well established - results by various methods differing by 1 to 2 orders of magnitude. In this work the equilibrium constant for each reaction was calculated from the standard free energy data compiled by Rossini, et al. (4). The equilibrium constant of a reaction is related to the change in standard free energy by

$$G^{\circ} = -RT \ln K \quad (23)$$

where

G° = change in standard free energy

R = universal gas constant

T = absolute temperature

K = equilibrium constant for the reaction

At 25°C. the values of G° were 9.53 kg.-cal./mole for Reaction (2) and 16.99 kg.-cal./mole for Reaction (3). Using these values in Equation (23), K_1 is 1.13×10^{-7} and K_2 is 3.48×10^{-13} .

REACTION CONSIDERATIONS

In any type of gas absorption apparatus the rate of absorption is affected by any reaction which might occur in the absorbing liquid. Three types of reactions will be encountered in this study. The first is the reversible dissociation of hydrogen sulfide as given by Reaction (2). The second is the reaction between hydrogen sulfide and the hydroxide ion:



This reaction is a neutralization reaction in which one of the reactants is an acidic molecule instead of the usual hydrogen ion.

The third reaction which will be studied is the reaction between an oxidizing agent and hydrogen sulfide:



The various oxidation reactions of hydrogen sulfide have not been studied extensively. To meet the needs of this study, certain properties were required of the oxidizing agent:

1. The oxidizing agent could not have an appreciable vapor pressure or be reduced to a product which had an appreciable vapor pressure.
2. The stoichiometry of the reaction between the oxidizing agent and hydrogen sulfide had to be known.

The two conditions were necessary in order to rigorously treat the data by the penetration theory. The second condition was required because of the procedure used in making the absorption runs. Also in this study it was advantageous to use the same oxidizing agent over a wide pH range. The oxidizing agent chosen for use in this thesis was sodium hypochlorite.

Hypochlorite Oxidation

A number of studies have been made on the oxidation of sulfides by hypochlorite solutions - primarily hypochlorite.

Willard and Cake (5) first studied the oxidation of sodium sulfide by hypochlorite and hypobromite ions in hydroxide solutions. They found that a mixture of elemental sulfur and sulfate ions was formed. Above a certain critical hydroxide concentration all of the sulfide was oxidized to a sulfate form (see Fig. 2). This critical hydroxide concentration was found to be $4N$ when hypochlorite

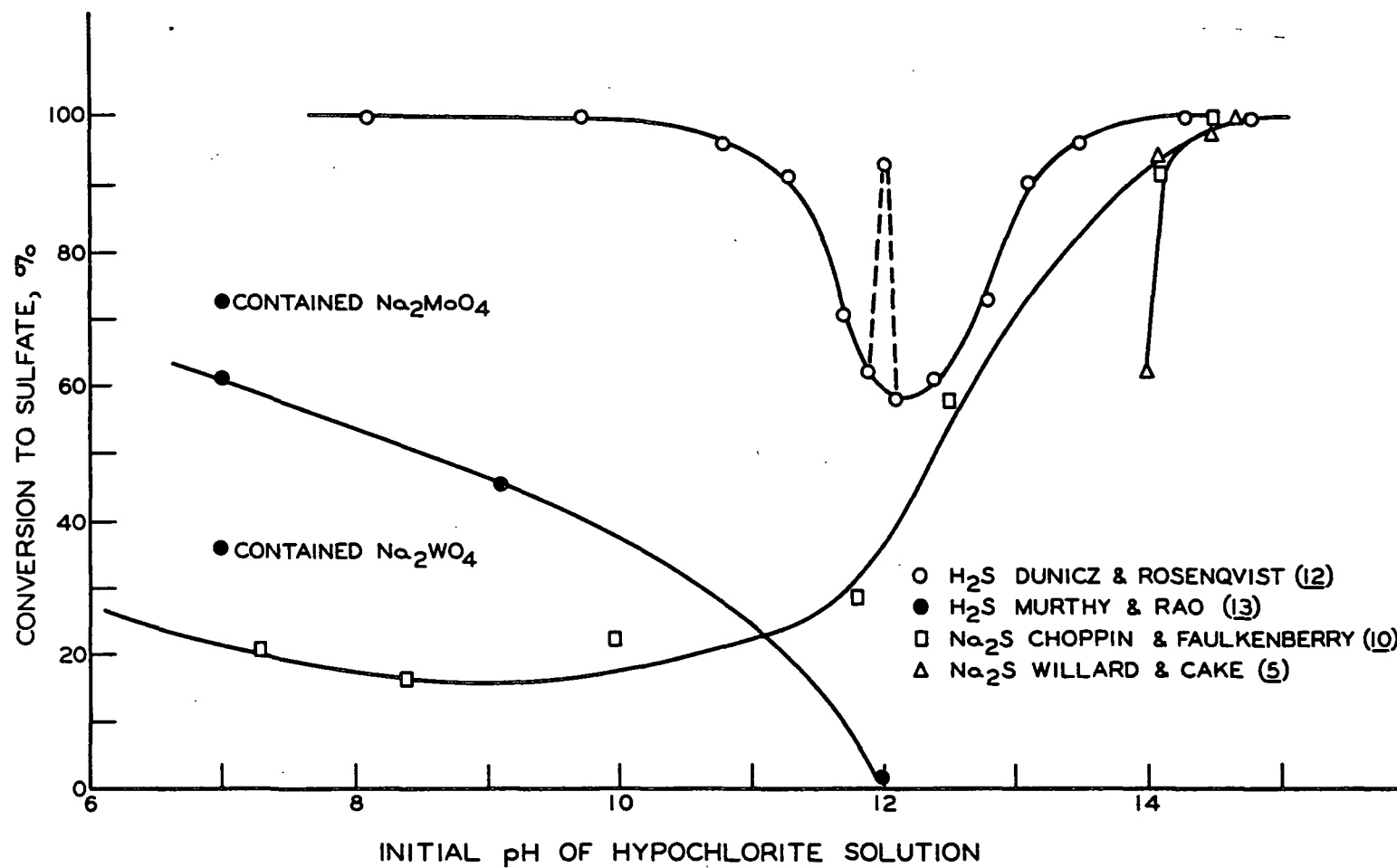
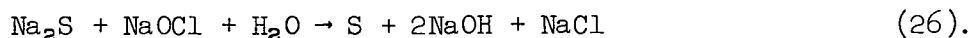
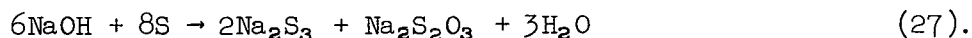


Figure 2. Oxidation of Sodium Sulfide and Hydrogen Sulfide by Sodium Hypochlorite - Previous Work

solutions were used and 2.7N when hypobromite solutions were used. The mechanism which they proposed was first the oxidation of the sulfide to elemental sulfur:



The hydroxide ions would dissolve the sulfur by Tartar's (6) reaction:



The polysulfide and thiosulfate formed would then be oxidized to the sulfate form.

Later Kitchener, et al. (7) determined the sulfur content in steel by liberating the sulfur as hydrogen sulfide and absorbing the gas in a solution of alkaline hypochlorite. They then boiled, cooled, and titrated the sample iodometrically. The sulfide content was calculated from the difference between the above titration and a blank titration, assuming that all of the sulfur was oxidized to a sulfate form. The above procedure was reported to be accurate to within $\pm 1\%$.

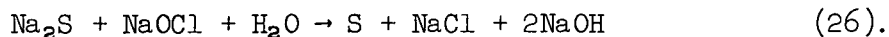
Pepkowitz (8) and Bethge (9) tried to oxidize sulfides to sulfates quantitatively using calcium hypochlorite at room temperature. They found that the reaction gave a mixture of elemental sulfur and sulfate ions, but could be used quantitatively if the conditions were standardized and an empirical correction factor was used.

Choppin and Faulkenberry (10) were the first to thoroughly investigate the effects of pH, temperature, and reactant concentrations on the stoichiometry of the reaction between sodium hypochlorite and sodium sulfide. The only two products found were sulfur and sodium sulfate. An increase in temperature was found to increase the relative amount of sodium sulfate formed. An increase in the relative amount of sodium hypochlorite caused an increase in the sulfate

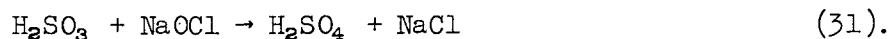
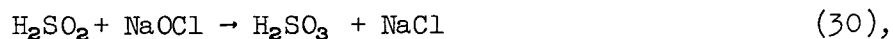
formation, while an increase in the amount of sodium sulfide caused an increase in the relative amount of sulfur formed. They found that if the molar ratio of the reactants remained constant, no matter what the actual reactant concentrations, the relative amounts of sulfur and sulfate formed remained constant.

The pH of the oxidizing solutions was found to have a very great effect on the reaction stoichiometry (see Fig. 2). The reaction was found to be quantitative with respect to sulfate formation above pH 14 (3N sodium hydroxide) and below pH 2 with a minimum at pH 10. It should be noted here that all of their solutions between pH 3-13 contained a buffering agent of some sort.

On the basis of this information the following reaction sequence for the oxidation of sodium sulfide to sodium sulfate was proposed.



The sulfur would then react in the following sequence:



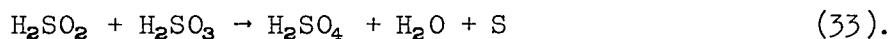
The increase which occurred on either side of the minimum was explained by a dissolving mechanism. On the alkaline side, the dissolution proceeded by Tartar's mechanism given earlier in Reaction (27). On the acid side, chlorine monoxide (Cl_2O) was believed to be responsible for the dissolving of the sulfur by the reaction



The reaction sequence would then continue as above.

Later, Bendall, Mann, and Purdie (11) oxidized hydrogen sulfide with chloramine-T and found that sulfuric acid was the principal product with a trace of sulfur being formed. On the other hand, when sodium sulfide was oxidized with chloramine-T, the principal product was sulfur and the resulting solution was markedly alkaline. They found that sulfur continued to be formed even when a large excess of chloramine-T was present. From these results they came to the conclusion that the oxidation of hydrogen sulfide was distinct from that of the sulfide ion and that elemental sulfur could not be an intermediate in the oxidation of hydrogen sulfide to sulfuric acid.

Dunicz and Rosenqvist (12) were the first to determine the effect of pH on the reaction between hypochlorite and hydrogen sulfide (see Fig. 2). They generated hydrogen sulfide by adding hydrochloric acid to a metallic sulfide and swept the gas into a solution of sodium hypochlorite. They found that the reaction proceeded quantitatively to the sulfate form from pH 8 to 11. There was a minimum sulfate formation at pH 12, and the reaction again became quantitative above pH 14.2. They found a reproducible peak at pH 12 which rose to almost 100% conversion of the sulfide to sulfate. No mechanism was proposed, but they suggested that the reaction probably proceeded through intermediate oxidation compounds such as sulfoxylic acid (H_2SO_2) or sulfurous acid. They attributed the failure to isolate these proposed intermediates to an autooxidation-reduction to sulfur and sulfate. For example,



None of their solutions contained buffering compounds.

Recently, Murthy and Rao (13) studied the effect of pH on the oxidation of hydrogen sulfide by chloramine-T (see Fig. 2). They found the reaction to be quantitative with respect to sulfate formation only in very strong acid solutions (2N H_2SO_4). They also noted that their data agreed with Choppin and Faulkenberry's (10). They stated that this was to be expected since the hypochlorite ion and hypochlorous acid have been shown to be the active species in a solution of chloramine-T (14). It should also be noted that their solutions contained the same buffering agents as were used by Choppin and Faulkenberry (10).

Murthy and Rao (13) explained their data by the initial formation of dihydrogen sulfoxide (H_2SO). This compound could then be oxidized further to sulfuric acid or decompose to form sulfur and water. They pointed out that dihydrogen sulfoxide (DHSO) was very similar to hydrogen peroxide and should behave in an analogous manner. They then added various compounds which were known to affect the rate of decomposition of hydrogen peroxide to their oxidizing solutions. Hydrogen peroxide stabilizers were found to increase the relative amount of sulfate formed while decomposition catalysts were found to increase the relative amount of sulfur formed. This was cited as evidence to support their proposed intermediate.

Kesler (15), in working up a scheme for the analysis of kraft pulping liquor, verified the findings of Willard and Cake (5). He also found that if an iodine solution was added dropwise to a 12N sodium hydroxide solution containing sulfide ions, the hypoiodite formed would quantitatively oxidize the sulfide ions to the sulfate form.

Thus, it appears that there are two different mechanisms for the oxidation of hydrogen sulfide and sodium sulfide. However, no direct proof of any mechanism has been reported. It is possible that a comparison of the stoichiometry of the

hypochlorite oxidation of hydrogen sulfide and sodium sulfide will clarify the picture. It is also possible that such data might suggest a revised mechanism which would fit both the hydrogen sulfide and sodium sulfide oxidation over an extended pH range.

KINETIC CONSIDERATIONS

The equilibrium and stoichiometry of the reactions which will be studied in this thesis were discussed in the preceding section. The rates of these reactions which will affect the rate of absorption of hydrogen sulfide are considered below.

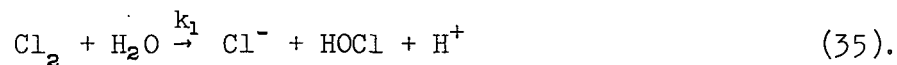
Rate of Dissociation

To date no one has made any attempt to measure the rate of association or dissociation of hydrogen sulfide. Therefore, one must use analogous systems to obtain an estimate of the rate of dissociation. One system very similar to aqueous hydrogen sulfide is pure water. Eigen and DeMaeyer (16) measured the relaxation times of water using a high voltage impulse, and determined the rate constants for the reaction



The value of k_1 was found to be 2.6×10^{-5} /sec., and k_2 to be 1.3×10^{11} liters/mole sec. Later Ertl and Gerisher (17) used a temperature-jump method and obtained the same values.

One can also make a comparison between hydrogen sulfide and another gas such as chlorine. Spalding (18) used a gas absorption technique and determined the rate constant for the reaction



He found that the reaction could be treated as a pseudo first-order reaction with a rate constant of 20.9/sec.

Because hydrogen sulfide has an ionization constant which is larger than that of water and smaller than that of chlorine, one would expect the rate constant to lie somewhere between the values for these two systems.

Rate of Reaction with Hydroxyl Ion

There has been no determination of the rate of reaction between a hydroxyl ion and hydrogen sulfide. Since hydrogen sulfide is an acid in its molecular form, the reaction can be compared with a neutralization reaction. The rate constant for a neutralization reaction between a hydrogen ion and a hydroxyl ion was given as 1.3×10^{11} liters/mole sec. in the previous section.

Because hydrogen sulfide is also a gas, it can be compared with gaseous compounds. Nijssing, et al. (19) used a gas absorption technique and found the rate constant for the reaction between carbon dioxide and the hydroxyl ion to be 4.7×10^3 liters/mole sec. Spalding (18), using similar techniques, obtained a rate constant of the order of 10^6 liters/mole sec. for the reaction between chlorine and the hydroxyl ion.

Because hydrogen sulfide lies between these two cases, the rate constant for the reaction between hydrogen sulfide and the hydroxyl ion should be of the order of 10^7 - 10^9 liters/mole sec.

Rate of Oxidation

To date there have been no good studies on the rate of oxidation of aqueous sulfide solutions. Satterfield, et al. (20) studied the rate of the reaction



They found the rate to be first order with respect to the peroxide concentration but did not determine the order with respect to the hydrogen sulfide. They also found a decrease in the rate constant by dropping the pH from 4.0 to 1.5. This suggested that one of the ionic species is probably the active species in the reaction. However, they did not pursue the study any further.

Carter (21) tried to study the rate of oxidation of sodium sulfide by molecular oxygen using a gas absorption technique. His results were not quantitative, but the limited amount of data indicated that the sulfide ion (S^{-2}) was probably the active species.

THE PENETRATION THEORY OF GAS ABSORPTION

THE MATHEMATICAL MODEL

The mathematical model for the unsteady-state diffusion of a gas into an absorbing liquid is given by Fick's first and second laws of diffusion. The solution to these equations under certain initial and boundary conditions is what comprises the penetration theory of gas absorption.

A physical picture of the model is that of a semi-infinite, stagnant liquid brought into contact with an atmosphere containing a soluble gas. The interface is usually considered to reach equilibrium with the gas phase instantaneously and remain at equilibrium over the entire exposure time. It is assumed that there are no concentration gradients initially present in the liquid phase and that the concentration of the dissolved gas remains constant at an infinite distance from the interface. Mathematically the initial and boundary conditions are

$$x = 0, t \geq 0, C_A = C_{A,o} \quad (37)$$

$$x \geq 0, t = 0, C_A = C_{A,o} \quad (38)$$

$$x = \infty, t > 0, C_A = C_{A,o} \quad (39).$$

Since the liquid-gas interface is assumed to be in equilibrium with the gas phase at all times, any molecule diffusing away from the interface is immediately replaced by another molecule from the gas phase. Thus, the rate of absorption is equal to the rate of diffusion away from the interface.

Physical Absorption

When a gas is absorbed into a liquid and no chemical reaction involving the dissolved gas accompanies absorption, Fick's second law for diffusion in one dimension is

$$\partial C_A / \partial t = D_A \partial^2 C_A / \partial x^2 \quad (40),$$

where $\underline{D_A}$ is the diffusion coefficient of the solute \underline{A} in the absorbent. An implied assumption is that $\underline{D_A}$ is independent of the concentration, $\underline{C_A}$.

The mathematical expression for Fick's first law is

$$J_A = -D_A (\partial C_A / \partial x) \quad (41),$$

where $\underline{J_A}$ is the flux past any plane. The rate of diffusion from a liquid-gas interface or the rate of absorption can then be found by solving Equation (40) using the boundary conditions (37)-(39) for $\underline{C_A}/\underline{x}$ as a function of \underline{x} and \underline{t} and utilizing Equation (41) for $\underline{x} = 0$,

$$N_A = -D_A (\partial C_A / \partial x)_{x=0} \quad (42).$$

The instantaneous rate of absorption, $\underline{N_A}$, after time \underline{t} can be shown to be given by

$$N_A^* = (C_{A,e} - C_{A,o}) \sqrt{D_A/\pi t} \quad (43).$$

One can then integrate Equation (43) over the exposure time, $\underline{t_e}$, and obtain the average rate of absorption for the period as

$$\bar{N}_A^* = 2(C_{A,e} - C_{A,o}) \sqrt{D_A/\pi t_e} \quad (44).$$

Absorption with Chemical Reaction

When the soluble gas undergoes a chemical reaction in the liquid phase, the concentration of the solute is less at any given plane (except at the interface) than if there was no chemical reaction. This would increase the concentration gradient in the liquid which would increase the rate of diffusion and, therefore, increase the rate of absorption. The change in concentration profiles due to chemical reaction is shown by Fig. 3.

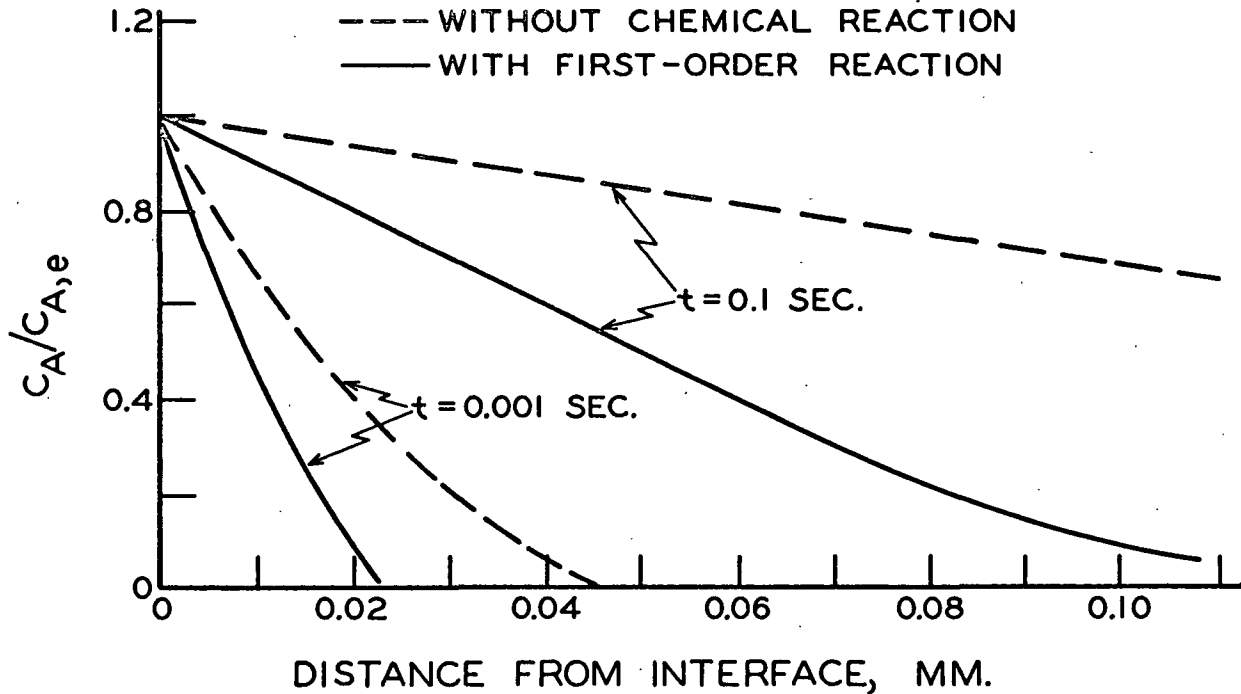


Figure 3. Typical Concentration Profiles

When a chemical reaction takes place, the rate of accumulation of a solute in a differential segment of the liquid becomes equal to the rate of diffusion into the segment minus the rate of diffusion out of the segment minus the rate of depletion due to chemical reaction, R_i . The differential equation which describes this situation is

$$\partial C_i / \partial t = D_i \partial^2 C_i / \partial x^2 - R_i \quad (45).$$

One must write one such equation for each molecular species taking part in the reaction to completely describe the system.

Solutions of Equation (45) under the conditions given earlier for various types of chemical reactions have been found by Danckwerts (22) and others (28-30). These solutions are usually given in the general form

$$\bar{N}_A = 2(C_{A,e} - C_{A,o}) \sqrt{D_A / t_e} \cdot \Phi \quad (46).$$

The function Φ is a function of some or all of the following: exposure time, initial product and reaction concentrations, product and reactant diffusivities, rate of reaction, and reaction equilibrium constant. The form of Equation (46) is very convenient to use because Φ becomes equal to the average rate of absorption with chemical reaction divided by the average rate of absorption without chemical reaction. This ratio is always greater than one for absorption with chemical reaction.

Mathematical expressions have been obtained for the function Φ for a limited number of types of chemical reactions. One type encountered in this thesis is a first-order, irreversible reaction where the rate of the chemical reaction is expressed as

$$R_i = k_1 C_A \quad (47).$$

The solution for this type of reaction is

$$\Phi = 1/2[\sqrt{\pi/k, t_e} (1/2 + k, t_e) \operatorname{erf}\sqrt{k, t_e} + \exp(-k, t_e)] \quad (48)$$

Another type of reaction is that of an "infinitely fast," second-order, irreversible reaction where rate of the reaction is given by

$$R_i = k_1 C_A C_B \quad (49)$$

and is very fast compared with diffusion. The solution to this type of reaction is

$$\Phi = 1/\operatorname{erf}(\alpha/\sqrt{D_A}) \quad (50)$$

where α is implicitly defined by

$$C_{A,e} \sqrt{D_A} \exp(-\alpha^2/D_A) \operatorname{erfc}(\alpha/\sqrt{D_B}) = C_{B,o} \sqrt{D_B} \exp(-\alpha^2/D_A) \operatorname{erf}(\alpha/\sqrt{D_A}) \quad (51).$$

The above solution was derived for a chemical reaction in which one mole of A reacts with one mole of B. In cases where either A or B reacts with one or more of the products of the initial reaction with an "infinitely fast" rate, the penetration theory solution is the same as before except that the left side of Equation (51) is multiplied by the stoichiometry coefficient, n. The constant α is then defined by

$$nC_{A,e} \sqrt{D_A} \exp(-\alpha^2/D_A) \operatorname{erfc}(\alpha/\sqrt{D_B}) = C_{B,o} \sqrt{D_B} \exp(-\alpha^2/D_B) \operatorname{erf}(\alpha/\sqrt{D_A}) \quad (52).$$

The other type of chemical absorption which required a mathematical solution was absorption accompanied by a first-order forward, second-order reverse reaction. No analytical solution exists for this case. Therefore, it was necessary to resort to a numerical analysis method to obtain a solution.

The mathematical details of the derivation of gas absorption equations and the numerical analysis procedures are given in Appendix I.

PENETRATION THEORY AS APPLIED TO HYDROGEN SULFIDE ABSORPTION

Previous Work

The only previous study of the absorption of hydrogen sulfide to which the penetration theory may be applied with any confidence is that of Astarita and Gioia (26). They used a wetted-wall column to study the absorption of hydrogen sulfide gas by water and by sodium hydroxide solutions up to 1 normal. They found almost perfect agreement between their data and the penetration theory solution of absorption accompanied by an "infinitely fast" reaction. They made certain simplifications in their theoretical treatment. However, these simplifications would not appreciably affect their conclusions.

They also investigated the absorption of hydrogen sulfide by sodium carbonate solutions. Again, they found very good agreement between their data and the "infinitely fast" reaction solution to the penetration theory. The active carbonate species was found to be the carbonate ion (CO_3^{--2}), while the bicarbonate ion (HCO_3^-) played little if any role in affecting the rate of absorption.

Information from Gas Absorption Measurements

Gas absorption studies have already supplied information about the reaction between hydrogen sulfide and hydroxide and carbonate solutions.

Absorption measurements made over a much wider pH range should provide kinetic information concerning the rate of dissociation and association of hydrogen sulfide. This study should also confirm the results obtained earlier by Astarita and Gioia (26).

Absorption measurements made using solutions containing oxidizing agents should provide information regarding the oxidation of hydrogen sulfide. The data should provide information regarding the mechanism and rate of the oxidation reaction.

APPARATUS AND PROCEDURES

THE SECONDARY EXPERIMENTS

In order to be able to analyze the absorption data obtained in this study in terms of the penetration theory, certain properties of the absorbents and of hydrogen sulfide had to be determined. These included the physical properties of the absorbents, the solubility and diffusivity of hydrogen sulfide in the absorbents, and the stoichiometry of any reaction which might occur in the absorbing liquid.

PHYSICAL PROPERTIES OF THE ABSORBENTS

The viscosities of the sodium hypochlorite solutions were measured with a Cannon viscometer with an efflux time of 74 seconds for distilled water at 25°C. The densities were measured in a 25-ml. pycnometer at 25°C.

SOLUBILITY MEASUREMENTS

Two methods were used in the determination of the equilibrium solubility of hydrogen sulfide in hydrochloric acid, sodium chloride, and sodium sulfate solutions - a static method which approached equilibrium from a state of supersaturation and a dynamic method which approached equilibrium from a state of unsaturation.

Static Method

The static method was a modification of the procedure used by Spalding (18) in the determination of the solubility of chlorine. First, about 200 ml. of the absorbent was placed in a 250-ml. gas washing bottle and the bottle was placed in an ice bath. Hydrogen sulfide gas was bubbled through the solution for about 20 minutes. The bottle was then removed from the ice bath and placed in a

constant-temperature bath at 25°C. As the temperature of the absorbent began to rise, the pressure in the bottle built up and was relieved by opening a valve to the atmosphere for a fraction of a second. This building up and relieving of pressure was continued until the pressure in the bottle was equal to atmospheric pressure.

After the solution had reached equilibrium, a sample was taken and analyzed. Care was taken to prevent any change in concentration during the sampling procedure.

Dynamic Method

The dynamic method was a modification of the procedure used by Parkison (27) in determining the solubility of sulfur dioxide. First, 200 ml. of the absorbent was placed in a 250-ml. gas washing bottle as before. The bottle was then placed in a constant-temperature bath at 25°C. After 2 hours in the bath, hydrogen sulfide gas was bubbled through the solution and exhausted through an exhaust jar. After bubbling the gas through the solution for 40 minutes, a sample was taken and analyzed. The total pressure on the system was atmospheric pressure plus the small amount of back pressure caused by the exhaust system.

It was determined by trial runs that saturation was reached after 20 minutes at the bubbling rate used in this study. This time was doubled so that equilibrium was virtually assured. Again, care was taken to prevent any change in the concentration of the absorbent as the sample was being taken.

Details of both the static and dynamic methods are given in Appendix V.

DIFFUSIVITY MEASUREMENTS

Four different techniques were used during the course of this study in an attempt to determine the diffusion coefficient of hydrogen sulfide in acidic

and salt solutions. Three of these techniques involved diffusion across a free boundary. The fourth was a gas absorption technique.

Free Boundary Techniques

Two different pieces of apparatus were employed in the free boundary techniques: a Beckman-Spinco Model H electrophoresis-diffusion apparatus and a Beckman Model E analytical ultracentrifuge.

Electrophoresis-Diffusion Apparatus Procedure

The procedure used with the electrophoresis-diffusion apparatus was identical to that used by Spalding (18) to determine the diffusion coefficient of chlorine. The procedure is also given in the instrument instruction manual (28) and therefore will not be discussed in detail in this report.

Briefly, the procedure called for the formation of a sharp boundary between a solution and its solvent in one of the legs of a U-shaped cell. The boundary was then allowed to spread and the rate of spread of the boundary was followed by photographing the Rayleigh interference fringe pattern produced by the optical system. The diffusion coefficient is ordinarily determined from the photographs.

Ultracentrifuge Apparatus Procedures

Two different techniques were tried using the ultracentrifuge. The first technique was a low-speed layering-in technique. In this procedure, a two-sector centrifuge cell with a minute capillary connecting the two sectors was used. The hydrogen sulfide solution was placed in one sector and water was placed in the other. The cell was then placed in the centrifuge and the centrifuge was accelerated gradually. The gravitational field built up in the rotor and caused the water to flow through the capillary and layer-in on top of the hydrogen sulfide solution. When the rotor had reached the desired speed (5000 r.p.m.), the

electrical system was balanced to maintain this speed. Diffusion took place across the boundary formed by the layering-in process.

The second technique was a high-speed sedimentation run. Here a two-sector cell without a capillary was used with water in one sector and a hydrogen sulfide solution on the other. The cell was then placed in the rotor and the centrifuge was accelerated to its maximum speed and held there. The diffusion coefficient was calculated from the rate at which the sedimentation equilibrium curve was approached.

The details of these two procedures can be found in the Beckman Model E Operating Manual (29).

Gas Absorption Technique

The gas absorption technique has been used by several authors (18,19,30) with excellent results. The basic requirement is that the absorption apparatus must satisfy the assumptions in penetration theory.

Earlier it was shown that in the case of gas absorption without chemical reaction, the rate of absorption is given by

$$\bar{N}_A^* = 2(C_{A,e} - C_{A,o}) \sqrt{D_A/\pi t_e} \quad (44).$$

Thus, one can determine the exposure time and rate of absorption of a gas under conditions of physical absorption and plot the rate of absorption against the inverse of the square root of the exposure time. The slope of the resulting line is

$$m = 2(C_{A,e} - C_{A,o}) \sqrt{D_A/\pi} \quad (53).$$

If one can then determine the solubility of the gas in the absorbent, the diffusion coefficient can be calculated from

$$D_A = \pi m^2/4(C_{A,e} - C_{A,o})^2 \quad (54).$$

In all the runs in this study the initial concentration of the gas in the liquid was zero. Thus, Equation (54) became

$$D_A = \pi m^2/4C_{A,e}^2 \quad (55).$$

The same apparatus and set of procedures were used in making the absorption runs for the determination of the diffusion coefficient as was used in all other absorption runs. The apparatus and procedures are described later in the report and will not be given here.

OXIDATION REACTIONS

In order to study the reaction between an oxidizing agent and either hydrogen sulfide or sodium sulfide, two techniques were used. The first was a determination of the stoichiometry of the reaction using iodometric procedures. The second was a determination of the amount of product formed.

Iodometric Technique

The iodometric technique for the analysis of the stoichiometry of the various oxidation reactions was begun by preparing a 0.1N solution of either hydrogen sulfide or sodium sulfide. The hydrogen sulfide solution was prepared by placing about 300 ml. of distilled water in a 500-ml. gas-washing bottle and bubbling hydrogen sulfide gas through the water for about 30 minutes. The gas-washing bottle was then inverted and connected to the side arm of a 50-ml. buret equipped with an extra long nozzle. This arrangement permitted the hydrogen sulfide solution to be added to the oxidizing solution without exposure to the atmosphere.

The sodium sulfide solution was prepared by washing reagent-grade crystals of sodium sulfide with distilled water. The clear crystals were then quickly weighed and dissolved in degassed distilled water. A regular 50-ml. buret was used to add the sulfide solution to the oxidizing solution. This procedure of washing the crystals and dissolving the crystals in degassed water permitted sodium sulfide solutions to be prepared which were free of sodium thiosulfate.

The oxidizing solution was prepared by placing an aliquot of a stock solution of the oxidizing agent in a 500-ml. ground-glass stoppered flask. Distilled water and either hydrochloric acid or sodium hydroxide were added to adjust the volume and pH of solution to predetermined values.

A quantity of the sulfide solution (either hydrogen sulfide or sodium sulfide) was run into the flask. After the sulfide solution had been added to all the flasks, an excess of potassium iodide was added and the solutions were acidified with hydrochloric acid. The iodine formed was titrated with standardized sodium thiosulfate. Blanks were run in exactly the same manner except that no sulfide solution was added.

The concentration of the sulfide solution was determined by adding a volume of the sulfide solution to an acidic iodine solution and titrating the excess iodine with sodium thiosulfate to the starch end point.

Product Analysis

The only product for which a quantitative determination was made was the sulfate ion. A modified barium sulfate gravimetric technique was used in this study.

First, a solution of either hydrogen sulfide or sodium sulfide was prepared as before. Then the oxidizing solution, distilled water, and either hydrochloric

acid or sodium hydroxide were added to a 600-ml. beaker to adjust the oxidizing strength, volume, and pH of solution to the desired values. A quantity of the sulfide solution was then added to the beaker which was under constant agitation from a magnetic stirrer.

Any sulfur which was formed was removed by centrifuging the solutions in an International analytical centrifuge at 4000 r.p.m. The solution was then acidified, placed on a hot plate and brought to a boil. The boiling was continued until the solution would no longer turn potassium iodide-starch paper blue. An excess of barium chloride was then added and the boiling was continued for at least two hours. The precipitate was filtered onto Whatman's No. 42 filter paper, ashed by a Meker burner, and ignited in a muffle furnace at 800°C. to constant weight.

The concentration of the sulfide solution was determined as before by adding a volume of the sulfide solution to an acidic iodine solution and titrating the excess iodine to a starch end point with standardized sodium thiosulfate.

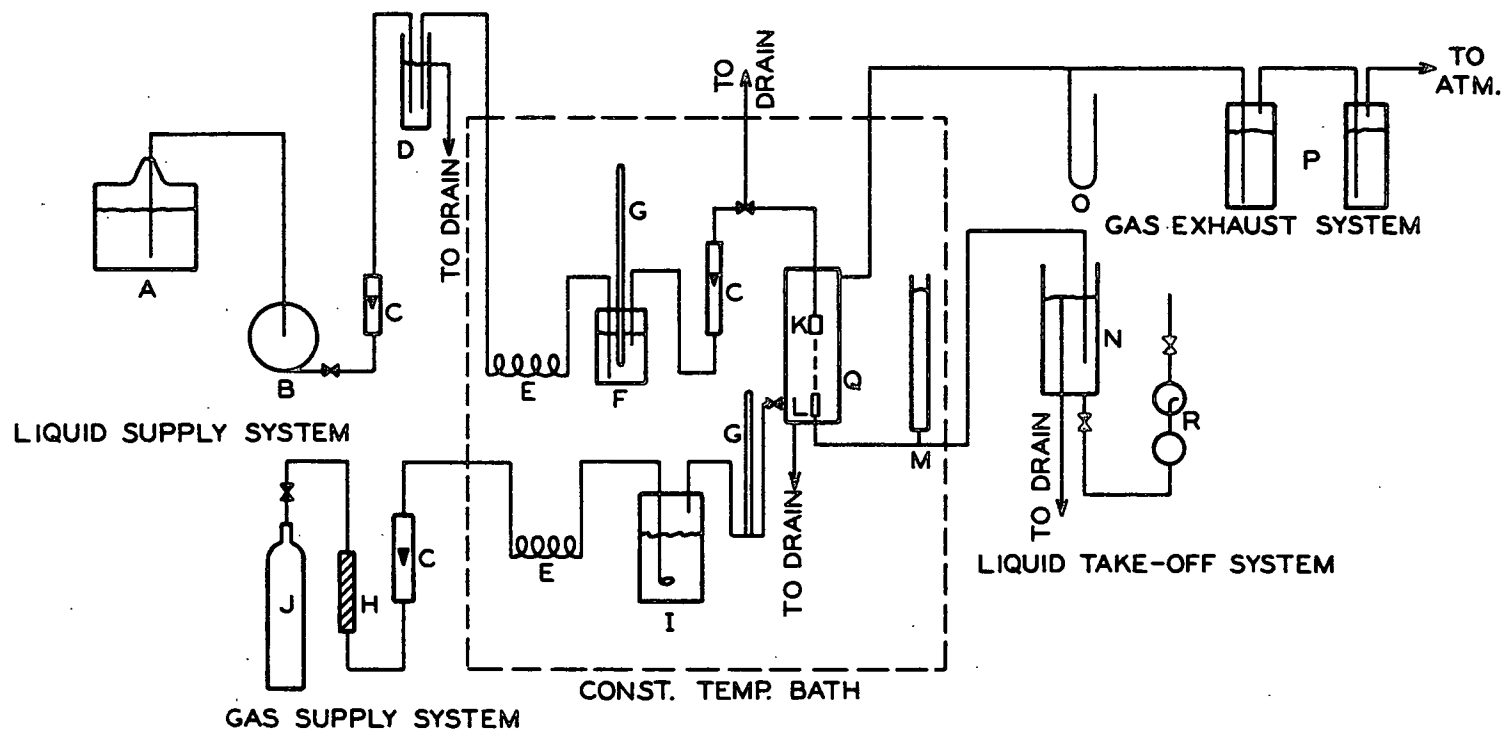
ABSORPTION EXPERIMENTS

ABSORPTION APPARATUS

The absorption apparatus used in this study is almost identical to that used by Spalding (18) and Scriven and Pigford (31). A schematic diagram of the apparatus is shown in Fig. 4. A complete description of the apparatus and its components has been given in Appendix III. A general description follows.

Liquid Supply System

During a run the absorbent was pumped to a constant-head device, and then run through a cooling cell, past a surge vessel, through a rotameter, into the



- | | | |
|----------------------|-----------------|----------------------|
| A STORAGE TANK | G THERMOMETER | M SURGE TUBE |
| B PUMP | H GAS FILTER | N LEVELING DEVICE |
| C ROTAMETER | I GAS SATURATOR | O MANOMETER |
| D CONST. HEAD DEVICE | J GAS CYLINDER | P EXHAUST BOTTLES |
| E COOLING COIL | K JET NOZZLE | Q ABSORPTION CHAMBER |
| F SURGE VESSEL | L TAKE-OFF TUBE | R SAMPLING PIPET |

Figure 4. Schematic Diagram of Absorption Apparatus

approach tube, and out the jet nozzle. The use of the constant-head device and a surge vessel allowed the flow to be controlled so that no noticeable variations could be detected.

The Jet Nozzle and Take-off Tube

The absorbent flowed down the straight approach tube and out a bell-shaped nozzle with a diameter of 1.644 mm. The position of the jet was adjusted by an aligning mechanism so that the absorbent stream flowed into the take-off tube. The liquid level in the take-off tube was adjusted to be level with the top of the tube so that no entrainment of hydrogen sulfide gas or loss of absorbent would occur.

Liquid Take-off System

After entering the take-off tube, the absorbent flowed past a surge tube, into a leveling device, through a sampling pipet, and to the drain. The surge tube was placed in the line to provide a means of escape for gas which became entrained during adjustment of the jet.

The level of the absorbent in the take-off tube was adjusted by means of a leveling device. The height of the liquid in the leveling device above the take-off tube was equal to the jet velocity head plus the pressure head inside the chamber minus the pressure loss caused by the flow of absorbent from the take-off tube to the leveling device. There was no danger of loss of hydrogen sulfide gas to the atmosphere since an overflow was always maintained at the downcomer. When the sampling pipet was in the sampling position, part of the absorbent stream flowed through the sampling pipet to the drain while the remainder flowed upward and then overflowed into the downcomer.

The Gas Supply and Exhaust System

Hydrogen sulfide gas was issued from a cylinder, filtered, metered, brought to temperature, saturated with water vapor, and allowed to flow into the jet chamber around the jet. After leaving the jet chamber, the gas was exhausted by bubbling it through two bottles to provide a back pressure and passing it to the atmosphere up a hood stack.

PROCEDURE FOR THE ABSORPTION RUNS

Preparation of Solutions

All of the absorbent solutions were prepared with degassed, distilled water. The degassing unit is described in Appendix III. The absorbent solutions were made by preparing concentrated solutions of hydrochloric acid, sodium hydroxide, and sodium hypochlorite, and diluting an aliquot to volume. A layer of n-heptane was placed on the prepared solutions to reduce air absorption during storage. The solutions were then allowed to sit overnight and a run was started the first thing the next morning. Thus, no solution was allowed to stand for more than 15 hours before use.

Starting a Run

To start a run the pump was turned on and the constant-head device was filled. After the constant-head device was filled and had started to overflow, part of the flow was directed through the absorbent system forcing out all of the air. Next, the flow was directed through the approach tube and the jet nozzle. The jet chamber was flooded. The gas was then turned on and the absorbent in the jet chamber was forced back into the jet nozzle and approach tube. This completed clearing the system of air.

After the approach tube had been cleared of air, the excess absorbent in the jet chamber was siphoned off to the drain and the jet was adjusted to hit the

take-off tube. The leveling device was filled and the flow was directed to the downcomer. The leveling device was then adjusted so that a bubble appeared at the top of the take-off tube. (see Fig. 5). The alignment of the jet was adjusted so that the bubble size was a minimum. This indicated proper alignment of the jet nozzle. The leveling device was then lowered until the bubble disappeared. The system was stable in this position until a change in the absorbent flow rate was made (see Fig. 6).

Continuing and Ending a Run

After the jet was in a stable position, the sampling pipet was filled. The pipet was then inverted and the flow was sent to the drain. After 5-10 volumes had passed through the sampling pipet, it was removed from the line and the volume of the upper bulb was allowed to drain into a flask. The sample was then set aside until the run was complete. If the pH of the absorbent was 13 or less, the flask contained an aliquot of standard iodine solution. If the pH was greater than 13, the flask was clean and dry.

A slight variation was made in the sampling procedure when the absorbent contained sodium hypochlorite. A tee was placed in line just before the leveling device. The sample was taken by diverting part of the flow into a clean, dry, tared flask. The flask was then reweighed in order to obtain the sample size. This flask was then set aside until the run was complete.

During times when all of the flow was directed to the downcomer, the absorbent was run into a tared beaker for a measured period of time. The beaker was then reweighed to obtain the flow rate. After the flow rate had been determined, the sampling pipet was refilled and another sample collected. Three such samples were collected for each run.



Figure 5. Centering the Jet



Figure 6. The Stable Jet

After all the samples had been collected, the pump and hydrogen sulfide cylinders were shut off, and the system was allowed to drain. If a highly concentrated solution had been used or if a different solution was to be used for the next run, the system was flushed with water.

After the system had been shut down and flushed out, the samples were analyzed for the sulfide content. The samples which had been run into the standard iodine solution were analyzed by titrating the excess iodine with standardized sodium thiosulfate. The strong sodium hydroxide solutions were analyzed by titrating the sulfide ions potentiometrically with standardized silver nitrate. The absorbents which contained sodium hypochlorite were analyzed by heating the solution, cooling it, and determining the excess hypochlorite iodometrically. The details of these procedures are given in Appendix IV.

RESULTS AND DISCUSSION

THE SECONDARY EXPERIMENTS

PHYSICAL PROPERTIES OF ABSORBENTS

The density and viscosity of the hydrochloric acid, sodium hydroxide, and sodium chloride absorbents were taken from the International Critical Tables (32) and are given in Table I. These values of density and viscosity were plotted as a function of concentration and are shown in Fig. 7 and 8. Values were taken from these graphs for use in the various calculations.

TABLE I

DENSITY AND RELATIVE VISCOSITY OF THE ACIDIC, BASIC, AND SALT
ABSORBENTS AS A FUNCTION OF CONCENTRATION AT 25°C.

Solute	Concentration, moles/liter	Density, g./cc.	Relative Viscosity, μ/μ_0
Water	--	0.9971	1.000
HCl	0.25	1.0012	1.017
HCl	0.50	1.0056	1.034
HCl	1.00	1.0137	1.067
NaOH	0.25	1.0092	1.056
NaOH	0.50	1.0188	1.109
NaOH	1.00	1.0381	1.236
NaOH	1.50	1.0572	1.391
NaCl	0.25	1.0073	1.024
NaCl	0.50	1.0171	1.047
NaCl	1.00	1.0368	1.097
NaCl	1.50	1.0563	1.151
NaCl	2.00	1.0752	1.212

Note: Specific viscosity of water at 25°C. = 0.8939 cp.

The densities and viscosities of the various sodium hypochlorite and sodium hypobromite solutions were determined for each set of runs. These data are presented in Table II.

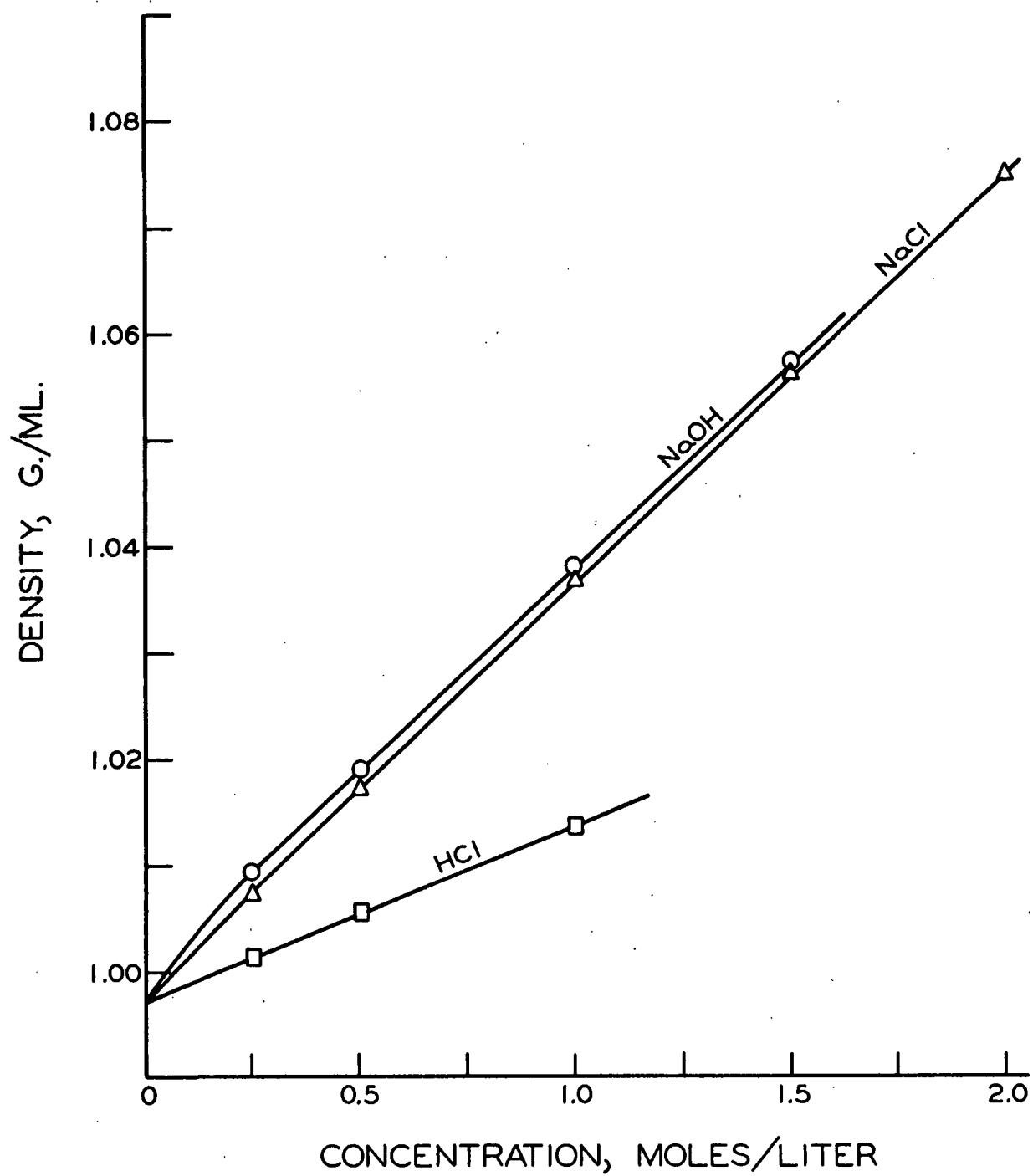


Figure 7. Density of Absorbents

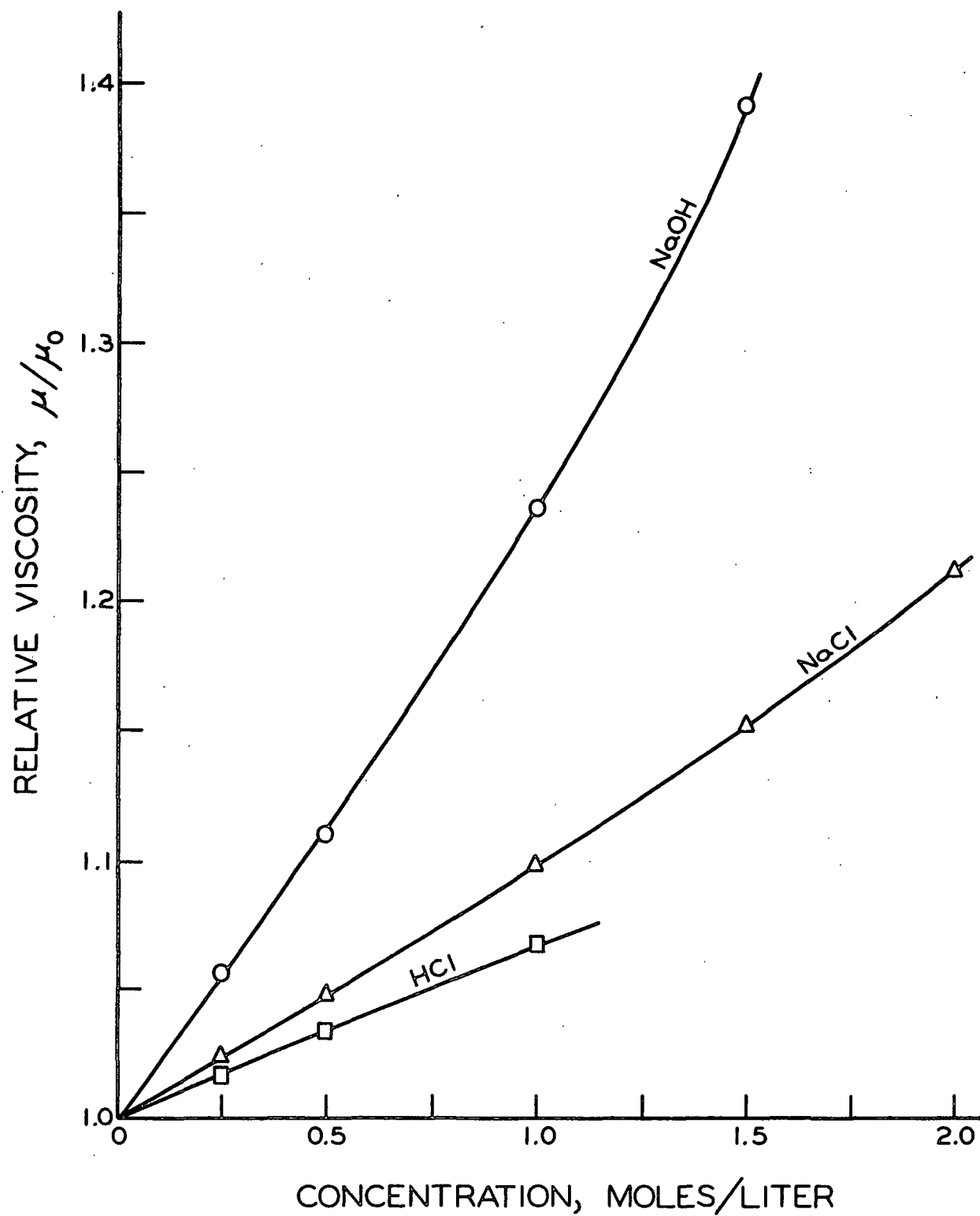


Figure 8. Viscosity of Absorbents

TABLE II

PHYSICAL PROPERTIES OF HYPOHALITE SOLUTIONS

Run No.	Density, g./cc.	Relative Viscosity, μ/μ_0
121-122	1.0026	1.021
123-124	1.0031	1.024
125-126	1.0066	1.040
127-129	1.0452	1.245
130-135	1.0245	1.132
136-138	1.0323	1.150
145-147	1.0118	1.064
148-150	1.0029	1.019
151-153	1.0020	1.014
154-159	1.0032	1.022
160-162	1.0042	1.023
163-165	1.0036	1.023
166-169	1.0031	1.022
170-172	1.0135	1.055
173-175	0.9997	1.009
176-178	1.0073	1.038

SOLUBILITY MEASUREMENTS

Solubility in Acidic and Salt Solutions

The results of the equilibrium solubility measurements of hydrogen sulfide in hydrochloric acid, sodium chloride, and sodium sulfate solutions are shown in Table III. The conditions for the data given in the table are 25°C. and a partial pressure of hydrogen sulfide of 760 mm. of mercury.

TABLE III
EQUILIBRIUM SOLUBILITY OF HYDROGEN SULFIDE

	Solubility, g./liter
Water	3.48
HCl, 0.2N	3.46
HCl, 0.4N	3.44
HCl, 0.6N	3.45
HCl, 0.8N	3.46
HCl, 1.0N	3.47
NaCl, 50 g./liter	2.96
NaCl, 100 g./liter	2.56
NaCl, 150 g./liter	2.23
NaCl, 200 g./liter	1.97
Na ₂ SO ₄ , 50 g./liter	2.68
Na ₂ SO ₄ , 100 g./liter	2.13
Na ₂ SO ₄ , 150 g./liter	1.72
Na ₂ SO ₄ , 200 g./liter	1.39

Duplicate determinations by either the static method or the dynamic method showed less than 1% difference. Also, the differences between the results obtained by the two methods were less than 1%.

Comparison of Results with Other Work

Wright and Maass (2) determined the solubility of hydrogen sulfide at 25°C. as a function of partial pressure, and at 760 mm. of Hg the equilibrium solubility was 3.47 g./liter. Kendall and Andrews (33) obtained 3.49 g./liter as the solubility at 25°C. and 1 atm. partial pressure. These two values agree with the value of 3.48 g./liter obtained in this study.

Kendall and Andrews (33) also determined the effect of hydrochloric acid on the equilibrium solubility at 25°C. and a hydrogen sulfide partial of 760 mm. of Hg. Their results agree with the values determined in this study to within $\pm 0.5\%$. The minimum also occurred at the same place in both studies.

The values for the equilibrium solubility of hydrogen sulfide in sodium chloride and sodium sulfate solutions taken from the International Critical Tables (34) differ from the results obtained in this study by more than 5%. The methods employed in the previous studies could not be determined from the literature. However, because of the close agreement between the two different experimental procedures employed in this study, the results presented in this study are felt to be correct and will be used throughout the course of this work.

Solubility in Basic and Oxidizing Solutions

In this study it was necessary to estimate the equilibrium solubility in solutions which will react with hydrogen sulfide. There are two principal methods of making this estimate. One is to calculate the solubility by analogy with other gases. The other method is to use the Debye-McAulay equation. Both methods give essentially the same values except at high (above 2N) salt concentrations. However, the analogy method could not be used for hypohalite solutions because no values could be found for the solubility of any gas in any hypohalite solution. Therefore, in order to be consistent, the Debye-McAuley (D-A) equation was used.

A modified form of the D-A equation for a 1-1 electrolyte can be written

$$\ln \gamma = K_D \sum_{i=1}^n M_i / b_i \quad (56)$$

where

K_D = a constant independent of the type of gas, but dependent on the temperature and solvent

M_i = molality of ionic species i

b_i = radius of ionic species i

One then solves for the value of $\underline{K_D}$ using a salt which does not react with the gas being employed. Having the value of $\underline{K_D}$, one can then estimate the solubility in any other solution.

The values for the various constants used in Equation (56) are as follows:

$$\underline{K_D} = 0.1818,$$

$$\underline{b_{Na^+}} = 1.51,$$

$$\underline{b_{Cl^-}} = \underline{b_{OCl^-}} = \underline{b_{Br^-}} = \underline{b_{OBr^-}} = 2.24, \text{ and}$$

$$\underline{b_{OH^-}} = 1.57.$$

A complete derivation of the modified D-A equation is given in Appendix V. Sources of the various constants mentioned above and sources of possible error are also discussed in detail.

DIFFUSIVITY MEASUREMENTS

Previous studies on the diffusion coefficient of hydrogen sulfide in water do not agree with each other. Exner (35) obtained a value of 1.77×10^{-5} cm.²/sec. at 16°C., Hagenbach (36) a value of 1.43×10^{-5} at 15.5°C., and Kamiike, et al. (37) a value of 1.36×10^{-5} at 25°C. Correcting Exner's and Hagenbach's values to 25°C. by assuming $\underline{D\mu/T} = \text{constant}$, one gets 2.27×10^{-5} and 1.84×10^{-5} , respectively.

An attempt to calculate the diffusion coefficient from theoretical (38) and empirical relationships (39,40) gave an equally wide range of values.

In order to use the penetration theory, an accurate estimate of the diffusion coefficient of hydrogen sulfide in water must be known. Also the effect of neutral salts on the diffusion coefficient must be known. Therefore, it was necessary to determine the diffusion coefficient as a part of this study.

Diffusion Coefficients by Free Boundary Techniques

A number of attempts were made to determine the diffusion coefficient using the electrophoresis-diffusion apparatus. Table IV gives a summary of the conditions employed. None of the attempts were successful because of a disturbance which kept disrupting the boundary.

TABLE IV

SUMMARY OF DIFFUSION RUN CONDITIONS

Run	Solvent	Hydrogen Sulfide Concentration, g./liter	Temperature, °C.
1	Water	3.2	25
2	Dil. HCl	3.1	25
3	0.1N HCl	3.1	25
4	Water	6.5	2
5	Water	3.2	2
6	0.01% ion agar	3.1	25

One run using water at 25°C. was attempted using the layering-in technique with the ultracentrifuge. This attempt also met with failure.

In all of the attempts described above, the boundary could be formed. Diffusion would occur normally for a very few minutes and then the boundary would be disrupted. The nature and cause of the disturbance was not determined but it is thought that the cause was due to mechanical vibrations from the instruments involved. In most systems the density differences between the solvent and solution are great enough to damp out mechanical disturbances. However, it was believed that the density differences in the system under study here were not great enough to form a stable boundary.

The sedimentation equilibrium run attempted also failed. The failure in this case can be attributed to a low sedimentation coefficient of hydrogen sulfide and again to the very slight density difference between water and a hydrogen sulfide solution.

Diffusion Coefficient by Gas Absorption Measurements

Since all attempts to use the free boundary techniques to determine the diffusion coefficient of hydrogen sulfide failed, it was necessary to use other techniques. The porous plug technique used by many workers had been found to have inherent sources of error (18). Thus, it was decided to use a gas absorption technique.

First, it was necessary to check the equipment and procedures used in this study. This was done using chlorine as the gas and 0.1N hydrochloric acid and 0.262N sodium hydroxide as the absorbents. Three runs were made using each of the absorbents, and the results agreed with those previously obtained (18) to within $\pm 1\%$.

It was then necessary to test the suitability of the laminar jet for studying hydrogen sulfide absorption. For this purpose, 15 runs were made using 0.1N hydrochloric acid as the absorbent and with exposure times varying from 0.013 to 0.06 second. Three runs were made with the same exposure times but different gas flow rates to test for the presence of a gas-film resistance which was found to be negligible. The runs were then plotted in accordance with Equation (44) which predicts a linear relationship between the rate of absorption and the inverse of the square root of exposure time. The results are shown in Fig. 9.

The slope of the line in Fig. 9 was determined by a least-squares regression analysis method which forced the solution through the origin. The slope of the

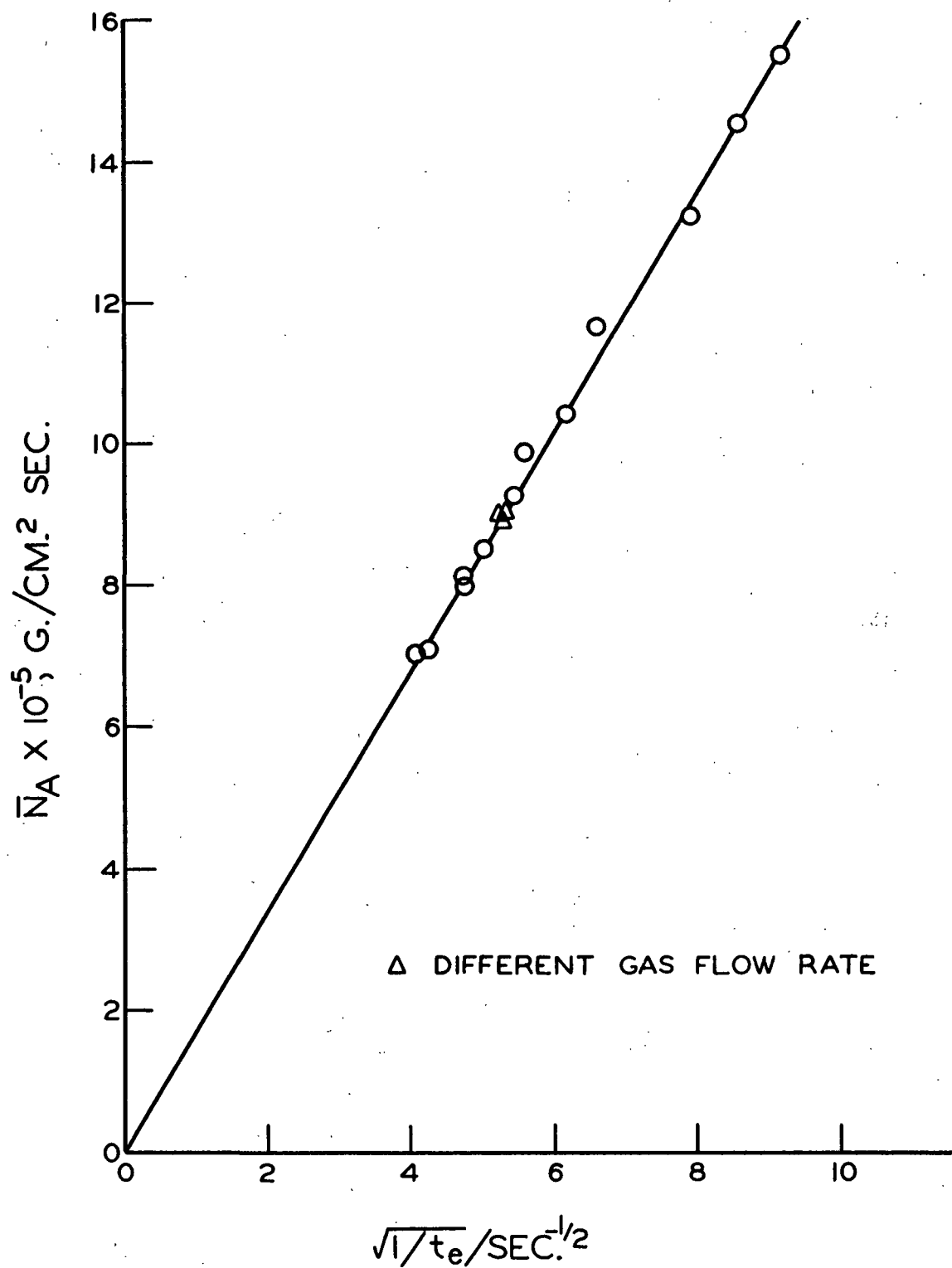


Figure 9. Absorption into 0.1N Hydrochloric Acid

line was found to be $(1.66 \pm 0.02) \times 10^{-5} \text{ g./cm.}^2 \text{ sec.}^{1/2}$. Using the equilibrium solubility value given in the previous section and the equation relating the slope and diffusion coefficient given earlier,

$$D_A = \pi m^2 / 4C_{A,e}^2 \quad (55),$$

the diffusion coefficient was found to be $1.86 \times 10^{-5} \text{ cm.}^2 \text{ /sec.}$

Because of the very good straight-line relationship obtained between the rate of absorption and the inverse of the square root of exposure time, it was concluded that the laminar jet was suitable for studying hydrogen sulfide absorption.

In order to determine the diffusion coefficient of hydrogen sulfide and the effect of a neutral salt on diffusion, absorption runs were made using sodium chloride solutions at a pH of 2.2. Six runs were made at each of four different salt concentrations with the exposure times varying from 0.015 to 0.040 second. The rate of absorption and exposure times were determined and plotted as before. The slope of the resulting line was again determined using the least-squares method of regression. The resulting slopes were used to calculate the diffusion coefficient for each salt concentration. The results are shown in Table V.

TABLE V

EFFECT OF A SALT ON THE DIFFUSION COEFFICIENT
OF HYDROGEN SULFIDE AT 25°C.

Sodium Chloride Concentration, g./liter	Slope, g./cm. ² sec. ^{1/2} x 10 ⁵	Solubility, g./liter	Diffusion Coefficient, cm. ² /sec. x 10 ⁵
25	1.48	3.23	1.77
50	1.34	2.96	1.72
75	1.22	2.76	1.63
100	1.11	2.56	1.53

The diffusion coefficient was then plotted against the salt concentration, and the resulting curve was extrapolated to zero salt concentration. The extrapolated value was very close to Hagenbach's (36) corrected value of 1.84×10^{-5} cm.²/sec. for the diffusion coefficient of hydrogen sulfide in water at 25°C.

In the Stokes-Einstein treatment of the diffusion of rigid spheres, the equation

$$D\mu/T = \text{constant} \quad (57)$$

is obtained. The constant is independent of the solvent but is a function of the diffusing species. The same general relationship is arrived at by Eyring's (38) treatment of diffusion.

The data for the diffusion of hydrogen sulfide through sodium chloride solutions were then put in the form of Equation (57), taking advantage of the fact that the temperature was a constant in this study. The results, together with Hagenbach's (36) value for the diffusion coefficient of hydrogen sulfide in water, are shown in Table VI.

TABLE VI

EFFECT OF VISCOSITY ON THE DIFFUSION COEFFICIENT OF HYDROGEN SULFIDE

Solvent	Diffusion Coefficient, cm. ² /sec. $\times 10^5$	Relative Viscosity, μ/μ_0	Diffusion Coefficient Viscosity Product, cm. ² /sec. $\times 10^5$
Water	1.84	1.000	1.84
NaCl, 25 g./liter	1.77	1.044	1.85
NaCl, 50 g./liter	1.72	1.077	1.85
NaCl, 75 g./liter	1.64	1.125	1.85
NaCl, 100 g./liter	1.53	1.177	<u>1.80</u>
Average:			1.84 \pm 0.01

Comparison of Results with Previous Work

Results from studies on the effect of neutral salts on the diffusion coefficients of other gases do not agree with those found in this study. Previous works have shown that at constant temperature the effect of a salt on the diffusion coefficient is best predicted by an equation of the form

$$D_{\mu}^a = \text{constant} \quad (58)$$

where a is a function of the type of salt.

As part of a study of the absorption of carbon dioxide by basic solutions, Nyjsing, et al. (19) determined the effect of the sulfate salts of sodium and magnesium on the diffusion coefficient of carbon dioxide. The values of a were found to be 0.90 and 0.80 for sodium sulfate and magnesium sulfate, respectively.

Ratcliff and Holdcroft (30) determined the effect of the chloride, nitrate, and sulfate salts of sodium and magnesium on the diffusion coefficient of carbon dioxide. They used a gas absorption technique in which the liquid was exposed to the carbon dioxide atmosphere by flowing over a sphere. Their data show considerable scatter, probably due to their experimental technique, and therefore any conclusions drawn must be very tentative. Despite the scatter, Equation (58) can be used to provide a reasonable fit of the data with a having the following values: NaCl 0.85, NaNO₃ 0.85, Na₂SO₄ 0.65, MgCl₂ 0.60, Mg(NO₃)₂ 0.40, and MgSO₄ 0.75. The values of a found by the two different studies for the common salts, sodium sulfate and magnesium sulfate, do not agree with each other.

Spalding (18) determined the effect of sodium chloride on the diffusion coefficient of chlorine. He found a maximum in the curve of diffusion coefficient versus sodium chloride concentration. He then recalculated his data using activity as a driving force for diffusion. Using these values, he found that the product

of the activity diffusion coefficient, \underline{D} , activity coefficient, γ , and viscosity, μ , ($\underline{D}\mu\gamma^{2.5}$) was a constant. From this he concluded that a diffusion coefficient based on a concentration driving force was a complicated function of salt concentration, while an activity-based diffusion coefficient was a simple function of salt concentration.

The fact that no other study shows a maximum in the diffusion coefficient-salt concentration curve would tend to indicate that either Spalding's (18) data were in error or that another means of mass transport was occurring. This author believed that it was the latter factor which affected the data. A sodium chloride solution contains an ion which is common to a chlorine solution. Thus, in a chlorine-sodium chloride solution, the chlorine could dissociate and recombine with a chloride ion which was originally present in conjunction with a sodium ion. If the chloride ion with which the hypochlorous acid recombined was farther along in the direction of diffusion than the chloride ion originally associated with the hypochlorous acid, there would be a net movement not due to diffusion. An increase in salt concentration would increase the probability of movement occurring by the mechanism described above. At the same time, the viscosity of the solution would be increasing which would slow up diffusion. Thus, the maximum in the rate of transport-salt concentration curve would be observed. This common ion effect has been observed for other systems (41-43).

In summary, Hagenbach's (36) corrected value of 1.84×10^{-5} cm.²/sec. was used as the diffusion coefficient of hydrogen sulfide in water at 25°C. The diffusion coefficient in all other solutions was estimated by assuming that ($\underline{D}\mu$) was constant.

OXIDATION REACTIONS

Preliminary investigations were carried out to determine the suitability of various oxidizing agents for use in the absorption apparatus. The oxidants tried included potassium permanganate, potassium dichromate, ceric ammonium nitrate, sodium hypochlorite, and sodium hypobromite. These investigations showed that all of the oxidizing agents except the hypohalites produced sulfur in a form which would interfere with operation of the absorption apparatus. Therefore, sodium hypochlorite and hypobromite were chosen as the oxidizing agents to be used in this study. The stoichiometry of the reaction between hydrogen sulfide and the hypohalites was then thoroughly investigated, and the results are reported below. The reaction between sodium sulfide and the hypohalites was also studied since this would help determine the mechanism of hypohalite oxidation of the sulfides. The results of the preliminary investigations using the other three oxidants are briefly discussed in a later section, "Oxidation of Hydrogen Sulfide by Miscellaneous Oxidants."

Oxidation Products

It had been reported that elemental sulfur and sulfate ions were the only two products of the hypohalite oxidation of hydrogen sulfide or sodium sulfide. To check this, a hypochlorite solution was prepared and an excess of hydrogen sulfide was added. The resulting solution gave a positive test for sulfate ions. The excess sulfide ions were precipitated by the addition of a zinc carbonate suspension formed by mixing equal volumes of 1 molar sodium carbonate and zinc sulfate solutions. The supernatant liquid gave a negative test for the presence of reducing compounds when iodine was used as the oxidizing agent.

An experiment was then performed to compare the results of two different methods - a volumetric and a gravimetric technique - for determining the per

cent conversion of sulfide to sulfate. The volumetric technique called for the addition of a sulfide solution to a solution containing an excess of hypochlorite which was determined iodometrically. The gravimetric technique involved a direct determination of the amount of sulfate formed by precipitating the sulfate ions with barium chloride and then weighing the amount of precipitate formed.

The results of the volumetric technique indicated that 25.2% of the sulfides had been converted to sulfate while the gravimetric technique gave a per cent conversion of 26.0%. Although this is a fairly large difference, it can be explained because of the differences in procedure. The volumetric technique called for the addition of 5 ml. of the hydrogen sulfide solution to a 50-ml. sample of hypochlorite, while the gravimetric procedure called for the addition of 40 ml. of the hydrogen sulfide solution to a 400-ml. sample of the hypochlorite. Because the time required for addition of the sulfide solution was greater in the gravimetric procedure, one would expect a slightly higher percentage of conversion of the sulfide to sulfate using the gravimetric procedure.

Thus, it was concluded that elemental sulfur and sulfate ions were the only products of the hypochlorite oxidation of hydrogen or sodium sulfide. It was also concluded that the percentage conversion of sulfide to sulfate could be determined using volumetric techniques alone. Since each mole of sulfide will consume two oxidizing equivalents in being oxidized to the sulfur form and eight equivalents in being oxidized to the sulfate form, it can be shown that the percentage of conversion of sulfide to sulfate can be calculated from

$$\% \text{ sulfate formed} = [(A - 2)/6] \times 100 \quad (58A)$$

where A is the number of oxidizing equivalents consumed per mole of sulfide added. In all subsequent experiments, Equation (58A) was used in calculating the relative amount of sulfate formed.

The other effect which was investigated in the preliminary experiments was the effect of time on the stoichiometry of the reaction. Using volumetric techniques, the percentage conversion of sodium sulfide to sodium sulfate rose from 25.2 to 27.1% over a period of 18 hours. Since, in all other experiments, the samples were only allowed to stand for a few minutes, the effect of time was concluded to be negligible.

Oxidation of Hydrogen Sulfide

The effect of pH on the stoichiometry of the hypochlorite and hypobromite oxidation of hydrogen sulfide was studied over the pH range 7.1-14.8 (6N sodium hydroxide). The percentage of conversion to sulfate was calculated and the results are shown in Fig. 10. The numerical data are given in Appendix VI.

The data showed that the reaction between hydrogen sulfide and the two hypohalite solutions proceeded quantitatively to a sulfate form in the pH range 7-11.9. At pH 11.9 there was a sudden drop in the relative amount of sulfate formed. The amount of sulfate formed then increased as the pH increased until the reaction again became quantitative above a sodium hydroxide concentration of 4 normal when sodium hypochlorite was used and 1 normal when sodium hypobromite was used.

It was noted during the course of the study that only in the hypochlorite solutions below pH 11.9 did the percentage of conversion rise above 100%. Here the results exhibited a normal scatter with the average being 100%. The points in the strong hydroxide solutions did not reach 100% conversion to sulfate except for one point. The conversion was only 98-99% complete. A possible explanation will be given later.

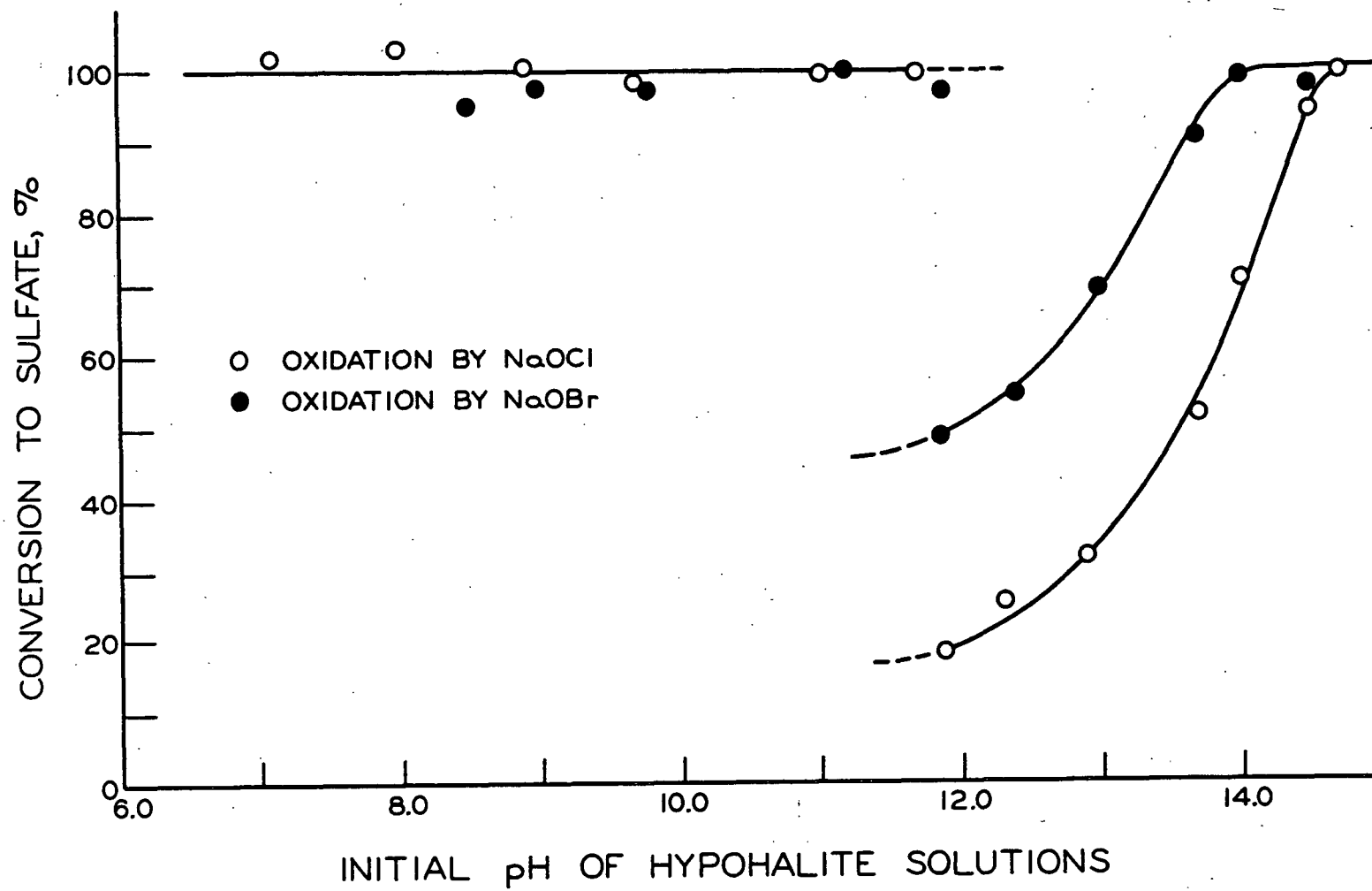


Figure 10. Oxidation of Hydrogen Sulfide

Comparison with Other Work

The results of this study agree with the work of Dunicz and Rosenqvist (12). Different methods of introduction of the hydrogen sulfide to the hypochlorite solution probably account for most of the differences. Also the previous workers determined the pH of their solutions with a glass electrode which was only recommended for use below pH 9.

This work does not agree with the work of Murthy and Rao (13). Buffering compounds present in the previous work can explain the difference. In one run in this study, 0.1N sodium borate was used to buffer the pH at 9.1. The conversion of hydrogen sulfide to sulfate fell from 100% for the unbuffered system to 7.9%. Another reason could be due to differences in the action of hypochlorite and chloramine-T.

Oxidation of Sodium Sulfide

The results of the oxidation of sodium sulfide are given in Fig. 11. As before, the numerical data are presented in Appendix VI.

The data showed that the reaction was quantitative below a certain pH — 7.2 for the hypochlorite system and 9.0 for the hypobromite system. As the pH was increased, the percentage of conversion of sulfate fell off sharply to a valley which continued to pH 11. The relative amount of sulfate formed then increased until the conversion to sulfate again became quantitative above a sodium hydroxide concentration of 4 normal for the hypochlorite system and 1 normal for the hypobromite system.

As was the case with oxidation of hydrogen sulfide, the percentage of conversion to sulfate did not attain 100% except for two isolated points. The percentage of conversion to sulfate in the quantitative regions was only 98-99%.

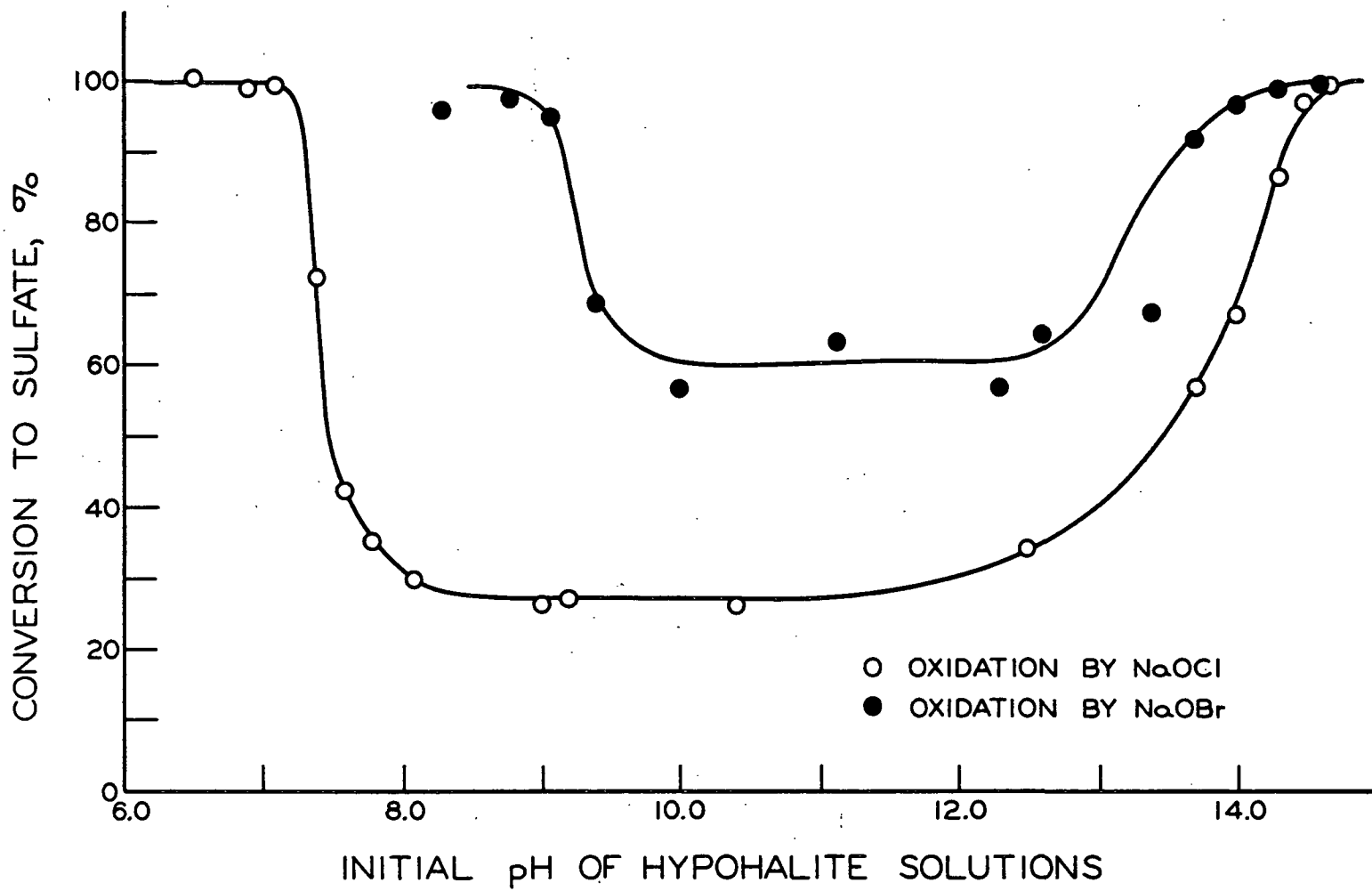


Figure 11. Oxidation of Sodium Sulfide

The effect of ionic strength on the stoichiometry was also determined using a 0.1N sodium hypochlorite - 0.5N sodium hydroxide as the base solution and adding sodium chloride as the neutral salt. The results are given in Table VII.

TABLE VII

EFFECT OF IONIC STRENGTH ON THE STOICHIOMETRY OF THE
HYPOCHLORITE OXIDATION OF SODIUM SULFIDE

Salt Concentration, moles/liter	Conversion to Sulfate, %
0.0	60.3
1.0	59.8
2.0	56.9
3.0	58.2
4.0	58.0
5.0	57.7

There appeared to be a slight decrease in the relative amount of sulfate formed with increase in ionic strength. This decrease could be coincidental because the difference between the two extremes was only 5% and the difference in duplicate determinations was about 2%. However, it was believed that the decrease was real even if it was small.

Comparison with Other Work

This work compared favorably with that of Willard and Cake (5). The differences in the two studies are probably due to differences in procedure, although the exact procedure was not given in the earlier report.

The results from this study agreed with those of Choppin and Faulkenberry (10) above pH 12. However, the results of the two studies differ below pH 12. This difference was believed to be due mainly to the use of buffering compounds by the previous workers.

No previous work had been done on the effect of ionic strength on the stoichiometry of the reaction.

Mechanism of Oxidation

From an analysis of the data obtained in this study and in previous studies, it was evident that the reaction sequence proposed by Willard and Cake (5) and refined by Choppin and Faulkenberry (10) was inadequate to explain the results over an extended pH range. The proposed sequence could occur in the alkaline solutions but it does not explain the difference between the action of hypobromite and hypochlorite. If the role of the hydroxide is merely to dissolve the sulfur as it is being formed, then there should be no difference between the action of hypobromite and hypochlorite.

Bendall's (11) and Murthy and Rao's (13) suggestion of dihydrogen sulfoxide (DHSO) as a possible intermediate appeared to be reasonable. However, Bendall's (11) idea that the oxidation of hydrogen sulfide and the sulfide ion occurred by different reaction sequences did not seem reasonable. Neither did Murthy and Rao's (13) theory that DHSO is the primary product of the oxidation of hydrogen sulfide and sulfur is the primary product of the oxidation of the bisulfide ion. If Murthy and Rao's theory is correct, their data should have agreed with Dunicz and Rosenqvist's (12) rather than with Choppin and Faulkenberry's (10).

In order to correctly analyze the absorption data in light of the penetration theory, the reaction sequence should be known. Since the two sequences presented earlier were believed to be incorrect, a revised reaction sequence based on the DHSO intermediate is proposed and presented in the next section.

Revised Reaction Sequence

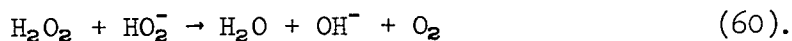
Dihydrogen sulfoxide has never been isolated. However, many organic sulfoxides are known and it would be reasonable to assume that DHSO could exist

even if for only a short time. Since it has never been isolated, its actions in solution have never been studied. However, it can be considered analogous to hydrogen peroxide which has been studied fairly extensively. Therefore, a discussion of the action of hydrogen peroxide in solution follows.

In aqueous solutions hydrogen peroxide ionizes to form the hypoperoxide anion by



The equilibrium constant for this reaction is quoted by Shanley and Greenspan (44) as 2.4×10^{-12} . Hydrogen peroxide will also decompose - the reaction being catalyzed by many different conditions. This decomposition has been studied by Duke and Haas (45) over a range of initial hydrogen peroxide concentration from 0.1 molar to 1.1 molar. They successfully eliminated heterogeneous catalysis and found that the rate of decomposition went through a maximum when the pH of a solution was equal to the pK_a of hydrogen peroxide. From this they concluded that the decomposition reaction must involve a hydrogen peroxide molecule and anion by



As further supporting evidence, they found that the rate of decomposition could be predicted by

$$-d[\text{H}_2\text{O}_2]/dt = k_1 [\text{H}_2\text{O}_2][\text{HO}_2^-] \quad (61).$$

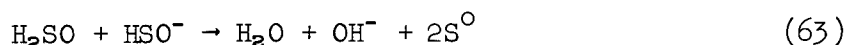
Similar results were obtained by Koubek, et al. (46) when the initial hydrogen peroxide concentration was 0.1 molar. However, when the latter authors used an initial concentration of 1 molar, the rate of decomposition decreased as the pH increased from 10.7 to 12.7. Also their rates were much lower than those obtained

by Duke and Haas (45), and they concluded that the former workers had not been able to eliminate homogeneous catalysis. Jones (47) has found that the rate of decomposition is very fast when the pH is in the vicinity of the pK_a and decreases as the pH is increased and is very slow in solutions where the ratio of hydroxide to hydrogen peroxide is greater than 2. He also found that the pH increased as the decomposition proceeded. This is consistent with the reaction proposed by Duke and Haas (45).

Thus, by analogy with hydrogen peroxide, DHSO would be expected to ionize into hydrogen ions and dihydrogen sulfoxide anions by



with an ionization constant of the order of 10^{-12} . DHSO would also be expected to decompose by



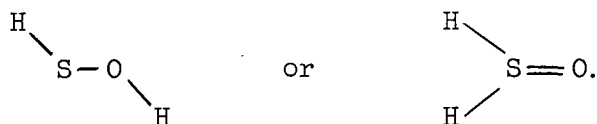
with the rate of decomposition

$$-d[H_2SO]/dt = k_1 [H_2SO] [HSO^-] \quad (64).$$

While Reaction (63) gives the stoichiometry probably involved in the decomposition of DHSO, the form of the sulfur is unknown. It could be as written, in a monoatomic state, but it could also be in a diatomic state (S_2) or in a chain (S_n). The final form is not important to this work and only the stoichiometry will be referred to.

It should be pointed out here that there are two possible molecular configurations for DHSO — one by continued analogy with hydrogen peroxide which has a skew chain configuration or by analogy with dimethyl sulfoxide which is usually

considered to have a planar trigonal configuration. Thus, the molecules in DHSO could be linked up



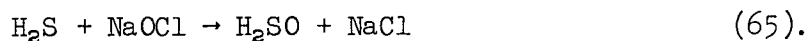
The results of this study can be explained on the basis of either structure, but because of the fact that the hydrogen atoms are originally associated with the sulfur atom and would have to transfer to the oxygen atom after oxidation, the latter configuration will be used throughout this thesis.

Before trying to draw any conclusions as to a probable reaction sequence, one must first understand the mechanism of hypohalite oxidation. Edwards (48) points out that these reactions probably occur by direct oxygen transfer to a reducing substrate. He states that isotopic studies and rate data are highly suggestive of a bimolecular nucleophilic displacement mechanism (S_N2 reaction). In the oxidation of hydrogen sulfide, this would involve the formation of the intermediate

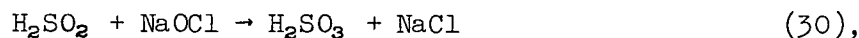
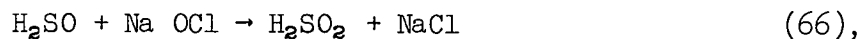


The halite atom, X, would then be displaced by the hydrogen sulfide molecule. The rate of such a reaction would be determined by the rate of formation of the intermediate and by the ability of the halite atom to leave the reaction site.

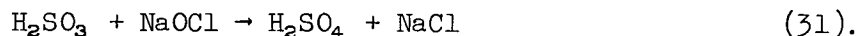
Since hypohalite oxidations probably occur through direct oxygen transfer, the initial reaction is probably



Three other reactions which may occur in series and give sulfate ions are



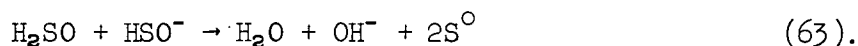
and



These last two reactions are identical to the last two reactions in the sequence proposed by Choppin and Faulkenberry (10).

While the above reaction sequence is written in molecular form, any one of the above reactants could be in ionic form, depending on the pH of the reactant solution. In fact, unless the pH is below 8, almost all of the hypochlorite is present as the hypochlorite anion (OCl^-). Even if the pH is below 8, the hypochlorite is present as hypochlorous acid (HOCl) and is never present as molecular sodium hypochlorite.

The sulfur is formed from the decomposition of DHSO given earlier by



Thus, according to the revised reaction sequence, the relative amounts of sulfur and sulfate formed are controlled by the relative rates of Reactions (66) and (63).

Oxidation on Basis of Revised Mechanism

Effect of the Oxidizing Agent

It has been well established (49) that a bromine atom will leave an $\text{S}_{\text{N}}2$ reaction site much more readily than will a chlorine atom. This means that for a given set of conditions, the rate of oxidation should be faster in the sodium hypobromite system. Therefore, at a given pH, sodium hypobromite should oxidize

more of the sulfide to sulfate than sodium hypochlorite. This is precisely what was shown in Fig. 10 and 11.

Effect of pH

Before discussing the effect of pH on the basis of the revised reaction sequence, it should be noted that the pH of the solutions were changing as the reaction proceeded. An attempt to use a buffering agent resulted in a very low per cent conversion to sulfate. Thus, the experiments were run at uncontrolled pH's. The variation in pH which occurred is shown in Fig. 12 where the final pH is plotted against the initial pH.

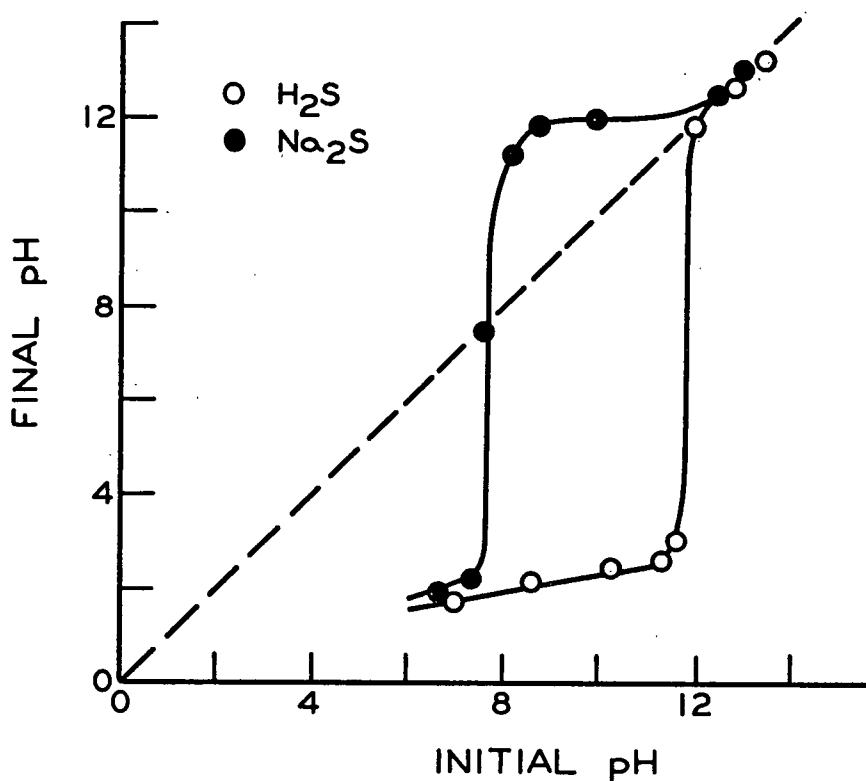


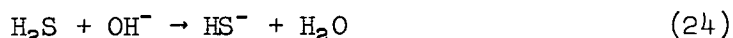
Figure 12. Effect of Initial pH on the Final pH for the Hypochlorite Oxidation of Sodium Sulfide and Hydrogen Sulfide

The decreased pH was due to two factors. First, in the low initial pH range, the oxidant was present as hypochlorous acid. The reduced form of this is hydrochloric acid which is a stronger acid. The other factor which caused a decrease in pH when hydrogen sulfide was used was that the sulfate form of hydrogen sulfide is sulfuric acid. The increase in pH observed for the sodium sulfide oxidation was due to the fact that one is adding equimolar quantities of hydroxide ions and bisulfide ions; and when sulfur is formed from the oxidation of the bisulfide ion, hydroxide ions are also a product of the reaction. Since the value of the pK_a of $DHSO$ is assumed to be 12, then the rate of decomposition would have a maximum at pH 12 and would decrease as the pH moved away from 12. The pH probably has little if any effect on the rate of oxidation (with one exception, noted later). This would predict a minimum sulfate formation at pH 12 and an increase in the sulfate formation as the pH moved away from 12. Essentially, this is what was observed for both the sodium and hydrogen sulfide systems.

The differences observed between the two systems below pH 12 were probably due to the difference in the form in which the sulfide was added to the oxidizing solution. In a 0.1M hydrogen sulfide solution, the pH is about 4 and the sulfide is present primarily as molecular hydrogen sulfide. The sulfate form of the oxidation products was sulfuric acid which would tend to lower the pH. Also, when sulfur was formed there was no net gain in hydroxide ions. Therefore, the tendency would always be to lower the pH.

In contrast, a 0.1M sodium sulfide solution has a pH of about 13 and the sulfide is present mainly as the bisulfide ion. The sulfate form of the oxidation products would be sodium sulfate. When sulfur was formed there was a net gain of hydroxide ions - one mole of hydroxide ions per mole of sulfur formed. Thus, the tendency would always be to raise the pH of the oxidizing solution.

There are two possible reasons for the sudden drop (at pH 11.9) in the relative amount of sulfate formed from the oxidation of hydrogen sulfide. The first is that this was almost the pH value (as will be shown later) at which the absorption of hydrogen sulfide by aqueous solutions switched from absorption accompanied by a slow, first-order, irreversible reaction to absorption accompanied by an "infinitely fast" reaction. In other words, this was near the pH where the reaction



became an important consideration in gas absorption. If the rate of Reaction (24) was faster than the rate of oxidation, then appreciable amounts of both DHSO and the DHSO anion would be formed. This would increase the rate of decomposition. Another fact which suggested that Reaction (24) occurred before the oxidation, was that above pH 12, the data for the oxidation of both sodium and hydrogen sulfide as shown by Fig. 13 fell on the same curve. This indicated that both species had the same initial oxidation reactant - the bisulfide ion. The second possible reason was that the change occurred very near the pH value where the rate of oxidation was predicted to be a minimum. The reason why the drop is so sharp is probably due to the fact that the solutions are not buffered. For some reason, it appeared that if the sulfur was the product from the first amount of hydrogen sulfide added then sulfur would be the principal product, while if sulfuric acid was the initial product then it was also the principal product.

The sharp increase in the relative amount of sulfate formed which occurred at pH 9.2 for the hypochlorite-sodium sulfide system and 8.0 for the hypobromite-sodium sulfide system can be explained by a change in the oxidant. At the two pH values mentioned above, appreciable quantities of the respective hypohalous

acids are present in a hypohalite solution. When a bisulfide ion is oxidized by the hypohalous acid in an S_N2 reaction, there would be a strong possibility of forming DHSO rather than the DHSO anion formed in the oxidation by the hypohalite ion. The further oxidation of DHSO and the DHSO anion will probably be more rapid since part of the oxidizing agent is present in the molecular form. Using ionization constants taken from Latimer (50), about 75% of the hypochlorite is present as hypochlorous acid at the pH value (7.2) where the oxidation to sulfate becomes quantitative. About 40% is present as hypobromous acid at this quantitative pH value (8.9) in the hypobromite system.

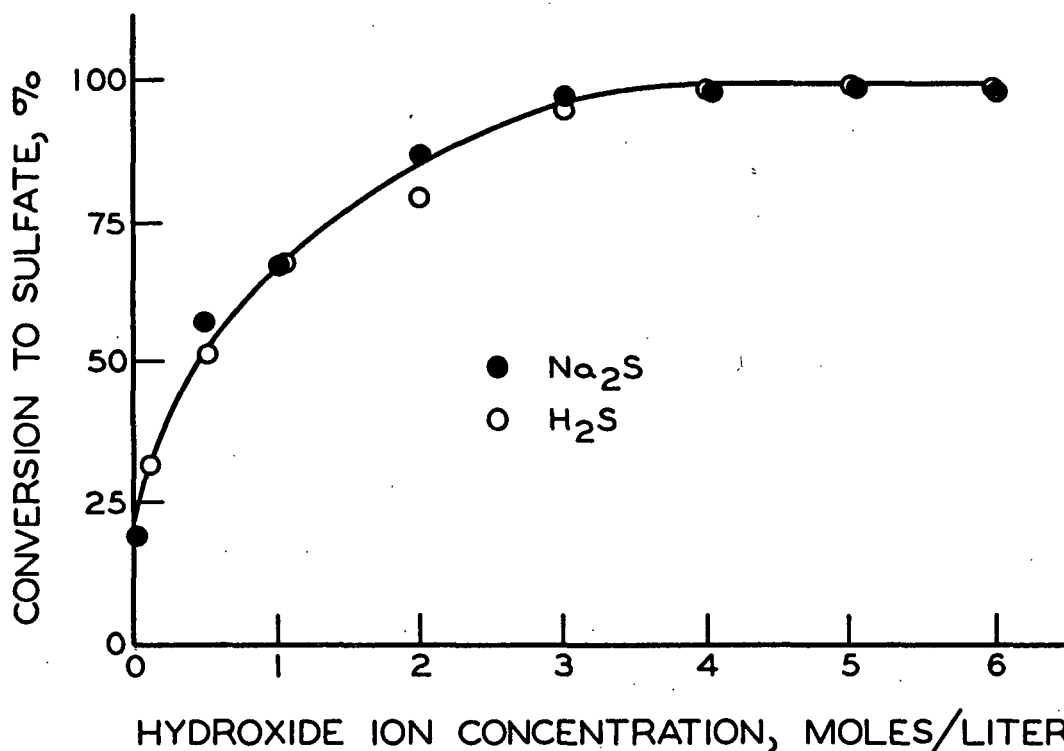


Figure 13. Effect of Hydroxide Ion Concentration on the Hypochlorite Oxidation of H₂S and Na₂S

In the proposed reaction sequence, the sodium hydroxide could influence the reaction in a number of ways. One way would be to raise the pH of the solution. This would decrease the concentration of DHSO and reduce the rate of decomposition.

A second function could be to increase the ionic strength. An increase in ionic strength would decrease the energy necessary to form the S_N2 intermediates. This would tend to increase the rate of oxidation. A third function could be that first proposed by Willard and Cake (5). The hydroxide ion could keep any sulfur initially formed in such a state that further oxidation could occur. At the present time, it is impossible to determine exactly the role of the hydroxide ion.

The fact that an increase in the sodium chloride concentration did not increase the relative amount of sulfate formed can be explained on the basis of a catalytic effect. The ferric ion is known to catalyze the decomposition of hydrogen peroxide and could have a similar effect on $DHSO$. The sodium chloride used in this study was reagent grade but contained about 2 p.p.m. ferric ion. This could offset the ionic strength effect and even give the slight decrease in percentage of sulfate formed with increasing ionic strength observed in this study.

Further Supporting Evidence

Some observations consistent with the assumption that the hypohalite oxidation of sulfides occurs by direct oxygen transfer rather than by electron transfer were seen in the form in which the sulfur appeared. In the oxidation of sulfides by chlorine gas, where oxidation probably occurs by electron transfer, the sulfur has a bright yellow color and is a rubberylike material. In the hypohalite oxidation of both sodium and hydrogen sulfide, the sulfur had a grayish-white color and a soft, powdery appearance in solution. This form of sulfur also passed through a qualitative-grade filter paper. This would seem to indicate that the sulfur is formed by different mechanisms in the two systems.

Another piece of information consistent with the revised mechanism was the fact that only in the hypochlorite oxidation of hydrogen sulfide in the pH range 7-11.9 did the percentage of conversion of sulfide to sulfate reach or exceed

100% (except for isolated cases). This incomplete conversion was also obtained by all other workers in the area although only Bethge (9) commented on the unusual result. This can be explained by the fact that one can slow up the decomposition of DHSO and reduce the formation of sulfur but can never stop it.

The 100% conversion results obtained in this study at the lower pH values for the hypochlorite oxidation of hydrogen sulfide were probably due to the formation of chlorates. After the hydrogen sulfide was added, the resulting pH was such that both hypochlorous acid and hypochlorite ions were present. This condition accelerates the decomposition of hypochlorite solutions to chlorate, and since chlorates will not oxidize iodide ions to iodine, an excessive consumption of chlorine was obtained.

The oxidation of organic sulfides by hydrogen peroxide (51) has also been shown to follow a mechanism which is consistent with the revised mechanism for the oxidation of sodium and hydrogen sulfide.

Oxidation of Hydrogen Sulfide by Miscellaneous Oxidants

In some preliminary experiments, it was noted in the permanganate oxidation of hydrogen sulfide that more than eight oxidizing equivalents were consumed by each mole of sulfide. Further investigation indicated that potassium permanganate could be used to oxidize sulfides to sulfates quantitatively if modified barium sulfate gravimetric procedure was used for the quantitative technique. Iodometric techniques gave erroneous results which were probably due to decomposition of the permanganate. Since this oxidizing agent was not used again in this study, the results and their significance are not discussed here but are presented in Appendix VII.

The results of the preliminary experiments using potassium dichromate and ceric ammonium nitrate as oxidizing agents showed that sulfur was formed in the

reaction and also more than two oxidizing equivalents were consumed per mole of sulfide. This indicated that more than one product was formed, probably due to the fact that oxidation by dichromate and ceric ions proceeds by electron transfer rather than by direct oxygen transfer. Since sulfur would interfere with the operation of the absorption apparatus, the experiments were not carried further.

THE ABSORPTION EXPERIMENTS

The primary purpose of this thesis was to study the factors affecting the rate of absorption of hydrogen sulfide. The two most important variables were pH and oxidizing strength. The pH was varied from 0.3 to 14.1. An oxidizing agent - sodium hypochlorite - was then added and the pH was varied from 7.0 to 14.0. The pH was held constant at a value of 10.5 and the oxidizing strength was varied from 0.05 to 0.3N. The results and conclusions drawn from these experiments are given below.

EFFECT OF pH ON ABSORPTION

A total of eighty-four runs were made to determine the effect of pH on absorption. Usually three runs with different exposure times were made at each pH value. The exposure times were varied from 0.012 to 0.059 sec. A summary of the runs is presented in Appendix VIII.

Summary of Results

For each set of runs at a given pH, the rate of absorption was plotted against the inverse of the square root of exposure time and the rate of absorption at 0.03 sec. was determined by interpolation. This was done so that the rates could be compared on an equal basis.

The rate of absorption without chemical reaction was then calculated from Equation (44) for each run. The equilibrium solubility of hydrogen sulfide in

the acidic absorbents was taken from the data in Table III. The solubility in the basic absorbents was calculated from Equation (56) using the constants presented on page 43. The diffusion coefficient was determined by assuming that (D_{μ}) was constant and that the diffusion coefficient of hydrogen sulfide in water was 1.84×10^{-5} cm.²/sec.

The function Φ at 0.03 sec. was then determined by dividing the experimentally determined rate of absorption by the rate of absorption without chemical reaction. The results of these calculations are presented as a function of pH in Table VIII and Fig. 14 and 15. Figure 14 covers the pH range 0.3-12, and Fig. 15 the pH range 11-14.1.

TABLE VIII
EFFECT OF pH ON RATE OF ABSORPTION OF HYDROGEN SULFIDE

Absorbent	pH	Experimental Rate of Absorption, g./cm. ² sec. x 10 ⁵	Rate of Absorption Without Chemical Reaction, g./cm. ² sec. x 10 ⁵	Φ
0.564N HCl	0.3	9.61	9.48	1.01
0.268N HCl	0.6	9.56	9.56	1.00
0.1N HCl	1.1	9.75	9.67	1.01
Dil. HCl	2.0	9.62	9.72	0.99
Dil. HCl	3.1	9.80	9.72	1.01
Dil. HCl	4.1	9.83	9.72	1.01
Dil. HCl	4.6	9.93	9.72	1.02
Dil. HCl	5.4	9.98	9.72	1.03
Dil. HCl	6.5	10.01	9.72	1.03
H ₂ O	7.1	9.97	9.72	1.03
Dil. NaOH	8.0	10.01	9.72	1.03
Dil. NaOH	8.3	9.95	9.72	1.02
Dil. NaOH	10.1	10.00	9.72	1.03
Dil. NaOH	11.0	10.02	9.72	1.03
Dil. NaOH	12.0	10.96	9.70	1.13
0.0421N NaOH	12.6	15.84	9.56	1.66
0.106N NaOH	13.0	27.6	9.43	2.93
0.206N NaOH	13.3	49.2	9.10	5.41
0.419N NaOH	13.6	97.1	8.49	11.44
0.657N NaOH	13.8	190.0	7.90	24.0
1.061N NaOH	14.0	347.0	7.14	48.6
1.231N NaOH	14.1	466.0	6.63	70.3

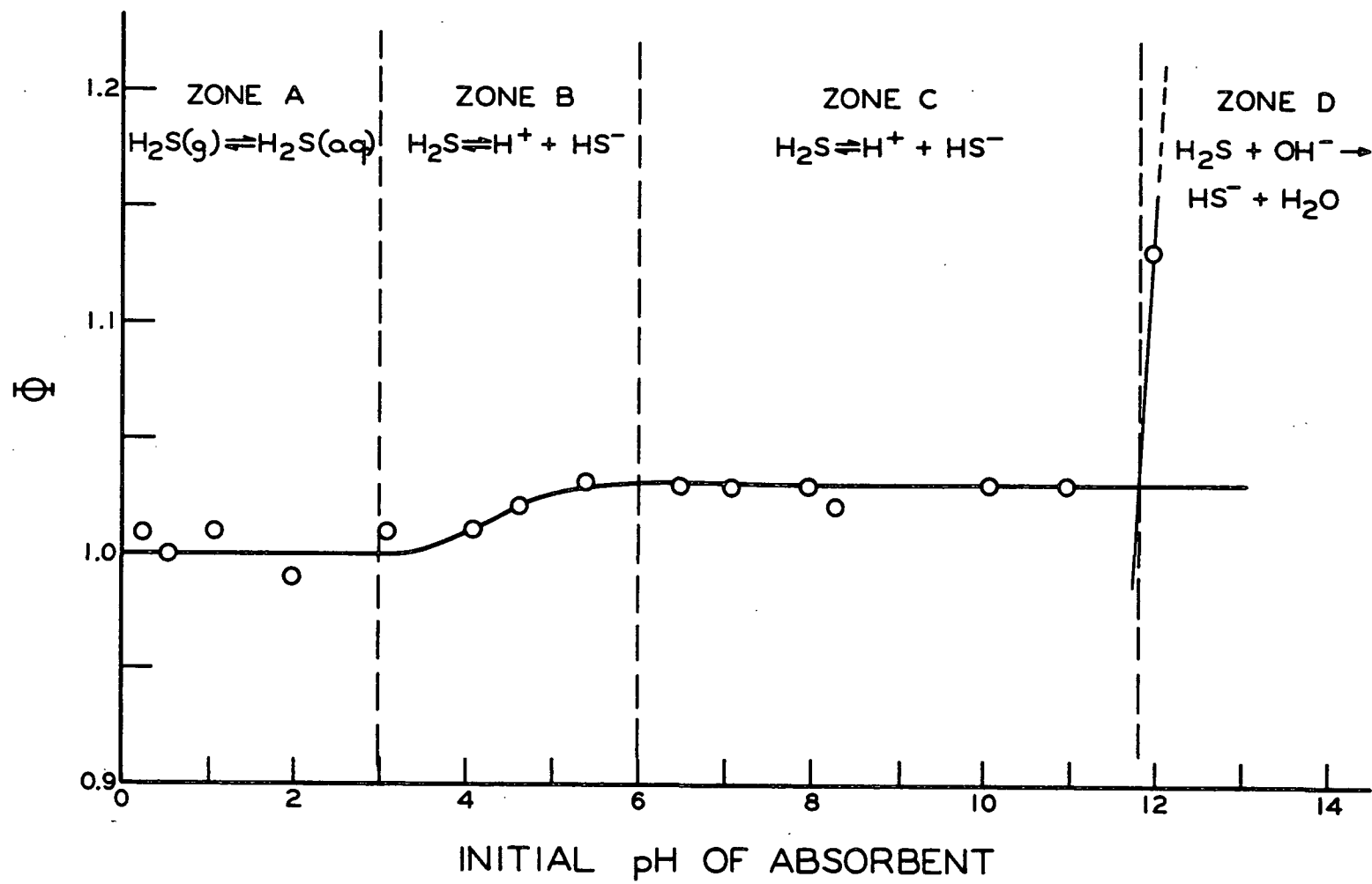


Figure 14. Effect of pH on the Rate of Absorption of Hydrogen Sulfide, pH Range 0.3-12

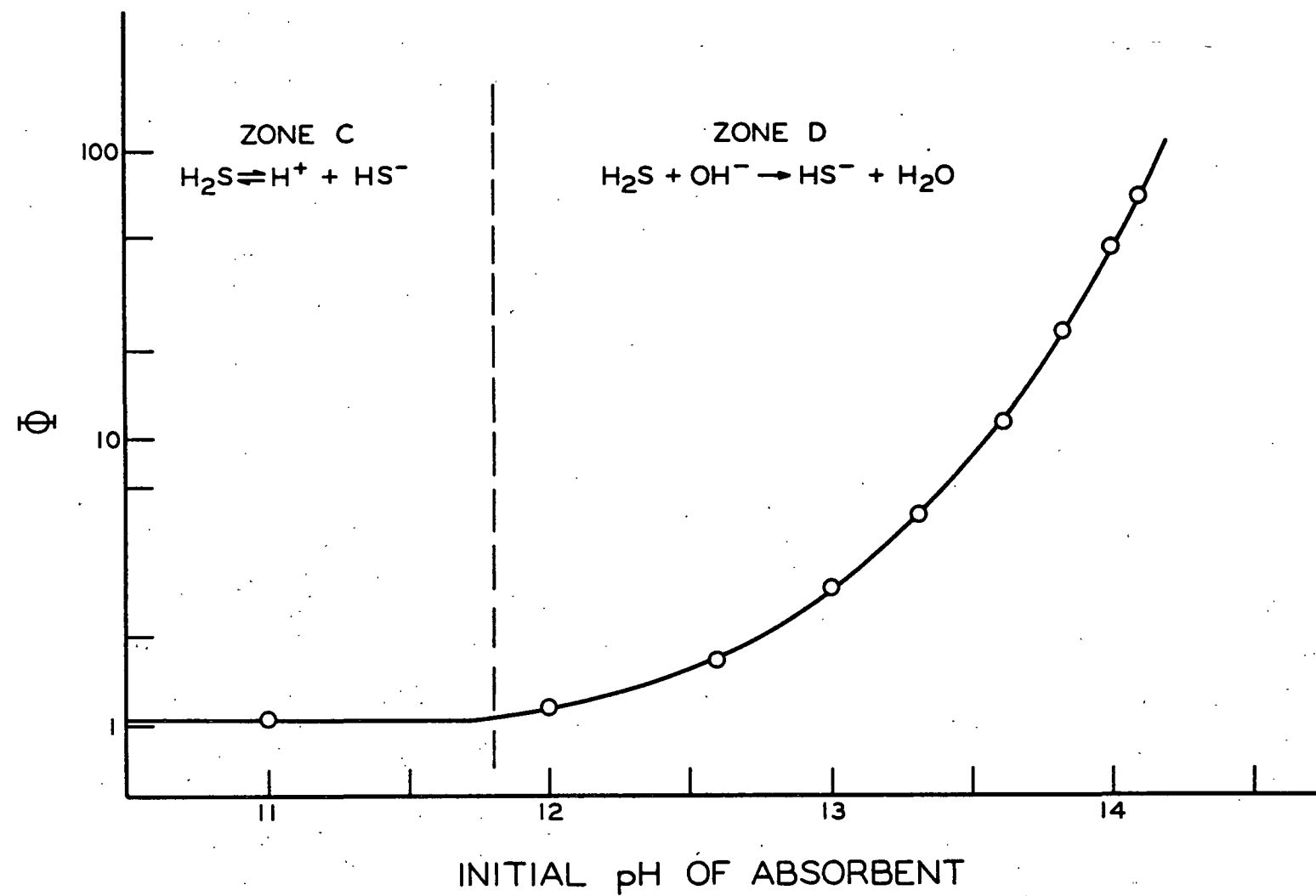


Figure 15. Effect of pH on the Rate of Absorption of Hydrogen Sulfide, pH Range 11-14.1

In Zone A, ϕ has a value of 1.0. This means that no chemical reaction is affecting absorption. Some ionization of the hydrogen sulfide was probably occurring, but the pH was such that the extent of ionization was negligible. Therefore, the only equilibrium which was considered was that between hydrogen sulfide in the gas and liquid phases.

As the pH increased above 3, some type of reaction began to affect the rate of absorption. This reaction could either have been the reversible ionization of hydrogen sulfide,



or the reaction between hydrogen sulfide and the hydroxide ion,



If Reaction (24) was the reaction which affected absorption, then the curve should have continued to rise as the pH increased. The fact that the curve leveled off at pH 6 tended to eliminate the possibility of Reaction (24) in this zone. Thus, it was the reversible ionization given by Reaction (2) which was believed to have affected absorption.

Above pH 6, the curve was level until pH 11.8 was reached. This indicated that the same reaction was affecting the absorption and that the reaction had the same rate over the entire zone. Thus, it was concluded that the ionization of hydrogen sulfide was the reaction to be considered. Also, it was concluded that the pH of the absorbent solution was such that the reverse reaction was negligible and that the reaction could be considered irreversible over the range of exposure times studied.

At pH 11.8, the rate of absorption began to increase rapidly as the initial pH of the absorbent was increased. Since Reaction (2) would have a constant effect from pH 6 and up, it was concluded that Reaction (24) began to affect absorption. Reaction (24) is a neutralization reaction and probably has a much faster rate than Reaction (2). Therefore, the neutralization reaction would overshadow the effect the ionization reaction has on absorption. There is probably a narrow transition region between Zones C and D where both Reaction (2) and Reaction (24) are important. However, this zone was not observed in this study.

Absorption Without Chemical Reaction

When hydrogen sulfide was absorbed by solutions whose initial pH was below 3, the rate of absorption could be predicted by the penetration theory solution for absorption without chemical reaction. This means that in acidic solutions, the equilibrium of Reaction (2) was shifted far to the left. Hydrogen sulfide probably ionized to some slight extent, but the reverse reaction proceeded so rapidly that all the hydrogen sulfide could be considered in a molecular form. This effect was expected since the ionization constant for hydrogen sulfide is small. Previous studies have shown that absorption can be predicted by Equation (44) when the initial pH of the absorbent is such that less than 2% of the gas present is in ionized form.

Absorption with Irreversible Reaction

As stated earlier, when hydrogen sulfide was absorbed by a solution whose initial pH was between 6 and 11.8, absorption was probably accompanied by an irreversible reaction. This reaction was believed to be the ionization of hydrogen sulfide given by Reaction (2) with the equilibrium shifted so far to the right that the reverse reaction was negligible. If this was so, then the absorption should

be predicted by the penetration theory solution of absorption accompanied by a first-order irreversible reaction. The function Φ for this case is given by

$$\Phi = 1/2[\sqrt{\pi/k_1 t_e} (1/2 + k_1 t_e) \text{erf}\sqrt{k_1 t_e} + \exp(-k_1 t_e)] \quad (48)$$

where k_1 is the first-order rate constant and t_e is the exposure time.

The value of the first-order rate constant, k_1 , was determined for each run in which the initial pH was between 7.0 and 11.5 using Equation (48). The results are shown in Table IX.

TABLE IX

FIRST-ORDER RATE CONSTANT FROM ABSORPTION DATA

Initial pH	Φ	Exposure Time, sec.	Rate Constant, sec. ⁻¹
7.1	1.035	0.0338	3.17
7.1	1.020	0.0306	1.98
7.1	1.025	0.0268	2.87
8.0	1.030	0.0343	2.68
8.0	1.020	0.0299	2.04
8.0	1.040	0.0265	4.61
8.3	1.010	0.0349	0.89
8.3	1.030	0.0302	3.05
8.3	1.030	0.0265	3.47
10.1	1.030	0.0308	2.99
10.1	1.025	0.0272	2.83
10.1	1.030	0.0238	3.87
11.0	1.030	0.0343	2.68
11.0	1.025	0.0304	2.53
11.0	1.040	0.0264	4.63

The average of all the statistically significant values gave a value of 3.1 sec.⁻¹ for the first-order rate constant. Although there was considerable scatter in the data, there appeared to be a slight decrease in the calculated rate constant with increasing exposure times. Statistical analysis showed that the trend was

significant. The data were then fitted to a line by the method of least squares and extrapolated to zero exposure time. This extrapolation gave a value of 8.4 sec.⁻¹ for the first-order rate constant.

Thus, evidence showed that there was a possibility that the liquid near the surface of the jet was approaching a state of equilibrium. Because of the scatter in the data, it was not possible at this time to say which value was the better estimate of the first-order rate constant. However, evidence discussed in the next section supports the idea that the surface did approach equilibrium.

Absorption with Reversible Reaction

In the pH range 3-6, it was shown that the reversible ionization of hydrogen sulfide given by Reaction (2) affected the rate of absorption. This is the case of absorption accompanied by a first-order forward, second-order reverse reaction. The set of differential equations describing this condition is as follows:

$$\partial C_A / \partial t = D_A \partial^2 C_A / \partial x^2 - k_1 C_A + k_2 C_B C_C \quad (67),$$

$$\partial C_B / \partial t = D_B \partial^2 C_B / \partial x^2 + k_1 C_A - k_2 C_B C_C \quad (68),$$

$$\partial C_C / \partial t = D_C \partial^2 C_C / \partial x^2 + k_1 C_A - k_2 C_B C_C \quad (69).$$

The subscripts A, B, and C refer to the molecular hydrogen sulfide, the hydrogen ion, and the bisulfide ion, respectively. The initial and boundary conditions are

$$x = 0, \quad t \geq 0; \quad C_A = C_{A,e}, \quad \partial C_B / \partial x = \partial C_C / \partial x = 0 \quad (70),$$

$$x > 0, \quad t = 0; \quad C_A = 0, \quad C_B = C_{B,0}, \quad C_C = C_{C,0} \quad (71),$$

$$\text{and} \quad x = \infty, \quad t > 0; \quad C_A = 0, \quad C_B = C_{B,0}, \quad C_C = C_{C,0} \quad (72).$$

No analytical solution exists for this set of equations and boundary conditions. Therefore, a numerical integration technique, described in Appendix I, was carried out for the specific conditions of the hydrogen sulfide-water system at 25°C. The theoretical values of Φ were calculated using 3.1 sec.^{-1} and 8.4 sec.^{-1} for the first-order rate constants. The rate constants for the reverse reaction, k_2 , were calculated from $k_2 = k_1/K$. The values used in conjunction with the forward rate constants were $2.9 \times 10^7 \text{ liters/mole sec.}$ and $7.3 \times 10^7 \text{ liters/mole sec.}$, respectively. The experimental Φ value at each pH was taken from Fig. 14. The values for the theoretical Φ_1 were those calculated using 3.1 sec.^{-1} as k_1 . The theoretical Φ_2 values were calculated using 8.4 sec.^{-1} as k_1 . The results are shown in Table X. All the Φ values were those at an exposure time of 0.03 sec.

TABLE X
COMPARISON OF EXPERIMENTAL AND THEORETICAL RATES OF
ABSORPTION FOR A REVERSIBLE REACTION

Initial pH	Experimental Φ	Theoretical Φ_1	Theoretical Φ_2
2.0	1.000	1.000	1.000
3.0	1.000	1.001	1.001
4.0	1.008	1.007	1.011
5.0	1.025	1.015	1.024
6.0	1.030	1.017	1.029
7.0	1.030	1.017	1.029

From Table X it can be seen that the theoretical values of Φ agree with the experimental values much more closely when 8.4 sec.^{-1} was used for k_1 than when 3.1 sec.^{-1} was used. It was also noted that values for the bisulfide ion concentration generated by the numerical analysis program for the liquid near the liquid-gas interface tended to approach a constant value after about 0.01 sec. exposure.

Therefore, it was concluded that the liquid near the interface was approaching a state of chemical equilibrium and that 8.4 sec.^{-1} was the better estimate of the first-order rate constant.

Absorption with "Infinitely Fast" Reaction

As the initial pH of the absorbent was increased above 11.8, the rate of absorption increased rapidly. The reason for this sudden increase was that there was a change in the rate-controlling reaction. As was stated earlier, below pH 11.8 the ionization of hydrogen sulfide is the reaction which affects the absorption. Above 11.8, the reaction between hydrogen sulfide and the hydroxide ions becomes important.

Earlier studies (18,19,26) have shown that when hydroxide ions react with an acidic gas which is being absorbed, the reaction can be considered as having an "infinitely fast" rate. The penetration theory solution for this case is given by

$$\Phi = 1/\text{erf}(\alpha/\sqrt{D_A}) \quad (50)$$

where α is implicitly defined by

$$nC_{A,e}\sqrt{D_A} \exp(-\alpha^2/\sqrt{D_A})\text{erfc}(\alpha/\sqrt{D_A}) = C_{B,0}\sqrt{D_B} \exp(-\alpha^2/\sqrt{D_B})\text{erf}(\alpha/\sqrt{D_A}) \quad (52).$$

Nijssing, et al. (19) showed that when $(C_{B,0}/C_{A,e})$ is large, the penetration theory solution can be approximated by

$$\Phi = \sqrt{D_A/D_B} + \sqrt{D_B/D_A} (C_{B,0}/nC_{A,e}) \quad (73)$$

where n is the number of moles of B consumed per mole of A. The approximation given by Equation (73) deviates from the true solution by about 2% when the second term is equal to 4 and becomes a better approximation as the second term becomes larger.

The data from this study were put in the form of Equation (73), and the results are shown in Fig. 16. The theoretical line given by Equation (73) was then calculated using $5.26 \times 10^{-5} \text{ cm.}^2/\text{sec.}^*$ as \underline{D}_B at infinite dilution, assuming that $(\underline{D}_B \mu)$ was a constant and that one mole of hydrogen sulfide would consume one mole of hydroxide ions ($\underline{n} = 1$). This line is shown by the dashed line in Fig. 16.

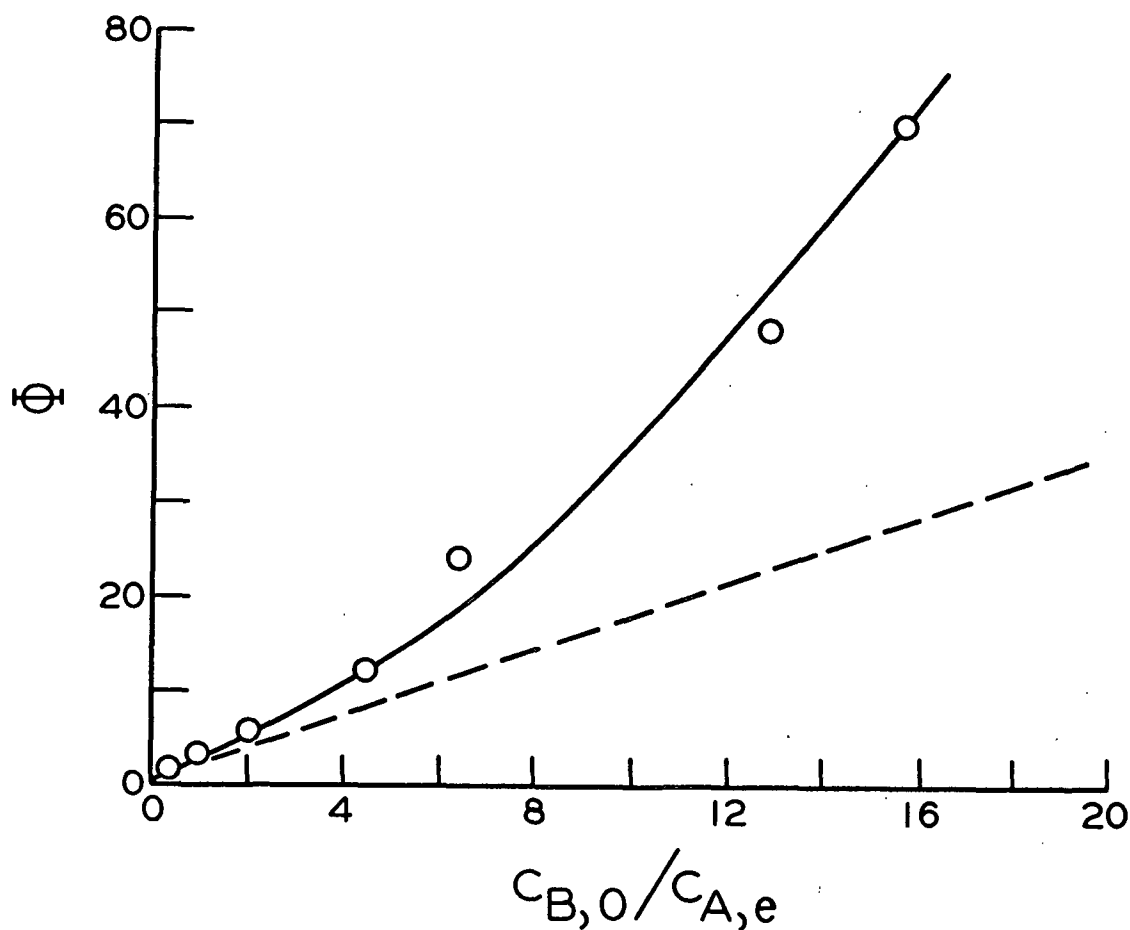


Figure 16. Effect of Hydroxide Ion on the Rate of Absorption

Thus, it appears that the experimental data and the penetration theory did not agree. The experimental data were believed to be valid for a number of reasons. First, the laminar liquid jet has previously been shown to give results

*Calculated from conductivity data (52) by $\underline{D}_B = (RT/zF^2)\lambda^0$.

which agree with the penetration theory (18,31). Second, the apparatus and techniques used in this study gave reproducible results, and when used with another system agreed with previous work (18) to within $\pm 1\%$. Third, three different techniques were used to determine the sulfide pickup by the absorbent solutions. An iodimetric technique was used to determine the final sulfide content of the two solutions of low hydroxide ion concentration. A hypochlorite-iodometric technique was used for one set of runs, and a silver nitrate technique was used to analyze the four strongest hydroxide absorbents.

Reasons for Disagreement with Theory

The first possibility for the source of difference between the experimental data and the theory was the values used for the equilibrium solubility and diffusion coefficient. However, a comparison of Equation (73) and the method for calculating the experimental value of ϕ shows that if the first term in Equation (73) is neglected, both ϕ values are inversely proportional to the equilibrium solubility and square root of the diffusion coefficient. Thus, any value, within reason, could be chosen for \underline{D}_A and $\underline{C}_{A,e}$, and the penetration theory solution and the experimental data should agree.

An examination of Equation (73) showed that the only unknown quantities which could make the experimental data agree with the theory were the factors \underline{n} and \underline{D}_B . The value of \underline{n} which would make the theory and data agree was then calculated. The values were found to decrease from 1.0 to 0.4 as the hydroxide ion concentration increased. A value of 0.4 for \underline{n} meant that each mole of hydroxide ions would have to react with 2.5 moles of hydrogen sulfide. This seemed illogical from a stoichiometric standpoint unless there was a reaction between hydrogen sulfide and bisulfide ions. While the latter reaction is possible, it has never been observed and was discounted. Thus, it was concluded that the estimate of diffusion coefficient of the hydroxide ions, \underline{D}_B , was in error.

Equations (50) and (52) were then used to calculate the values of $\frac{D}{B}$ which would make the penetration theory agree with the data. The results are shown in Table XI and Fig. 17 as a function of initial hydroxide concentration. As was seen in Fig. 17, the value for the diffusion coefficient of the hydroxide ion at infinite dilution was about 9.0×10^{-5} cm.²/sec. There was also a noticeable break in the curve at a hydroxide concentration of 0.3 mole/liter. The break point in the curve could be merely coincidental, but it occurs at the same concentration where Fary (42) first observed ion-pair formation in the sodium hydroxide-water system.

TABLE XI

HYDROXIDE ION DIFFUSION COEFFICIENT AT 25°C.

Initial Hydroxide Ion Concentration, moles/liter	Diffusion Coefficient, cm. ² /sec. x 10 ⁵
0.0421	8.9
0.106	9.3
0.206	9.5
0.419	10.1
0.657	16.4
1.061	21.4
1.231	28.9

The diffusion coefficients of the hydroxide ion seem abnormally large when compared with the diffusion coefficients of other similar-size ions. The large values could be due to the counterdiffusion of two anions. If one neglects the formation of the sulfide (S⁻²) ion, then a typical set of concentration gradients for the absorption of hydrogen sulfide are shown in Fig. 18. Thus, there would be a net flux of bisulfide ions in one direction and of hydroxide ions in the other.

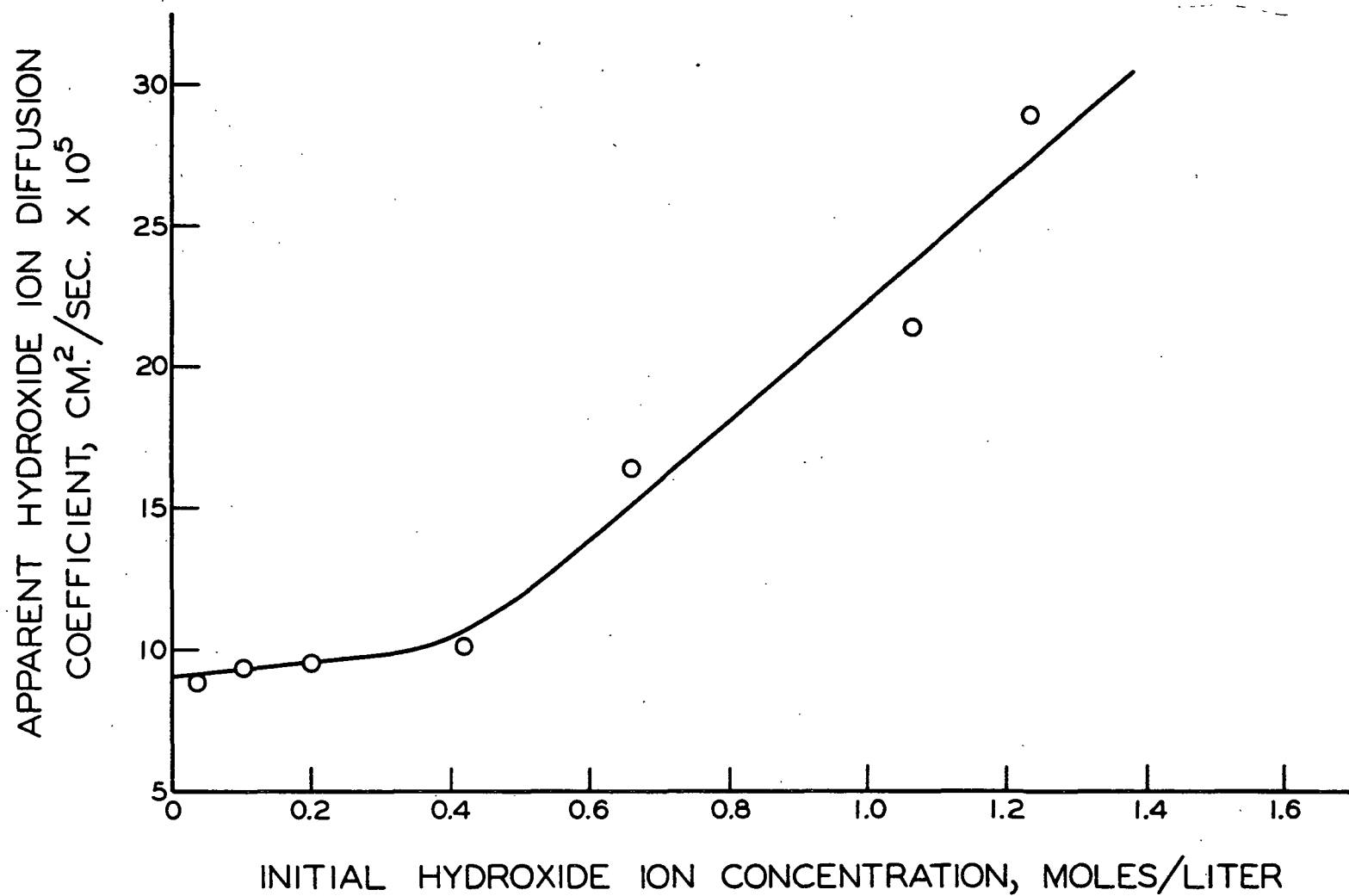


Figure 17. Effect of Initial Hydroxide Concentration on Apparent Diffusion Coefficient of the Hydroxide Ion

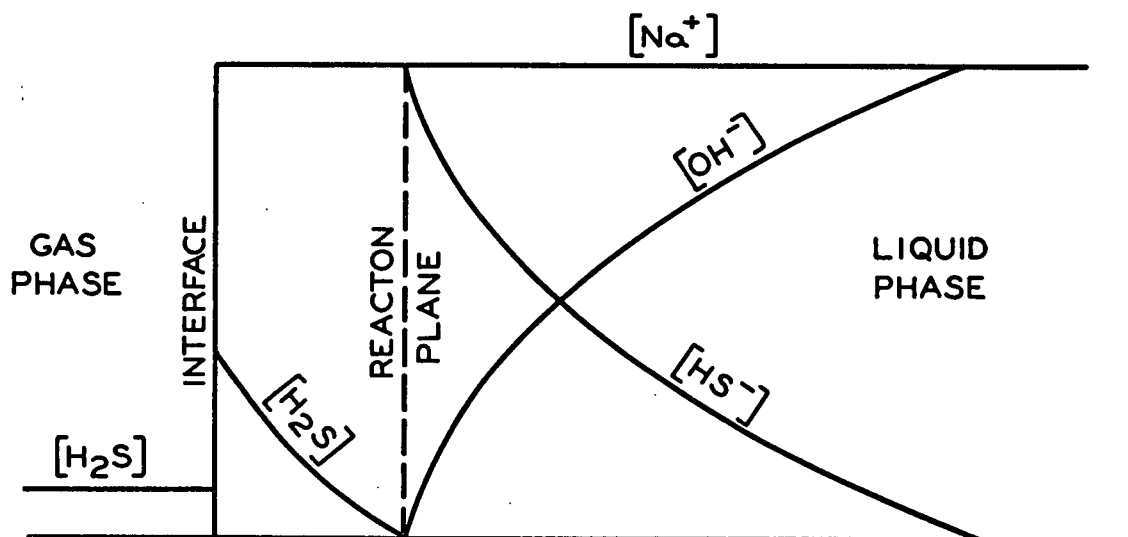


Figure 18. A Typical Concentration Profile for the Absorption of Hydrogen Sulfide by Hydroxide Solutions

It has been shown (43) that the addition of a neutral salt with an ion in common with the diffusing species will speed up the rate of transport. This is illustrated by the work of McBain and Dawson (41) who studied the diffusion of hydrochloric acid through, against, and with potassium chloride. Their results are shown in Table XII.

TABLE XII

DIFFUSION OF 0.1N HYDROCHLORIC ACID THROUGH, WITH, AND AGAINST 0.01N POTASSIUM CHLORIDE AT 25°C.

Diffusion Coefficient of, cm. ² /sec. x 10 ⁵	H ⁺	K ⁺	Cl ⁻
Through	4.62	(-1.17)	3.04
With	3.67	1.11	2.27
Against	4.40	2.51	(-1.17)

As a basis for comparison, the diffusion coefficient of 0.1N hydrochloric acid is 2.71×10^{-5} cm.²/sec. (53), and of 0.1N potassium chloride is 1.79×10^{-5} cm.²/sec. (54).

To date, no transport mechanism has been proposed which can be used to explain the increased diffusion coefficient. In fact, no one has done very much work in this area. The effect of the concentrations of the various species is unknown. Thus, there is evidence to show that such large values are possible. However, much future work needs to be done in this area before any definite conclusions can be drawn.

Comparison with Previous Work

As was stated earlier, Astarita and Gioia (26) determined the rate of absorption of hydrogen sulfide by sodium hydroxide solution using a wetted-wall column. Using a value of 3.41×10^{-5} cm.²/sec. as the diffusion coefficient of the hydroxide ion at infinite dilution and assuming n equal to one, they got good agreement between their data and the penetration theory solution for absorption accompanied by an "infinitely fast" reaction. This did not agree with the results of this study as was shown in Fig. 16.

There are a number of reasons why the data from the two studies do not agree. The previous workers observed ripples in their column. This was taken as evidence that surface renewal was taking place. To correct for this surface renewal they determined the rate of absorption of hydrogen sulfide by water and then determined the function Φ by dividing the rate of absorption by hydroxide solutions by the rate of absorption by water at the same flow rate. This can be shown to be valid (55) provided the rates of surface renewal are the same in both cases. However, because of increasing density and viscosity with increasing hydroxide concentrations, the rate of surface renewal is likely to decrease. This would tend to decrease the function Φ .

Also, it appears from a schematic diagram of their apparatus that they did not use degassed water. The dissolved gases could desorb into the absorption

chamber and introduce a gas-film resistance. Their method of determining rates of absorption would also enhance the buildup of this gas-film resistance. They had no outlet for the gas stream into their absorption chamber and determined the rate of absorption by measuring the flow rate of gas required to keep a constant pressure in the chamber. This would allow the buildup of a stagnant film which would tend to decrease the experimental determination of the function Φ .

The factors mentioned above were probably responsible for part of the difference observed between the previous work and this study. However, it is believed that there is a basic difference between the data collected from a laminar jet and a wetted-wall column. Both the laminar jet (18,19) and the wetted-wall column (56) have been shown to conform to the requirements of the penetration theory when a gas is absorbed under conditions of physical absorption. However, no comparison has been made of the two techniques under conditions of absorption accompanied by an "infinitely fast" reaction.

There are two other studies which support the idea that there is a basic difference between the laminar jet and the wetted-wall column. Nijsing, et al. (19) studied the rate of absorption of carbon dioxide by sodium hydroxide and potassium hydroxide solutions with a wetted-wall column. Using a value of 2.8×10^{-5} cm.²/sec. as the hydroxide ion diffusion coefficient and assuming that the reaction stoichiometry was given by



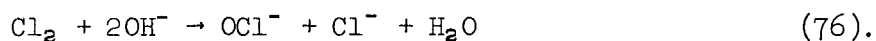
they found very good agreement between the experimental data and the penetration theory solution for absorption accompanied by an "infinitely fast" reaction given by Equation (73).

In part of his work, Spalding (18) determined the rate of absorption of chlorine into sodium hydroxide solutions. He used the diffusion coefficient of sodium hydroxide for $\underline{D_B}$ and assumed that the reaction stoichiometry was given by



Using these assumptions, he got good agreement between his data and the penetration theory solution for absorption with an "infinitely fast" reaction.

Since the ionization constant of hypochlorous acid is several orders of magnitude larger than the second ionization constant of carbonic acid (10^{-7} to 10^{-11}), it seemed illogical that carbon dioxide should consume two moles of hydroxide ions per mole while chlorine only appeared to consume one. Spalding's (18) data were then recalculated using the value of the diffusion coefficient of the hydroxide ion determined in this study ($9.0 \times 10^{-5} \text{ cm}^2/\text{sec.}$ at infinite dilution) and assuming that the reaction stoichiometry was given by



The results are shown in Fig. 19.

The agreement between the penetration theory solution given by Equation (73) and the experimental data was well within the experimental limits of accuracy. The leveling out of the experimental curve can be explained on the basis of a change in the type of reaction. It has been shown (19) that for a given reaction rate, the absorption will change from absorption accompanied by an "infinitely fast" reaction to absorption accompanied by a pseudo first-order reaction as the reactant concentration in the absorbent builds up. Therefore, the rate of absorption will tend to level out as the initial reactant concentration is increased.

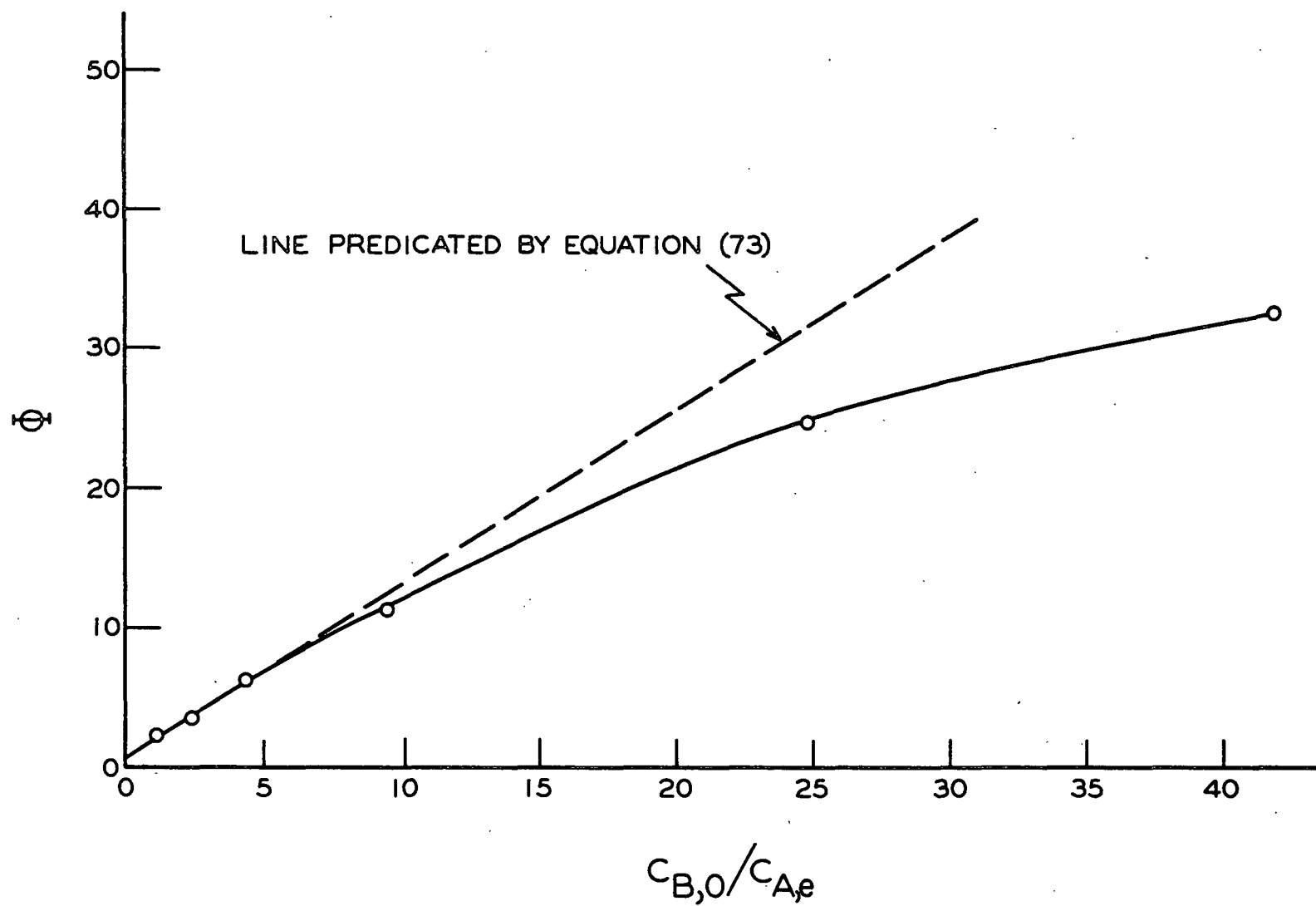


Figure 19. Absorption of Chlorine Gas into Sodium Hydroxide Solutions (18).

The reason why both sets of data analysis for the chlorine system appear to fit the theory is that, when \underline{n} was equal to 1, $\underline{D_B}$ was equal to $2.13 \times 10^{-5} \text{ cm.}^2/\text{sec.}$ and when \underline{n} was 2, $\underline{D_B}$ was equal to $9.0 \times 10^{-5} \text{ cm.}^2/\text{sec.}$ Since the square root of 9.0 is almost exactly equal to twice the square root of 2.13, one would essentially be multiplying both the numerator and denominator of the second term in Equation (73) by 2 when one substitutes 2 and 9.0×10^{-5} for Spalding's values of \underline{n} and $\underline{D_B}$, respectively.

While an argument can be raised in favor of \underline{n} being either 1 or 2, it was believed that the more logical choice for the stoichiometric coefficient is 2. This belief is based upon a comparison of the chlorine system with the carbon dioxide system mentioned earlier. The absorption of hydrogen sulfide by basic solutions supports this belief. Since each mole of hydrogen sulfide will consume one mole of hydroxide ions, each mole of hypochlorous acid should consume one mole of hydroxide ions because the first ionization constant of hydrogen sulfide is of the same order of magnitude as the ionization constant of hypochlorous acid (10^{-7}). Therefore, each mole of chlorine should consume two moles of hydroxide ions.

Thus, a value of approximately $3.0 \times 10^{-5} \text{ cm.}^2/\text{sec.}$ for the diffusion coefficient of the hydroxide ion will make the experimental data and the penetration theory agree for two studies in which the rates of absorption were determined from a wetted-wall column. Likewise, a value of $9.0 \times 10^{-5} \text{ cm.}^2/\text{sec.}$ for the diffusion coefficient of the hydroxide ion will make the experimental data and the penetration theory agree for two studies in which the rates of absorption were determined from a laminar liquid jet.

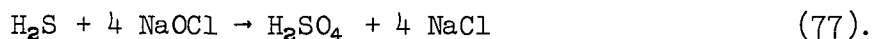
EFFECT OF OXIDIZING AGENTS

In studying the effect of the oxidizing agents on the rate of absorption of hydrogen sulfide, a total of 46 runs were made using sodium hypochlorite as the oxidizing agent. Usually three runs at different exposure times were made for each set of conditions. However, ten runs were made for the 0.1N sodium hypochlorite at pH 10.5 and six runs were made at a pH of 13.7 (0.5N sodium hydroxide). Also, six runs were made using sodium hypobromite as the oxidizing agent - three at a pH of 10.7 and three at a pH of 13.7. A summary of the runs is presented in Appendix VIII.

Summary of Results

For each set of runs at a given pH and oxidant concentration, the rate of absorption was plotted against the inverse of the square root of the exposure time and the rate of absorption at an exposure time of 0.03 second was determined by interpolation.

In calculating the experimental rates of absorption, the quantities actually determined were the initial and final hypohalite concentrations. The amount of hypochlorite consumed in passing through the jet was assumed to have reacted with hydrogen sulfide by the following stoichiometry:



Equation (56) was used to calculate the equilibrium solubility of hydrogen sulfide in the absorbents. The concentration of the various ionic species was taken from Table XVII in Appendix III. The diffusion coefficient in each absorbent was calculated by assuming that (D_u) was a constant and that the diffusion coefficient of hydrogen sulfide in water was $1.84 \times 10^{-5} \text{ cm}^2/\text{sec}$. The rate of absorption without chemical reaction was then calculated from Equation (44).

The function Φ was calculated by dividing the experimental rate of absorption by the rate of absorption without chemical reaction. The results of these calculations are shown as a function of pH in Table XIII and Fig. 20.

TABLE XIII
EFFECT OF OXIDIZING AGENT ON THE RATE OF ABSORPTION
AT 0.03 SECOND EXPOSURE TIME

Initial pH	Rate of Absorption With Chemical Reaction, g./cm. ² sec. x 10 ⁵	Rate of Absorption Without Chemical Reaction, g./cm. ² sec. x 10 ⁵	Φ
7.1	23.8	9.48	2.51
8.1	24.3	9.48	2.56
9.5	22.8	9.48	2.42
10.5	24.1	9.48	2.55
11.8	27.4	9.48	2.90
12.3	28.5	9.37	3.04
12.8	43.4	9.18	4.73
13.3 (0.2N NaOH)	100.5	8.86	11.34
13.7 (0.5N NaOH)	229.0	8.07	28.4
14.0 (1.0N NaOH)	371.0	6.84	54.2

It appeared that there were three regions in Fig. 20. The first was the level portion of the curve which extended from pH 7 to pH 11.8 (Zone A). From these data alone; it was impossible to predict exactly what type of oxidation reaction was affecting absorption. However, the data showed that the reaction (or reactions) had the same effect over this pH range. In this pH range, it had been shown that the ionization of hydrogen sulfide affected absorption. However, its effect was negligible in comparison with the effect of the oxidation reaction. Therefore, the ionization reaction was ignored in the discussion of these results.

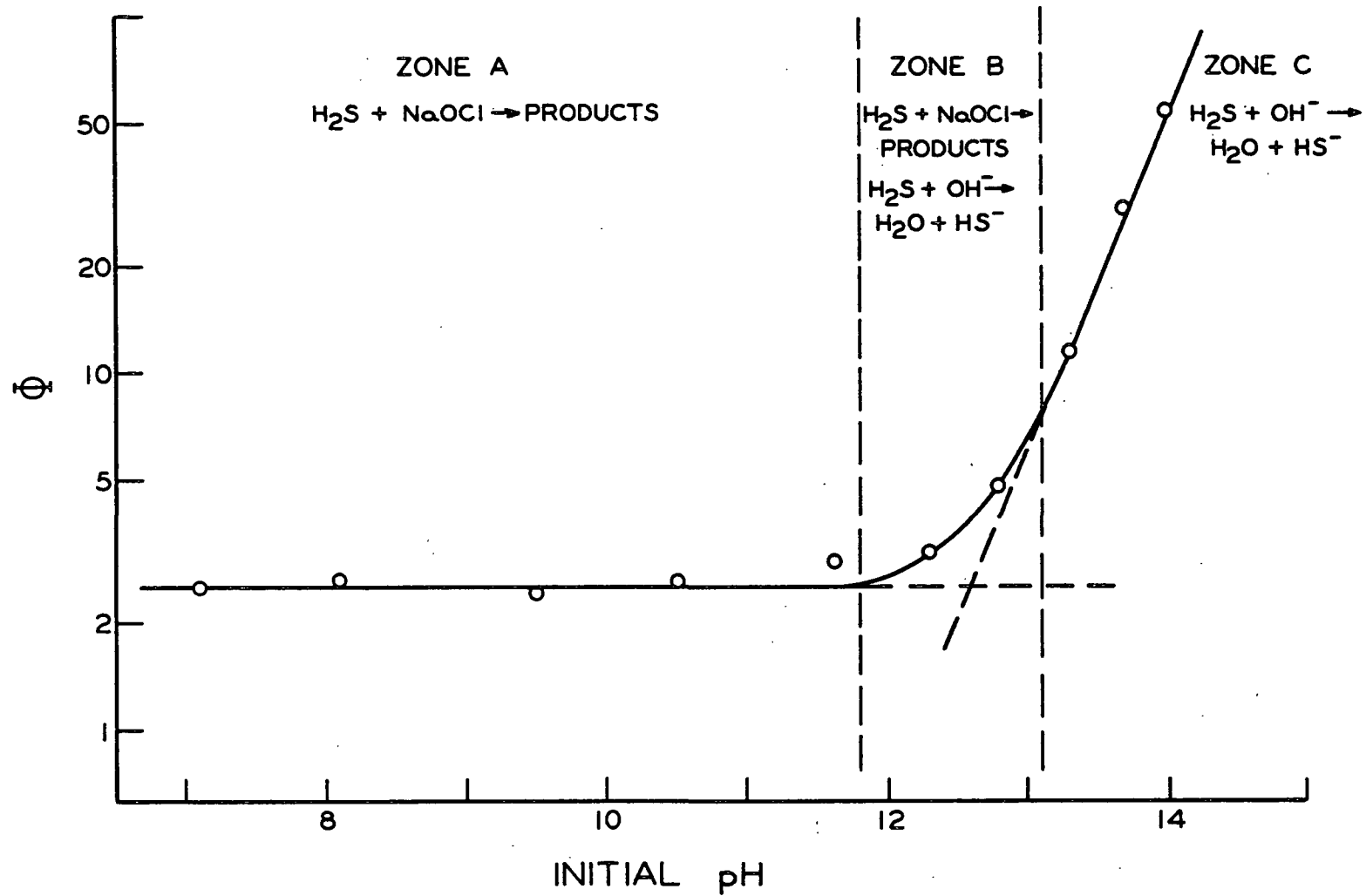


Figure 20. Effect of Oxidizing Agent on the Rate of Absorption at 0.03 Second Exposure Time

In Zone C, above pH 13.1, it appeared that another reaction became predominant. It had already been shown that this was the region where the reaction between hydrogen sulfide and the hydroxide ion became an important consideration in gas absorption. Thus, it was concluded that this was the predominant reaction which affected absorption in this zone.

In Zone B, from pH 11.8 to 13.1, both the oxidation reaction and the neutralization reaction appeared to affect absorption.

The equations of the reactions which were believed to have affected absorption in the various zones are shown in Fig. 20.

Effect of the Oxidation Reaction Upon Absorption

From the data presented in Table XIII and Fig. 20, it was concluded that the oxidation reaction had the same effect over the pH range 7-11.8. The pH could not be extended below pH 7 because sulfur began to be formed and interfered with the operation of the absorption apparatus. Another reason why the pH could not be decreased was that when the pH of a hypochlorite solution falls below 7.5, significant quantities of both the hypochlorite anion and hypochlorous acid are present. This condition speeds up the decomposition of hypochlorites into chlorates.

In order to determine the rate of oxidation of hydrogen sulfide, ten runs were made at exposure times ranging from 0.0092 to 0.0467 sec. The absorbent was a 0.1N sodium hypochlorite solution at a pH of 10.5. Also three runs were made with 0.1N sodium hypobromite as the absorbent. The results are shown in Table XIV and Fig. 21.

The data seem to fit the penetration theory solution for absorption accompanied by a first-order irreversible reaction. Danckwerts (22) has shown that

if the product of the exposure time and the first-order rate constant ($k_1 t$) is large, the rate of absorption can be approximated by

$$N_A = C_{A,e} \sqrt{D_A k_1} \quad (78).$$

The approximation differs from the true solution by less than 2% if ($k_1 t$) is greater than 4. Equation (78) predicts a constant rate of absorption which is in agreement with the experimental data.

TABLE XIV

ABSORPTION BY 0.1N SODIUM HYPOCHLORITE AND HYPOBROMITE AT pH 10.5

Absorbent	Exposure Time	Rate of Absorption With Chemical Reaction, g./cm. ² sec. x 10 ⁵	ϕ
NaOCl	0.0092	22.80	1.33
NaOCl	0.0102	22.2	1.36
NaOCl	0.0161	22.7	1.68
NaOCl	0.0184	22.4	1.86
NaOCl	0.0214	22.0	1.97
NaOCl	0.0259	22.1	2.17
NaOCl	0.0296	22.7	2.38
NaOCl	0.0340	22.5	2.65
NaOCl	0.0413	22.3	2.76
NaOCl	0.0467	22.3	2.93
NaOBr	0.0261	19.5	1.92
NaOBr	0.0294	20.8	2.17
NaOBr	0.0336	21.8	2.44

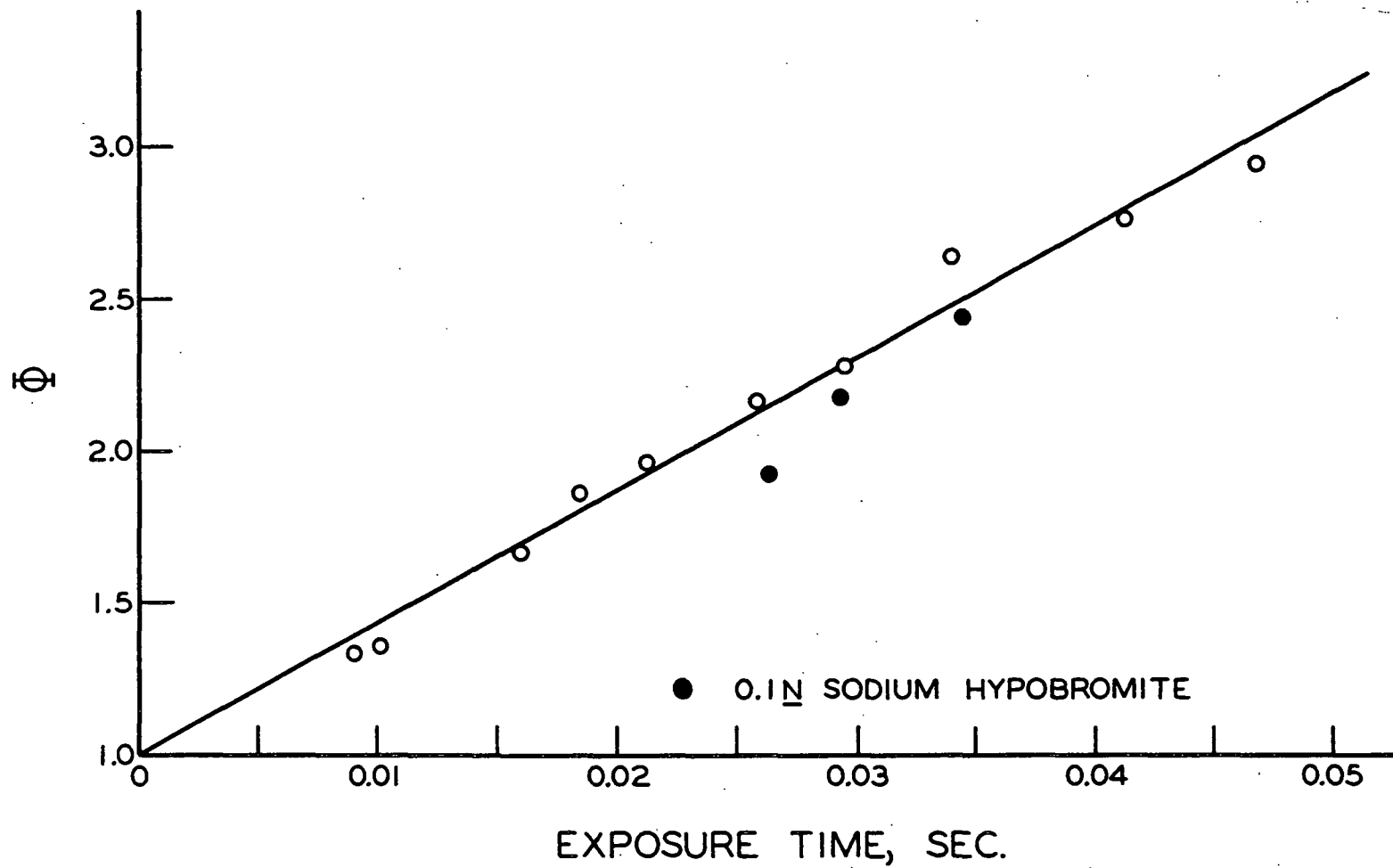


Figure 21. Absorption of Hydrogen Sulfide Into 0.1N Sodium Hypochlorite, pH - 10.5

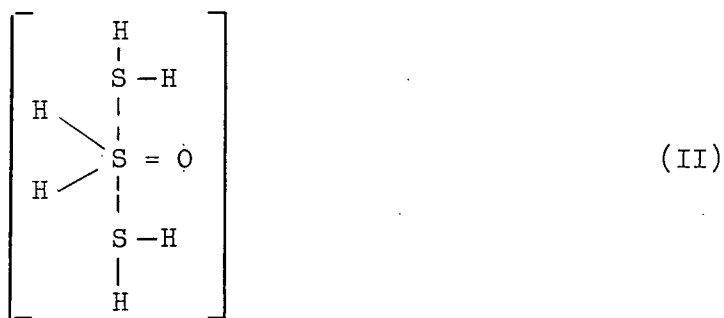
The first-order rate constant was then calculated from Equation (78) using the average rate of absorption by the hypochlorite solutions. The value of k_1 turned out to be approximately 240/sec. Since the product ($k_1 t$) was greater than 4 over most of the exposure time range, the use of Equation (78) was valid.

It seemed odd that a concentration of only 0.1N sodium hypochlorite solution should give such a large first-order rate constant. The reaction was then assumed to be "infinitely fast" and the function Φ was calculated from Equations (50) and (52), using values of $n = 1$ and $D_B = 1.6 \times 10^{-5} \text{ cm.}^2/\text{sec.}$ The theoretical value of Φ turned out to be 1.48. This is the largest value Φ can have for a given reactant concentration. The fact that the experimental values of Φ became larger than 1.48 indicated that more than one mole of hydrogen sulfide was being consumed per mole of hypochlorite.

The excessive consumption of hydrogen sulfide by sodium hypochlorite can be explained if one assumes that dihydrogen sulfoxide (DHSO) is an intermediate in the hypohalite oxidation of sulfides to sulfates.

First, one must consider the shapes of the various electron probability functions (electron clouds) in DHSO. No one has ever worked out the probable shapes of the electron clouds in DHSO, but they should be analogous to those of dimethyl sulfoxide which are discussed in detail by Burg (57). The evidence indicates that some of the electrons around the sulfur atom are shifted from the 3p orbitals which are used in compounds such as hydrogen sulfide to the 3d orbitals. It is believed that there is a sigma bond between the kernels of the sulfur atom and the oxygen atom. Pi bonds are believed to be formed between two electrons in the 2p orbitals of the oxygen atom and two electrons in the 3d orbitals of the sulfur atom. Thus, the bond is electronically a triple bond but has a bond order of about 2.

Burg (57) stated that organic sulfides form complexes with metallic ions. Since most metallic ions have electrons in 3d orbitals, it is highly probable that hydrogen sulfide could form complexes with DHSO which, if it exists, probably has electrons in 3d orbitals. Because protons have a very small steric effect, it is also possible that two or more hydrogen sulfide molecules could bond to each DHSO molecule. A possible complex is shown by



Supporting evidence for this type of complex is discussed by Tarbell (58). Organic thiols are easily oxidized to disulfides by many oxidizing agents. No one has established any mechanism for this oxidation. However, it has been suggested that the reaction may proceed through a thiosulfinate ($\text{R}-\overset{\text{O}}{\text{S}}-\text{S}-\text{R}$) intermediate. The formation of an intermediate



is also possible.

Further supporting evidence is discussed by Campaigne (59). Thiols will add readily and reversibly to the carbonyl group of aldehydes and ketones to form hemimercaptals (IV). These compounds



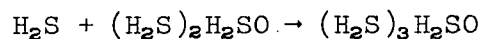
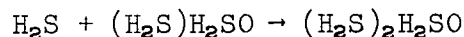
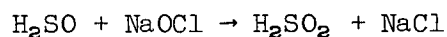
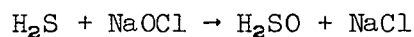
are ordinarily unstable, but can be isolated in some instances. Since sulfur can expand its octet and delocalize centers of electron density, this type of addition should be even more probable with a sulfur atom as the base of an intermediate such as (IV).

The proposed intermediate can also be used to explain why the rate of absorption by hypobromite solutions was less than by hypochlorite solutions. Sodium hypobromite will normally react faster in a given system than sodium hypochlorite. If the hypohalite ions had been the only reactants in solution, the hypobromite solutions should have had the higher rate of absorption.

If one again assumes that the initial reaction is the formation of DHSO, then a second reaction could be either further oxidation of DHSO to sulfoxylic acid or the complexing of DHSO with hydrogen sulfide. The former reaction will in effect reduce the amount of DHSO available for complexing with hydrogen sulfide, and will, therefore, reduce the effect of this reaction on absorption. Since sodium hypobromite has a faster rate of reaction than sodium hypochlorite, more of the sulfoxylic acid will be formed in the hypobromite system and less DHSO will be available for complexing, thereby reducing the rate of absorption.

Rate of Oxidation

In the preceding section, evidence was given which led to the conclusion that a number of reactions occurring in series and in parallel affected the rate of absorption of hydrogen sulfide by hypohalite solutions. The following are some of the reactions which could occur in the absorbent stream.



It should be pointed out here that the reactions given above would occur in the absorbent stream between the nozzle and the take-off tube. After the liquid enters the take-off tube, it is thoroughly mixed. Since there is an excess of hypochlorite present, the complexes would break down and all of the sulfur would eventually end up in the sulfate form.

Absorption runs were then made using three different hypochlorite concentrations to try to separate the effect of the various reactions and possibly determine the rate constants.

For each of the different hypochlorite concentrations the rate of absorption was constant over the exposure time range 0.025-0.035. Therefore, the pseudo first-order rate constant was calculated for each concentration using Equation (78). The second-order rate constant was calculated by dividing the first-order rate constant by the original hypochlorite concentration. The results are shown in Table XV.

TABLE XV

FIRST-ORDER AND SECOND-ORDER RATE CONSTANTS FROM ABSORPTION DATA

Initial Hypochlorite Concentration, moles/liter	First-Order Rate Constant, sec. ⁻¹	Second-Order Rate Constant, liters/mole sec.
0.0258	129	5000
0.0499	240	4800
0.0999	607	6070
0.1496	1810	12070

The extremely large value obtained for the 0.1496M hypochlorite solution was believed to be due to difficulties in operating the jet. Because of high concentration of hypochlorite, chlorine was formed in the bottom of the absorption apparatus. This caused sulfur to build up on the take-off tube. As a result of this, there was a noticeable amount of gas entrainment at times and some entrainment probably occurred over the entire course of the run. The same difficulty was also experienced with the 0.099M hypochlorite run but to a smaller extent.

From an analysis of the various rates of absorption and the values of the various rate constants obtained, it was not possible to separate the effect of the various reactions. There are a number of combinations of reactions and rate constants which could give the observed results.

Combined Effect of Oxidation and Neutralization Reactions

Earlier, it was concluded that in the pH range 11.8-13.1 both the oxidation reaction sequence and the neutralization reaction given by Reaction (24) affected absorption. Also, it was concluded that above pH 13.1 the neutralization reaction overshadowed the oxidation reaction which could then be neglected.

Spalding (18) hypothesized that when more than one reaction occurred in the absorbing liquid, the rate of absorption could be approximated by

$$\bar{N}_A \text{ (reactions 1 \& 2)} = \bar{N}_A \text{ (no reaction)} + \Delta\bar{N}_A \text{ (reaction 1)} + \Delta\bar{N}_A \text{ (reaction 2)} \quad (79).$$

There was a narrow pH range in his study in which two parallel reactions occurred and the one experimental datum point in this pH range fitted Equation (79).

The data from this study were then put in the form of Equation (79). The results are shown in Fig. 22. The solid horizontal line is the line which best fits the experimental data of absorption by 0.1N sodium hypochlorite solution in the pH range of 7-11. The solid slanted line is the line which best fits the experimental data of absorption by sodium hydroxide solutions (Table VIII). The dashed line was obtained by adding the two solid lines in accordance with Equation (79).

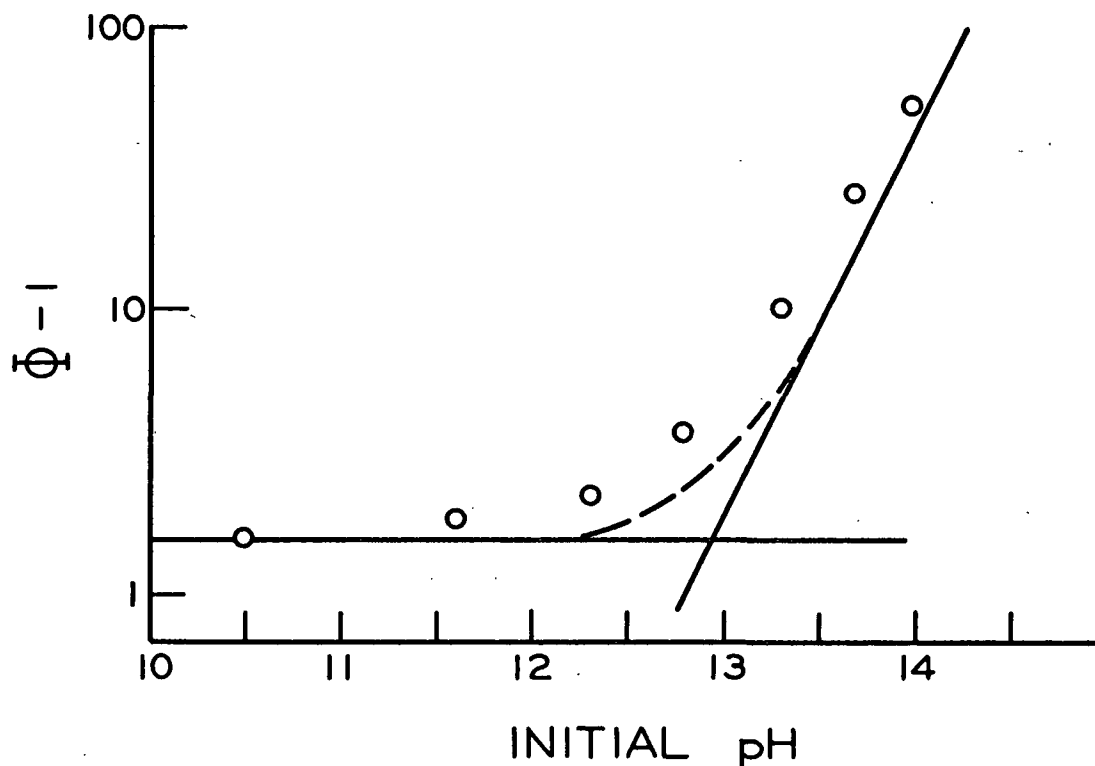
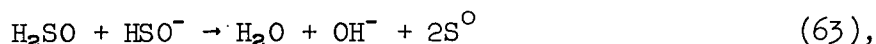


Figure 22. Effect of Simultaneous Reactions Upon Absorption

The fact that the experimental data did not lie on the predicted curve indicated that either Equation (79) was not applicable or that another reaction was affecting absorption. It was believed to be the latter case in this system. The other reaction was believed to be a hydroxide ion regeneration and subsequent reaction with hydrogen sulfide.

This hydroxide ion regeneration is again based on the DHSO intermediate. In a preceding section, it was shown that above pH 12 the reaction between hydrogen sulfide and sodium hypochlorite gives sulfur as one of the products. The sulfur was believed to be formed by the reaction between a DHSO molecule and a DHSO anion,



in which the hydroxide ion is also one of the products. There are a number of possible paths which could lead to Reaction (63). All involve at least three reactions. Therefore, the hydroxide ion would be regenerated behind the hydrogen sulfide-sodium hydroxide reaction plane and would have a large effect on the hydrogen sulfide concentration gradient.

This reaction sequence can also be used to explain the difference in the rates of absorption by hypochlorite and hypobromite solutions shown in Table XVI.

TABLE XVI

RATES OF ABSORPTION BY 0.1N HYPOCHLORITE AND 0.1N
HYPOBROMITE SOLUTIONS IN 0.5N SODIUM HYDROXIDE

Sodium Hypochlorite		Sodium Hypobromite	
Exposure Time, sec.	Rate of Absorption, g./cm. ² sec. x 10 ⁵	Exposure Time, sec.	Rate of Absorption, g./cm. ² sec. x 10 ⁵
0.0348	227	0.0351	213
0.0301	232	0.0301	213
0.0269	231	0.0264	208
0.0214	233		
0.0184	230		
0.0160	238		

It has already been shown that at a given pH level less sulfur is formed in a hypobromite system than in a hypochlorite system. Therefore, there would be less hydroxide ion regeneration behind the sodium hydroxide-hydrogen sulfide reaction plane to affect the hydrogen sulfide concentration gradient. Thus, the rate of absorption by hypobromite solutions would be less.

SUMMARY AND CONCLUSIONS

The equilibrium solubility of hydrogen sulfide in water, hydrochloric acid, sodium sulfate, and sodium chloride solutions at 25°C. and a partial pressure of 1 atm. was determined. The values obtained for the water and hydrochloric acid systems agreed with those previously reported (2,33), but the values obtained for the salt solutions did not agree with earlier determinations (34). Since two methods were used in this study, the values reported here were believed to be the most reliable.

The diffusion coefficient of hydrogen sulfide in a 0.1N hydrochloric acid solution and in sodium chloride solutions was calculated from gas absorption data. From these results it was concluded that the best estimate for the diffusion coefficient in water at 25°C. was $1.84 \times 10^{-5} \text{ cm.}^2/\text{sec.}$ The addition of a neutral salt caused a decrease in the diffusion coefficient. For the system being studied here, this decrease could be predicted by ($D\mu = \text{a constant}$) at constant temperature.

The effect of pH and ionic strength on the stoichiometry of the hypochlorite and hypobromite oxidation of hydrogen and sodium sulfide was determined. The results gave evidence which indicated that sulfur could not be an intermediate in the oxidation of sulfides to sulfates as had previously been proposed (5,10). A revised reaction sequence based on an intermediate originally suggested by Murthy and Rao (13) was then proposed. The initial step in the revised reaction sequence was the formation of dihydrogen sulfoxide (DHSO). The DHSO would then undergo further oxidation to give sulfate ions or decompose to sulfur.

The rate of absorption of hydrogen sulfide into aqueous solutions whose initial pH ranged from 0 to 14 was determined by means of a laminar liquid jet.

These rates were compared to the rates of absorption which would occur when no chemical reaction was accompanying absorption. From this comparison, it was established that hydrogen sulfide would react with hydroxide ions already present in the absorbent or will ionize into bisulfide ions and hydrogen ions. The controlling reaction depends upon the initial pH of the solution. For an exposure time of 0.03 second and at an initial pH of less than 3, neither reaction affected absorption and the rate of absorption could be predicted by the penetration theory solution for physical absorption. Between pH 3 and 11.8, the reversible ionization of hydrogen sulfide influenced the rate of absorption. Above pH 11.8, the reaction between hydrogen sulfide and the hydroxide ion controlled the rate of absorption.

The first-order rate constant for the ionization of hydrogen sulfide was determined from an analysis of the data in terms of the penetration theory. Two values for the rate constant were obtained - one by considering the reaction as irreversible in the pH range 7-11.5 and another by considering the reversible nature of the ionization reaction. It was believed that the value obtained by considering the reversible nature of the reaction was the better estimate. This value was found to be 8.4 sec.^{-1} .

Analysis of the rates of absorption into sodium hydroxide solutions indicated that the rates could be predicted by the penetration theory solution for absorption accompanied by an "infinitely fast" reaction provided an unusually large value was used for the diffusion coefficient of the hydroxide ion. This large value for the hydroxide ion diffusion coefficient was believed to be due to the fact that there was a net flux of hydroxide ions toward the liquid-gas interface and a net flux of bisulfide ions away from the interface. Analysis of data for the absorption of chlorine into sodium hydroxide solutions (18)

indicated that the hydroxide ion diffusion coefficient determined in this study was valid. Further analysis of the data mentioned above and examination of the previous data for absorption of hydrogen sulfide (26) and carbon dioxide (19) into basic solutions indicated that there was a basic difference in the data taken from a laminar liquid jet and a wetted-wall column.

The rate of absorption of hydrogen sulfide into sodium hypochlorite and hypobromite solutions whose initial pH ranged from 7 to 14 was determined and compared to the rate of absorption without accompanying chemical reaction. Hydrogen sulfide was found to react with both the hypochlorite and hydroxide ions. The reaction with the hypochlorite ions was found to be the rate-controlling reaction in the pH range 7-11.8. Above pH 13.1, the reaction with the hydroxide ions was rate-controlling. In the pH range 11.8-13.1, both reactions influenced the rate of absorption.

Analysis of the absorption data in the pH range 7-11.8 showed that the rate of absorption could be predicted by the penetration theory solution for absorption with a first-order irreversible reaction when the first-order rate constant was $(500 \frac{C_B}{C_P})\text{sec.}^{-1}$. Further analysis showed that the only way in which such a large rate constant could be attained was that more than one mole of hydrogen sulfide was being consumed per mole of hypochlorite. This could be explained on the basis of the DHSO intermediate proposed earlier. Evidence was cited which indicated that it was possible for hydrogen sulfide to form complexes with compounds such as DHSO. Thus, it was believed that hydrogen sulfide would react with the hypochlorite ions to form DHSO which would then form a sulfur-sulfur complex with additional hydrogen sulfide molecules.

Analysis of the absorption data above pH 11.8, indicated that both the oxidation and neutralization reactions proceeded simultaneously with the neutralization

reaction becoming more and more important at higher pH values. However, the observed absorption rates were higher than could be accounted for by the addition of the effects of the two reactions. The increased absorption rate was believed to be due to the production of hydroxide ions in the region between the liquid-gas interface and the hydrogen sulfide-hydroxide ion reaction plane by the decomposition of DHSO . The effect of this hydroxide ion regeneration became less pronounced as the pH increased.

Many of the conclusions drawn from the data gathered in this study are speculative. However, all of the data from both the secondary experiments and the absorption runs are consistent. The same general reaction scheme can be used to explain all of the data for systems involving hypohalite solutions. The fact that the value of the hydroxide ion diffusion coefficient determined in this study fits the data for the chlorine-sodium hydroxide system supports the conclusions drawn from data on the hydrogen sulfide-sodium hydroxide system. While much more work needs to be done before any of the conclusions can be definitely established, it was believed that on the basis of the information available, the conclusions are correct.

FUTURE WORK

It has been long recognized that much theoretical and experimental work needs to be done on the solubility and diffusivity of gases. Work also needs to be done on the diffusivity of ionic species, particularly on the effect of common ions and on the effect of the counterdiffusion of ionic species.

The results of this thesis suggest the possibility that the wetted-wall column might not meet the requirements of the penetration theory as well as had previously been assumed. A comparison of the wetted-wall column and the laminar liquid jet needs to be made for absorption accompanied by various types of chemical reactions.

Another area in which work needs to be done is that of the oxidation of sulfides. While all of the data obtained in this study are consistent with the proposed reaction sequence, much more work needs to be done before the reaction sequence can be verified or disproved. Since protons are easily lost or gained during a reaction, direct evidence of the proposed reaction sequence might be difficult to obtain. The hypohalite oxidation of organic sulfides, such as methyl mercaptan and dimethyl sulfide, might result in reactions which are easier to follow and might possibly give intermediates which could be isolated.

ACKNOWLEDGMENTS

I wish to thank Mr. S. T. Han, Dr. B. L. Browning, and Dr. H. D. Wilder, of my thesis advisory committee for their guidance during the course of this study.

The assistance of Dr. E. O. Dillingham and Mr. J. A. Carlson in running the Spinco Model-H apparatus and the ultracentrifuge is greatly appreciated.

NOMENCLATURE

\underline{a}	=	interfacial area, cm.^2
\underline{a}_i	=	activity of species \underline{i}
$\underline{A}_{m,n}$	=	concentration of hydrogen sulfide in numerical integration, moles/liter
\underline{b}	=	relative boundary layer thickness, δ/\underline{R}_O
\underline{b}_j	=	radius of ion species \underline{j}
$\underline{B}_{m,n}$	=	concentration of the bisulfide ion in numerical integration, moles/liter
\underline{C}	=	initial hydrogen ion concentration in numerical integration, moles/liter
\underline{C}_i	=	concentration of species \underline{i} , moles/liter or g./liter
\underline{D}_i	=	diffusion coefficient of species \underline{i} defined in terms of a concentration driving force, $\text{cm.}^2/\text{sec.}$
\underline{D}_O	=	diameter of nozzle opening, cm.
\underline{D}_S	=	dielectric constant of the solvent
\underline{D}	=	diameter of jet, cm.
\underline{e}_j	=	electrical charge of ion species \underline{j}
\underline{f}_i	=	fugacity of species \underline{i}
$\underline{F}(\underline{s})$	=	Laplace integral, Equation (82)
\underline{g}	=	gravitational constant, $\text{cm.}^2/\text{sec.}^2$
\underline{G}	=	Gibbs free energy, cal./mole
\underline{h}	=	intermediate jet length, cm.
\underline{h}'	=	grid spacing in space, cm.
\underline{H}	=	enthalpy, cal./mole; total jet length, cm.; Henry's law constant, atm. liters/g.
\underline{J}	=	mass flux past any plane, $\text{g./cm.}^2 \text{ sec.}$
\underline{k}	=	Boltzmann's constant
\underline{k}_1	=	rate constant for forward reaction
\underline{k}_2	=	rate constant for reverse reaction
\underline{K}	=	ionization constant in general

K_1	= first ionization constant of hydrogen sulfide, moles/liter
K_2	= second ionization constant of hydrogen sulfide, moles/liter
K_i	= Henry's law constant for species i , atm.
K_D	= constant in modified Debye-McAuley equation
L	= grid spacing in time, sec.
m	= constant in Equation (88)
M	= molecular weight, g./mole
N_A	= instantaneous rate of absorption, g./cm. ² sec.
\bar{N}_A	= average rate of absorption, g./cm. ² sec.
P_i	= partial pressure of species i
P	= total pressure, atm.
q	= jet flow rate, ml./sec.
R	= universal gas constant, cal./mole °K.
R_i	= rate of reaction, moles/liter sec.
R_o	= nozzle radius, cm.
s	= Laplace transform variable
S	= entropy, cal./mole °K.
t	= intermediate time, sec.
t_e	= total exposure time, sec.
T	= absolute temperature, °K.
\bar{U}	= mean velocity of jet, cm./sec.
\bar{U}_o	= mean velocity of jet at nozzle, cm./sec.
U_s	= velocity at jet surface, cm./sec.
U_∞	= velocity of jet core, cm./sec.
U	= velocity vector parallel to bulk flow, cm./sec.
V	= velocity vector perpendicular to bulk flow, cm./sec.
x	= direction of mass movement, cm.
X_i	= mole fraction of species i

\underline{x}	= direction in \underline{x} co-ordinate system
\underline{y}	= direction perpendicular to mass movement, cm.
α	= relative concentration, Equation (77); constant in Equation (118)
$\bar{\alpha}$	= Laplace transform of α
β_1	= $\underline{k}_1, \underline{K}$ in numerical integration
β_2	= $\underline{k}_2, \underline{K}$ in numerical integration
$\gamma_{\underline{i}}$	= activity coefficient of species \underline{i}
δ	= boundary layer thickness, cm.
η	= viscosity relative to water
λ_1	= $\underline{D}_A \underline{K} / \underline{h}'$ in numerical integration
λ_2	= $\underline{D}_B \underline{K} / \underline{h}'$ in numerical integration
μ	= viscosity of solution, g./cm. sec.
$\mu_{\underline{i}}$	= chemical potential of species \underline{i}
ρ	= density of solution, g./cm. ³
Φ	= function defined by Equation (47)
$\underline{\ell}$	= equivalent flat plate length, cm.
$\underline{\ell}'$	= characteristic nozzle length, cm.
$\underline{\mathcal{L}}$	= Laplace transform operator
\underline{m}	= diffusion coefficient defined in terms of an activity driving force, cm. ² /sec.

Subscripts:

\underline{A}	= the gaseous solute
\underline{B}	= the reactant in solution
\underline{e}	= equilibrium at interface
\underline{i}	= species \underline{i}
\underline{j}	= species \underline{j}
\underline{m}	= the \underline{m} th position in space

n = the nth position in time
o = pure water or bulk phase
s = salt solution

Superscripts:

o = standard value
s = solution phase
v = vapor phase
* = absorption without chemical reaction

Mathematical definitions:

$\exp \underline{z}$ = exponential of z, i.e., $e^{\underline{z}}$

$\operatorname{erf} \underline{z}$ = error function of z, i.e., $2/\sqrt{\pi} \int_0^{\underline{z}} e^{-\underline{u}^2} d\underline{u}$

$\operatorname{erfc} \underline{z} = 1 - \operatorname{erf} \underline{z}$

LITERATURE CITED

1. Higbie, R., Trans. Am. Inst. Chem. Engrs. 31:365(1935).
2. Wright, R. H., and Maass, O., Can. J. Res. 6:94-101(1932).
3. West, C. J. International critical tables. Vol. III. p. 3. New York McGraw-Hill, 1927.
4. Rossini, D. F., Wagman, D. D., Evans, W. H., Levine, S., and Jaffe, I. Selected values of chemical thermodynamic properties. Washington, D. C., U. S. Printing Office, 1952.
5. Willard, H. H., and Cake, W. E., J. Am. Chem. Soc. 43:1610-14(1921).
6. Tartar, H. V., J. Am. Chem. Soc. 35:1714-17(1913).
7. Kitchener, J. A., Bockris, J. O. M., and Liberman, A., Discn. Faraday Soc. 4:57-8(1948).
8. Pepkowitz, L. P., Anal. Chem. 20:268-70(1948).
9. Bethge, P. O., Anal. Chim. Acta 9:129-39(1953).
10. Choppin, A. R., and Faulkenberry, L. C., J. Am. Chem. Soc. 59:2203-7(1937).
11. Bendall, J. R., Mann, F. G., and Purdie, D., J. Chem. Soc. 1942:157-63.
12. Dunicz, B. L., and Rosenqvist, I., Anal. Chem. 24:404-6(1952).
13. Murthy, A. R. V., and Rao, B. S., Proc. Indian Acad. Sci. 35A:7-13(1952).
14. Afans'co, J. Phys. Chem. U.S.S.R. 22:499(1948); C.A. 42:7169(1948).
15. Kesler, R. B., Tappi 40:802-9(1957).
16. Eigen, I. M., and DeMaeyer, L., Z. Electrochem. 59:986-93; C.A. 50:4600e (1956).
17. Ertl, G., and Gerisher, H., Z. Electrochem. 65:629-33(1961); C.A. 57:649 (1963).
18. Spalding, C. W. The absorption of chlorine into aqueous media in light of the penetration theory. Doctor's Dissertation. Appleton, Wis., The Institute of Paper Chemistry, 1961. 186 p.
19. Nijssing, R. A. T. O., Hendriks, R. H., and Kramers, H., Chem. Eng. Sci. 10:88-104(1959).
20. Satterfield, C. N., Reid, R. C., and Briggs, D. R., J. Am. Chem. Soc. 76:3922-3(1954).
21. Carter, C. N. Unpublished work, 1963.

22. Danckwerts, P. V., Trans. Faraday Soc. 46:300-4(1950).
23. Danckwerts, P. V., Trans. Faraday Soc. 46:701-12(1950).
24. Olander, D. R., A.I.Ch.E. Journal 6:233-9(1960).
25. Brian, P. L. T., Hurley, J. F., and Hasseltine, E. H., A.I.Ch.E. Journal 7:226-31(1961).
26. Astarita, G., and Gioia, F., Chem. Eng. Sci. 19:963-71(1964).
27. Parkison, R. V., Tappi 39:517-19(July, 1956).
28. Beckman/Spinco Model H Electrophoresis - Diffusion Instrument Instruction Manual. p. 48-56.
29. Beckman Model E. Analytical Ultracentrifuge Instruction Manual E - IM - 3, Section 5.
30. Ratcliff, G. A., and Holdcroft, J. G., Trans. Inst. Chem. Engrs. (London) 41:315(1963).
31. Scriven, L. E., and Pigford, R. L., A.I.Ch.E. Journal 4:439-44(1958).
32. West, C. J. International critical tables. Vol. III & V. New York, McGraw-Hill, 1928.
33. Kendall, J., and Andrews, J. C., J. Am. Chem. Soc. 43:1545-60(1921).
34. West, C. J. International critical tables. Vol. III. New York, McGraw-Hill, 1928.
35. Exner, F., Pogg, Ann. 155:321(1875); Taken from Himmelblau, D. M., Chem. Rev. 64:527-50(1964).
36. Hagenbach, A., Weid, Ann. 65:673(1898); Taken from Himmelblau, D. M., Chem. Rev. 64:527-50(1964).
37. Kamiike, O., Kataoka, S., and Inaba, S., J. Chem. Soc. (Japan) 63:1007-14(1942).
38. Kincaid, J. F., Eyring, H., and Stern, A. E., Chem. Revs. 28:301-65(1941).
39. Wilke, C. R., and Chang, P., A.I.Ch.E. Journal 1:264-70(1955).
40. Othmer, D. F., and Thakar, M. S., Ind. Eng. Chem. 45:589-93(1953).
41. McBain, J. W., and Dawson, C. R., J. Am. Chem. Soc. 56:52-6(1934).
42. Fary, A. D. The diffusional properties of sodium hydroxide. Doctor's Dissertation. Appleton, Wis., The Institute of Paper Chemistry, 1966. 140 p.
43. King, C. V., and Cathcart, W. H., J. Am. Chem. Soc. 58:1639-42(1936).

44. Shanley, E. S., and Greenspan, F. P., Ind. Eng. Chem. 39:1536(1947).
45. Duke, F. R., and Haas, T. W., J. Phys. Chem. 65:304-6(1961).
46. Koubek, E., Haggett, M. L., Battaglia, C. J., Ibne-Rasa, K. M., Pyun, H. Y., and Edwards, J. O., J. Am. Chem. Soc. 85:2263-8(1963).
47. Jones, D. D. Personal communication, 1965.
48. Edwards, J. G. Inorganic reaction mechanisms. p. 88. New York, W. A. Benjamin, 1964.
49. Gould, E. S. Mechanism and structure in organic chemistry. p. 261. New York, Holt, Rinehart, and Winston, 1959.
50. Latimer, W. M. Oxidation potentials. 2d ed. p. 55. New York, Prentice Hall, 1952.
51. Barnard, D., Bateman, L., and Cunneen, J. I. Oxidation of organic sulfides. In Kharasch's Organic sulfur compounds. Vol. 1. p. 229. New York, Pergamon Press, 1961.
52. Hetland, E., J. Am. Chem. Soc. 68:2532-5(1946).
53. Robinson, R. A., and Stokes, H. H. Electrolyte solutions. p. 515. London, Butterworths, 1959.
54. Harned, H. S., and Owen, B. B. The physical chemistry of electrolyte solutions. p. 700. New York, Reinhold, 1958.
55. Portalski, S., Ind. Eng. Chem. Fundam. 3:49(1964). Quoted in Astarita, G., and Gioia, F., Chem. Eng. Sci. 19:963-71(1964).
56. Lynn, S., Straatemeier, J. R., and Kramers, H., Chem. Eng. Sci. 4:63-70 (1955).
57. Burg, A. B. The bonding characteristics of the sulfur atom. In Kharasch's Organic sulfur compounds. Vol. 1. p. 30. New York, Pergamon Press, 1961.
58. Tarbell, D. S. The mechanism of oxidation of thiols to disulfides. In Kharasch's Organic sulfur compounds. Vol. 1. p. 97. New York, Pergamon Press, 1961.
59. Campaigne, E. Addition of thiols or hydrogen sulfide to carbonyl compounds. In Kharasch's Organic sulfur compounds. Vol. 1. p. 134. New York, Pergamon Press, 1961.
60. Cranck, J. The mathematics of diffusion. London, Oxford Press, 1956.
61. Campbell, G. A., and Foster, R. M. Fourier integrals for practical applications. New York, D. Van Nostrand Company, 1948.
62. Sherwood, T. K., and Pigford, R. L. Absorption and extraction. 2d ed. New York, McGraw-Hill, 1952.

63. Hansen, M. NACA Tech. Memo. No. 585, 1930; Quoted in Schlichting, H. Boundary layer theory. p. 111. New York, McGraw-Hill, 1955.
64. Nikuradse, J. Quoted in Schlichting, p. 219.
65. Goldstein, S., Proc. Cambr. Phil. Soc. 26:Part 1(1930); Quoted in Schlichting, p. 142.
66. Peaceman, D. W. Liquid-side resistance in gas absorption with and without chemical reaction. Sc.D. Thesis in Chem. Eng., Mass. Inst. of Tech., 1951. 426 p.
67. Danckwerts, P. V., Appl. Sci. Research A3:385-90(1952).
68. Rideal, S., and Stewart, G. G., Analyst 26:141-8(1901).
69. Kolthoff, I. M., and Elving, P. J., Treatise on analytical chemistry. Part II. Vol. 7. New York, Interscience, 1961. p. 108-9.
70. Maurice, M. J., Anal. Chem. 157:89-96(1957); Anal. Abstr. 5:474(1958).
71. Bethge, P. O., Anal. Chim. Acta. 10:113-16(1954); C.A. 48:5732e(1954).
72. Borlew, P. B., and Pascoe, T. A., Paper Trade J. 122, no. 10:31-4(March 7, 1946); Paper Trade J. 123, no. 15:178-80(Oct. 10, 1946).
73. Lingane, J. J., Electroanalytical chemistry. p. 70. New York, Interscience, 1953.
74. Debye, P., and McAuley, J., Physik. Z. 26:22(1925); Quoted in Harned, H. S., and Owen, B. B. The physical chemistry of electrolytic solutions. 3rd ed. p. 80. New York, Reinhold, 1958.
75. Setchenow, M., Ann. Chim. Phys. 25:226(1892); Quoted in Harned, H. S., and Owen, B. B. The physical chemistry of electrolytic solutions. 3rd ed. p. 531. New York, Reinhold, 1958.
76. Stern, K. H., and Amis, E. S., Chem. Revs. 59:1-64(1959).
77. Pierce, W. C., and Haenisch, E. L. Quantitative analysis. 3rd ed. New York, John Wiley & Sons, 1948.

APPENDIX I

MATHEMATICAL DETAILS OF THE PENETRATION THEORY

PHYSICAL ABSORPTION

The basic differential equation describing absorption without chemical reaction has been shown to be

$$D_A \partial^2 C_A / \partial x^2 - \partial C_A / \partial t = 0 \quad (40).$$

The boundary conditions for the penetration theory are

$$x > 0, \quad t = 0; \quad C_A = C_{A,0} \quad (38),$$

$$x = \infty, \quad t \geq 0; \quad C_A = C_{A,0} \quad (37),$$

$$x = 0, \quad t > 0; \quad C_A = C_{A,e} \quad (39).$$

Equation (40) can be solved by making the following substitution:

$$\alpha = (C_A - C_{A,0}) / (C_{A,e} - C_{A,0}) \quad (80).$$

Equation (40) and the boundary conditions then become

$$D_A \partial^2 \alpha / \partial x^2 - \partial \alpha / \partial t = 0 \quad (81)$$

and

$$x = 0, \quad t > 0; \quad \alpha = 1 \quad (82),$$

$$x = \infty, \quad t \geq 0; \quad \alpha = 0 \quad (83),$$

$$x > 0, \quad t = 0; \quad \alpha = 0 \quad (84).$$

Partial differential equations such as Equation (81) are frequently encountered in heat and mass transfer problems. Solutions have been established for many initial and boundary value situations. The use of the Laplace transform

technique discussed by Cranck (60) gives a readily available solution for the boundary conditions here.

The Laplace transform of any function, \underline{u} , is given by:

$$\mathcal{L}(u) = \bar{u} = \int_0^{\infty} e^{-st} u dt = F(s) \quad (85).$$

The transforms of many functions have been tabulated (61) and therefore are not given here. The inverse Laplacian operation is defined by

$$\mathcal{L}^{-1}(\bar{u}) = u \quad (86).$$

Operating on Equation (81) gives

$$D_A d^2 \bar{\alpha} / dx^2 - s \bar{\alpha}^2 + (\alpha)_{x=0} = 0 \quad (87).$$

Using boundary condition (84), $(\alpha)_{\underline{x}=0}$ becomes equal to zero, and Equation (87) becomes

$$D_A d^2 \bar{\alpha} / dx^2 - s \bar{\alpha} = 0 \quad (88).$$

The function \underline{s} is only a function of \underline{t} ; and the function $\bar{\alpha}$ is only a function of \underline{x} and \underline{s} . Therefore, \underline{s} may be regarded as a constant in Equation (87) and the ordinary second derivative is permissible. Operating on the boundary conditions gives

$$x = 0, \quad \bar{\alpha} = 1/s \quad (89),$$

$$x = \infty, \quad \bar{\alpha} = 0 \quad (90).$$

Equation (88) may then be solved by substituting

$$\bar{\alpha} = e^{mx} \quad (91).$$

Equation (88) then becomes

$$e^{mx} (m^2 - s/D_A) = 0 \quad (92).$$

This leads to a general solution for Equation (88) of

$$\bar{\alpha} = C_1 \exp(\sqrt{s/D_A} x) + C_2 \exp(-\sqrt{s/D_A} x) \quad (93).$$

Using boundary conditions (89) and (90), the values of C_1 and C_2 are 0 and $1/s$, respectively. Thus,

$$\bar{\alpha} = 1/s \exp(-\sqrt{s/D_A} x) \quad (94).$$

Performing the inverse Laplace operation gives

$$\alpha = \text{erfc}(x/2\sqrt{D_A t}) \quad (95),$$

or

$$(C_A - C_{A,0})/(C_{A,e} - C_{A,0}) = 1 - \text{erf}(x/2\sqrt{D_A t}) \quad (96).$$

It has already been shown that the rate of absorption is equal to the rate of diffusion away from the interface.

$$N_A = -D_A (\partial C_A / \partial x)_{x=0} = -D_A (C_{A,e} - C_{A,0}) (\partial \alpha / \partial x)_{x=0} \quad (40).$$

Because

$$\partial \alpha / \partial x = \mathcal{L}^{-1}(\partial \bar{\alpha} / \partial x) \quad (97),$$

one can differentiate Equation (94) and perform the inverse Laplace operation.

This gives

$$\mathcal{L}^{-1}(\partial \bar{\alpha} / \partial x) = \partial \alpha / \partial x = -1/\sqrt{D_A \pi t} \quad (98).$$

Therefore, from Equation (40),

$$N_A = (C_{A,e} - C_{A,0}) \sqrt{D_A / \pi t} \quad (43).$$

The average rate of absorption, \bar{N}_A , is then obtained by integrating Equation (43) over the exposure time period, $\underline{t_e}$, and dividing the result by the exposure time. This gives

$$\bar{N}_A^* = 1/t_e \int_0^{t_e} N_A dt = 2(C_{A,e} - C_{A,0}) \sqrt{D_A/\pi t_e} \quad (44).$$

ABSORPTION WITH SIMULTANEOUS FIRST-ORDER IRREVERSIBLE CHEMICAL REACTION

For the case of absorption accompanied by a first-order irreversible reaction, the equation of continuity reduces to

$$D_A \partial^2 C_A / \partial x^2 - \partial C_A / \partial t = k_1 C_A \quad (99).$$

The boundary conditions are

$$x = 0, \quad t > 0; \quad C_A = C_{A,e} \quad (39),$$

$$x > 0, \quad t = 0; \quad C_A = 0 \quad (100),$$

$$x = \infty, \quad t > 0; \quad C_A = 0 \quad (101).$$

Operating on Equation (49) and making use of boundary condition (100) gives

$$D_A \partial^2 \bar{C}_A / \partial x^2 - s \bar{C}_A = k_1 \bar{C}_A \quad (102)$$

where

$$\bar{C}_A = \mathcal{L}(C_A).$$

The boundary conditions (39) and (101) become

$$x = 0; \quad \bar{C}_A = C_{A,e}/s \quad (103),$$

$$x = \infty; \quad \bar{C}_A = 0 \quad (104).$$

Rearranging Equation (102) gives

$$d^2\bar{C}_A/dx^2 - \bar{C}_A(s + k_1)/D_A = 0 \quad (105).$$

Performing a substitution similar to that used in solving Equation (87) gives the solution for Equation (105) of

$$\bar{C}_A = C_1 \exp[\sqrt{(s + k_1)/D_A} x] + C_2 \exp[-\sqrt{(s + k_1)/D_A} x] \quad (106).$$

From the boundary conditions (103) and (104),

$$C_1 = 0 \quad (107),$$

$$C_2 = C_{A,e}/s \quad (108).$$

Therefore,

$$\bar{C}_A = (C_{A,e}/s) \exp[-\sqrt{(s + k_1)/D_A} x] \quad (109).$$

Differentiating Equation (109) gives

$$d\bar{C}_A/dx = -(C_{A,e}/s) \sqrt{(s + k_1)/D_A} \exp[-\sqrt{(s + k_1)/D_A} x] \quad (110),$$

and at $x = 0$,

$$(d\bar{C}_A/dx)_{x=0} = -(C_{A,e}/\sqrt{D_A}) [1/\sqrt{s + k_1} + k_1/s\sqrt{s + k_1}] \quad (111).$$

The inverse Laplacian of Equation (111) gives

$$(dC_A/dx)_{x=0} = -(C_{A,e}/D_A) [1/\pi t \exp(-k_1 t) + k_1 \operatorname{erf} k_1 t] \quad (112).$$

The rate of absorption, then, is

$$N_A = C_{A,e} \sqrt{D_A} [\sqrt{1/\pi t} \exp(-k_1 t) + \sqrt{k_1} \operatorname{erf} \sqrt{k_1 t}] \quad (113).$$

When $\underline{k_1 t}$ is large, $\exp(-\underline{k_1 t})$ equals zero and $\text{erf}\sqrt{\underline{k_1 t}}$ equals one. Therefore,

$$N_A = C_{A,e} \sqrt{D_A k_1} \quad (78),$$

which differs from the true solution by less than 2% if $\underline{k_1 t}$ is larger than 4 (22).

The average rate of absorption over the exposure time, $\underline{t_e}$, is

$$\bar{N}_A = 1/t_e \int_0^{t_e} N_A dt = -D_A/t_e \int_0^{t_e} (\partial C_A / \partial x)_{x=0} dt \quad (114).$$

Recalling the Laplacian function

$$\mathcal{L} \int_0^t u dt = 1/sF(s) \quad (115),$$

one can combine it with the integral in Equation (111) as

$$\mathcal{L} \int_0^{t_e} (\partial C_A / \partial x)_{x=0} dt = -C_{A,e} / \sqrt{D_A} [1/s\sqrt{s + k_1} + k_1/s^2\sqrt{s + k_1}] \quad (116).$$

The inverse Laplace operation gives

$$\begin{aligned} \int_0^{t_e} (\partial C_A / \partial x)_{x=0} dt &= C_{A,e} / \sqrt{D_A} [-1/\sqrt{k_1} \cdot \text{erf}\sqrt{k_1 t_e} \\ &\quad - t_e \sqrt{k_1} \text{erf}\sqrt{k_1 t_e} + 1/2\sqrt{k_1} \text{erf}\sqrt{k_1 t_e} \\ &\quad - \sqrt{t_e/\pi} \exp(-k_1 t_e)] \end{aligned} \quad (117).$$

Substituting Equation (116) into (114) and rearranging gives

$$\bar{N}_A = C_{A,e} \sqrt{D_A/\pi t_e} \left\{ \sqrt{\pi/k_1 t_e} [1/2 + k_1 t_e] \text{erf}\sqrt{k_1 t_e} + \exp(-k_1 t_e) \right\} \quad (118).$$

The function Φ therefore is

$$\Phi = \bar{N}_A / \bar{N}_A^* = N_A / 2C_{A,e} \sqrt{D_A/\pi t_e} = 1/2 [\sqrt{\pi/k_1 t_e} (1/2 + k_1 t_e) \text{erf}\sqrt{k_1 t_e} + \exp(-k_1 t_e)] \quad (119).$$

ABSORPTION WITH SIMULTANEOUS, SECOND-ORDER, "INFINITELY FAST," IRREVERSIBLE REACTION

The solution to this problem is based upon Danckwerts' (23) treatment of the more general problem of diffusion with a moving boundary. This problem has also been solved by Sherwood and Pigford (62) and by Cranck (60). One starts by considering a gas, A, in contact with a liquid containing a reactant, B. If the reaction which takes place between A and B is second order, irreversible, and very fast compared with diffusion, there will exist a plane in the liquid where the chemical reaction takes place. At this reaction plane, the concentrations of A and B will be zero because they cannot exist together. Thus, the rate of absorption of A is controlled by the rate of diffusion of A to the reaction plane. The depth of the reaction plane within the liquid or the distance A must diffuse to reach B is in turn controlled by the rate of diffusion of B to the other side of the plane.

To simplify the derivation, a two-scale co-ordinate system was chosen. In medium A, above the reaction plane where only the gaseous solute exists, position is designated by a co-ordinate in the \underline{x}_A system. In medium B, below the reaction plane where only the reactant B exists, position is designated by a co-ordinate in the \underline{x}_B system. The surface of the liquid remains permanently at $\underline{x}_A = \underline{x}_B = 0$ so that the distance from the reaction plane to the liquid surface is the same in both co-ordinate systems: $-\underline{x}_A = \underline{x}_B$. The co-ordinate system is depicted in Fig. 23.

The equations which govern the diffusion of A and B in their respective media are as follows:

$$\partial C_A / \partial t = D_A \partial^2 C_A / \partial x^2 \quad (40),$$

$$\partial C_B / \partial t = D_B \partial^2 C_B / \partial x^2 \quad (119).$$

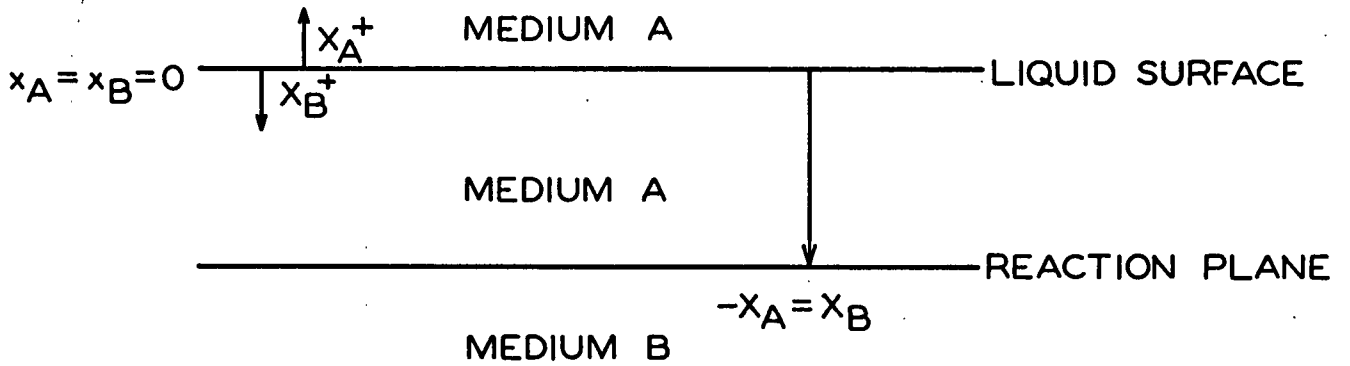


Figure 23. The Co-ordinate System

The boundary conditions for A are:

$$x_A < 0, \quad t = 0; \quad C_A = C_{A(-\infty)} \quad (120),$$

$$x_A = 0, \quad t \geq 0; \quad C_A = C_{A,e}$$

and for B are:

$$x_B < 0, \quad t = 0; \quad C_B = C_{B(-\infty)} \quad (121).$$

$$x_B = 0, \quad t > 0; \quad C_B = C_{B,0}$$

The solution for Equation (40) and boundary conditions (120) is

$$(C_{A(-\infty)} - C_A) / (C_{A(-\infty)} - C_{A,e}) = 1 - \operatorname{erf}(x_A / 2\sqrt{D_A t}) \quad (122).$$

The solution for Equation (119) and boundary conditions (121) is

$$(C_{B(\infty)} - C_B) / (C_{B(\infty)} - C_{B,0}) = 1 - \operatorname{erf}(x_B / 2\sqrt{D_A t}) \quad (123).$$

The solutions of Equations (118) and (119) are for infinite media. However, the equations can apply to regions bounded by one or two \underline{x} -planes, providing the presence of restricting planes does not alter the general shape of the concentration-distance curves. The restriction planes do affect the position of the concentration-distance curves. This is the reason for the $\underline{C}_A(-\infty)$ and $\underline{D}_{B,0}$ boundary values. These values are negative because they lie outside the respective media and, as such, they have no physical meaning. Figure 24 shows this situation. $\underline{C}_A(-\infty)$ and $\underline{C}_{B,0}$ are the hypothetical boundary value concentrations which must be chosen so that $\underline{C}_A = \underline{C}_B = 0$ at the reaction plane at all times.

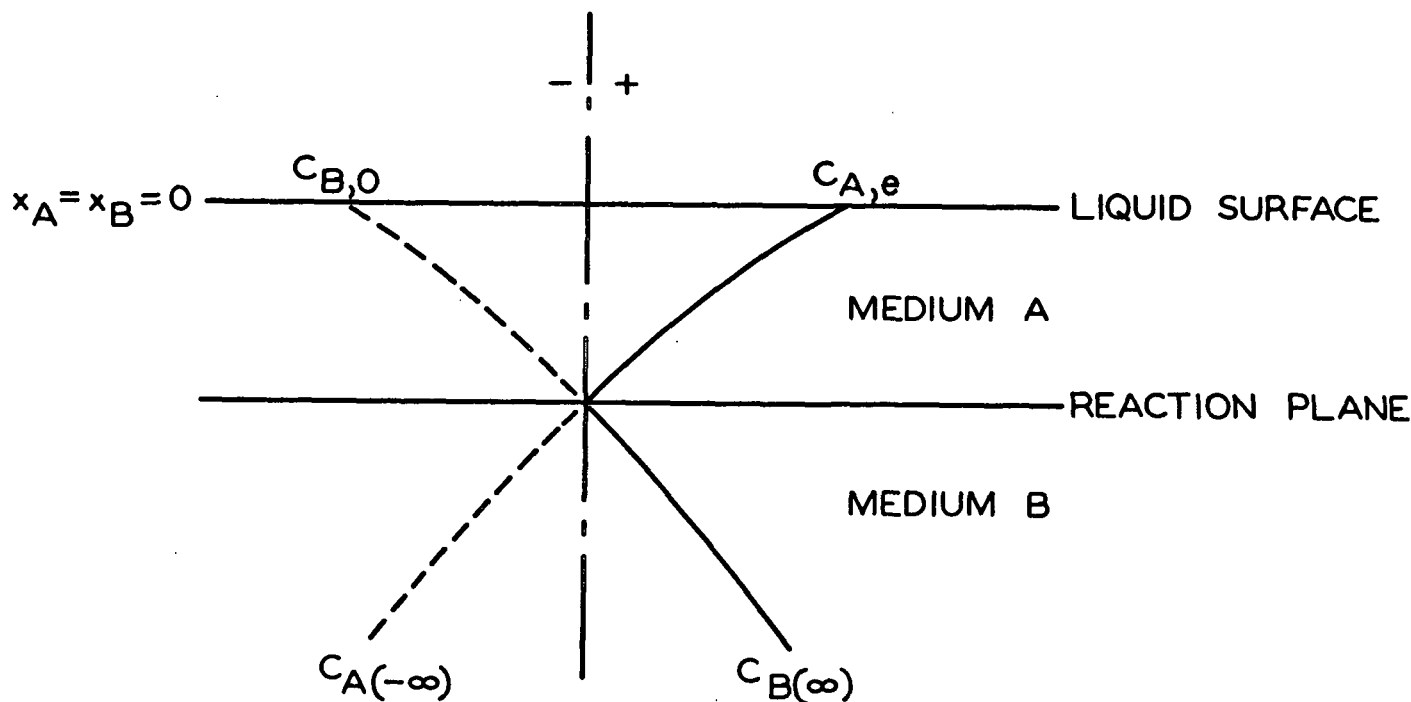


Figure 24. Concentration Gradients of A and B

In the general case, \underline{n} moles of B react per mole of A and no accumulation takes place at the reaction plane. Thus,

$$nD_A(\partial C_A/\partial x)_{x_A=-x_A} = D_B(\partial C_B/\partial x)_{x_B=x_B} \quad (124).$$

Substituting (122) and (123) into (124) gives

$$n(C_{A,e} - C_{A(\infty)})(D_A/\pi t)^{1/2} \exp(-x^2/4D_A t) - (C_{B(\infty)} - C_{B,0})(D_B/\pi t)^{1/2} \exp(-x^2/4D_B t) = 0 \quad (125).$$

It is seen that Equation (125) is true for all values of t only if $x/t^{1/2}$ is a constant. After putting

$$x = 2\alpha t^{1/2} \quad (126),$$

Equation (125) becomes

$$n(C_{A,e} - C_{A(-\infty)})D_A \exp(-\alpha^2/D_A) = (C_{B(\infty)} - C_{B,0})D_B \exp(-\alpha^2/D_B) \quad (127).$$

From (122) and (123) at the reaction plane,

$$C_{A(-\infty)} = -C_{A,e} \operatorname{erfc}(x/2\sqrt{D_A t})/\operatorname{erf}(x/2\sqrt{D_A t}) \quad (128)$$

and

$$C_{B,0} = -C_{B(\infty)} \operatorname{erf}(x/2\sqrt{D_B t})/\operatorname{erfc}(x/2\sqrt{D_B t}) \quad (129).$$

Substituting (128) and (129) into (127) gives

$$n C_{A,e} \sqrt{D_A} \exp(-\alpha^2/D_A) \operatorname{erfc}(\alpha/\sqrt{D_B}) = C_{B(\infty)} \sqrt{D_B} \exp(-\alpha^2/D_B) \operatorname{erf}(\alpha/\sqrt{D_A}) \quad (130).$$

The rate of diffusion away from the liquid surface can be found by differentiating Equation (122) just as was done for physical absorption:

$$\bar{N}_A = [C_{A(-\infty)} - C_{A,e}] 2\sqrt{D_A/\pi t} \quad (131).$$

Substituting (128) into (131),

$$\bar{N}_A = 2C_{A,e} \sqrt{D_A/\pi t_e} / \operatorname{erf}(\alpha/\sqrt{D_A}) \quad (132).$$

Equations (132) and (130) are the solution to this problem.

ABSORPTION ACCOMPANIED BY A REVERSIBLE REACTION

The reversible reaction which is encountered in this study is the reversible ionization of hydrogen sulfide given by



This is the case of a first-order forward, second-order reverse reaction.

If one assumes that the diffusion of the hydrogen ion is controlled by the diffusion of the bisulfide ion and that there is no net movement of the hydrogen ions originally present in the absorbent, the partial differential equations describing the system are

$$\partial A/\partial t = D_A \partial^2 A/\partial x^2 - k_1 A + k_2 B(B + C) \quad (133),$$

and

$$\partial B/\partial t = D_B \partial^2 B/\partial x^2 + k_1 A - k_2 B(B + C) \quad (134),$$

where A and B are the concentrations of the molecular hydrogen sulfide and the bisulfide ions, respectively. C is the concentration of the hydrogen ions originally present in the solution. The boundary conditions are

$$x = 0, \quad t > 0; \quad A = A_e, \quad \partial B/\partial x = 0 \quad (135),$$

$$x > 0, \quad t = 0; \quad A = 0, \quad B = 0 \quad (136),$$

$$x = \infty, \quad t \geq 0; \quad A = 0, \quad B = 0 \quad (137).$$

As stated earlier, no analytical solution exists for this set of equations and boundary conditions. Therefore, a numerical analysis technique had to be used to obtain $(\partial A / \partial x)_{\underline{x}=0}$ as a function of time.

Expressing (133) and (134) as first approximate difference equations gives

$$\begin{aligned} (1/L)(A_{m,n+1} - A_{m,n}) &= D_A/h'^2(A_{m+1,n} - 2A_{m,n} + A_{m-1,n}) \\ &\quad - k_1 A_{m,n} + k_2 B_{m,n}(B_{m,n} + C) \end{aligned} \quad (138)$$

and

$$\begin{aligned} (1/L)(B_{m,n+1} - B_{m,n}) &= D_B/h'^2(B_{m+1,n} - 2B_{m,n} + A_{m-1,n}) \\ &\quad + k_1 A_{m,n} - k_2 B_{m,n}(B_{m,n} + C) \end{aligned} \quad (139)$$

where:

\underline{h}' is the step length in the space dimension

\underline{L} is the step length in the time dimension

subscript \underline{m} is the position in the space dimension

subscript \underline{n} is the position in the time dimension

Solving (138) and (139) for $A_{\underline{m},\underline{n}+1}$ and $B_{\underline{m},\underline{n}+1}$ gives

$$\begin{aligned} A_{m,n+1} &= (1 - 2\lambda_A)A_{m,n} + \lambda_A(A_{m+1,n} + A_{m-1,n}) \\ &\quad - \beta_1 A_{m,n} + \beta_2 B_{m,n}(B_{m,n} + C) \end{aligned} \quad (140),$$

and

$$\begin{aligned} B_{m,n+1} &= (1 - 2\lambda_B)B_{m,n} + \lambda_B(B_{m+1,n} + B_{m-1,n}) \\ &\quad + \beta_1 A_{m,n} - \beta_2 B_{m,n}(B_{m,n} + C) \end{aligned} \quad (141),$$

where $\lambda_A = D_A \underline{L} / \underline{h}'^2$, $\lambda_B = D_B \underline{L} / \underline{h}'^2$, $\beta_1 = k_1 \underline{L}$, and $\beta_2 = k_2 \underline{L}$.

It can be seen from Equations (140) and (141) that the values of \underline{A} and \underline{B} in the $(\underline{n} + 1)$ position in time can be generated from values of \underline{A} and \underline{B} in the \underline{n} position in time. In the \underline{B} grid, the boundary condition $(\partial \underline{B} / \partial \underline{x})_{\underline{x}=0} = 0$ is satisfied by making $\underline{B}_{0,\underline{n}}$ equal to $\underline{B}_{1,\underline{n}}$.

Since only the $(\partial \underline{A} / \partial \underline{x})_{\underline{x}=0}[(\underline{A}_{\underline{e}} - \underline{A}_{1,\underline{n}})/\underline{h}]$ is of interest here, there is a short cut which will greatly reduce the amount of computer time required. To illustrate this short cut, assume that nine points in time are required. The ordinary grid is shown in Fig. 25. As can be seen from Equations (140) and (141), only the points with a check mark need to be calculated in order to obtain $(\underline{A}_{\underline{e}} - \underline{A}_{1,\underline{n}})$ for ten points in time. Use of this short cut will give a program which has one fourth the running time of a program which calculates the full grid.

10	$\underline{A}_{\underline{e}}$	$\underline{A}_{1,10}$ ✓	$\underline{A}_{2,10}$	$\underline{A}_{3,10}$	$\underline{A}_{4,10}$	$\underline{A}_{5,10}$	$\underline{A}_{6,10}$	$\underline{A}_{7,10}$	$\underline{A}_{8,10}$	$\underline{A}_{9,10}$	$\underline{A}_{10,10}$
9	$\underline{A}_{\underline{e}}$	$\underline{A}_{1,9}$ ✓	$\underline{A}_{2,9}$ ✓	$\underline{A}_{3,9}$ ✓	$\underline{A}_{4,9}$	$\underline{A}_{5,9}$	$\underline{A}_{6,9}$	$\underline{A}_{7,9}$	$\underline{A}_{8,9}$	$\underline{A}_{9,9}$	0
8	$\underline{A}_{\underline{e}}$	$\underline{A}_{1,8}$ ✓	$\underline{A}_{2,8}$ ✓	$\underline{A}_{3,8}$ ✓	$\underline{A}_{4,8}$ ✓	$\underline{A}_{5,8}$	$\underline{A}_{6,8}$	$\underline{A}_{7,8}$	$\underline{A}_{8,8}$	0	0
7	$\underline{A}_{\underline{e}}$	$\underline{A}_{1,7}$ ✓	$\underline{A}_{2,7}$ ✓	$\underline{A}_{3,7}$ ✓	$\underline{A}_{4,7}$ ✓	$\underline{A}_{5,7}$	$\underline{A}_{6,7}$	$\underline{A}_{7,7}$	0	0	0
6	$\underline{A}_{\underline{e}}$	$\underline{A}_{1,6}$ ✓	$\underline{A}_{2,6}$ ✓	$\underline{A}_{3,6}$ ✓	$\underline{A}_{4,6}$ ✓	$\underline{A}_{5,6}$ ✓	$\underline{A}_{6,6}$	0	0	0	0
5	$\underline{A}_{\underline{e}}$	$\underline{A}_{1,5}$ ✓	$\underline{A}_{2,5}$ ✓	$\underline{A}_{3,5}$ ✓	$\underline{A}_{4,5}$ ✓	$\underline{A}_{5,5}$ ✓	0 ✓	0	0	0	0
4	$\underline{A}_{\underline{e}}$	$\underline{A}_{1,4}$ ✓	$\underline{A}_{2,4}$ ✓	$\underline{A}_{3,4}$ ✓	$\underline{A}_{4,4}$ ✓	0 ✓	0	0	0	0	0
3	$\underline{A}_{\underline{e}}$	$\underline{A}_{1,3}$ ✓	$\underline{A}_{2,3}$ ✓	$\underline{A}_{3,3}$ ✓	0 ✓	0	0	0	0	0	0
2	$\underline{A}_{\underline{e}}$	$\underline{A}_{1,2}$ ✓	$\underline{A}_{2,2}$ ✓	0 ✓	0	0	0	0	0	0	0
1	$\underline{A}_{\underline{e}}$	$\underline{A}_{1,1}$ ✓	0 ✓	0	0	0	0	0	0	0	0
0	$\underline{A}_{\underline{e}}$	0 ✓	0	0	0	0	0	0	0	0	0
	0	1	2	3	4	5	6	7	8	9	10

$\underline{m}, \text{ space}$

Figure 25. A Grid

A program was written for the IBM 1620 II computer in Fortran language. This program would calculate the triangular grids from Equations (140) and (141) and would print out the rate of absorption after each time interval for as many time intervals as was desired.

Care had to be taken in choosing values for the step lengths, $\underline{h'}$ and \underline{L} . λ cannot be greater than $1/2$; and if $\underline{h'}$ is too large, the numerical analysis is not a good approximation of the true solution. Trial runs were made using progressively smaller values of $\underline{h'}$ until reducing $\underline{h'}$ further did not appreciably change the values obtained by the numerical procedure. The value of $\underline{h'}$ finally chosen was 0.0001. \underline{L} was chosen as 0.0002. The diffusion coefficients, $\underline{D_A}$ and $\underline{D_B}$, were assumed to be the same and equal to the diffusion coefficient of hydrogen sulfide in water (1.84×10^{-5} cm.²/sec.).

It had previously been noted that this type of procedure does not get off to a very good start (18). This was believed to be caused by the very short exposure times where the rate of absorption is very fast. To compensate for this, the equation for physical absorption was used to calculate the rate of absorption at very short exposure times. When the rate of absorption calculated by

$$N_A = 2C_A \sqrt{D_A/\pi t} \quad (43)$$

became equal to the rate of absorption calculated by the numerical analysis procedure, the numerical integration took over and proceeded with the integration.

The program was tested by making values of $\underline{k_1}$ and $\underline{k_2}$ equal to zero. The numerical analysis procedure was found to agree very nicely with Equation (43) at short exposure times but began to become slightly less as the time increased. The difference was only about 2% at an exposure time of 0.05 second. The error

was believed to be due to truncation in the machine. This error was not believed to be serious because the average rate of absorption was taken to calculate the function Φ . This would tend to cancel out any errors involved.

The program was then run using various values of \underline{C} , \underline{k}_1 , and \underline{k}_2 . The results have already been reported.

APPENDIX II

DETAILS OF THE LAMINAR JET

The mathematical details of the laminar liquid jet have been discussed at length by Scriven and Pigford (31) and Spalding (18). Therefore, only a review is included in this section. The review follows very closely the detailed discussion given by Spalding (18).

LAMINAR FLOW

In the derivation of the absorption equations it will be necessary to assume that the flow in the jet is laminar. Hansen and van der Hegge Zijnen (63) have shown that the transition from laminar to turbulent flow in a boundary layer of a fluid flowing past a flat plate occurs at a Reynolds number of 300,000 based on the flat plate length. The largest Reynolds number encountered in this work is 4500 based on the nozzle exit length. While the flow in a pipe and across a flat plate are not exactly the same, it is an indication that the flow is laminar. Also, the Reynolds number in the approach tube never exceeded 1000 and the bell-shaped nozzle accelerated the flow in the jet to the exit velocity very quickly. This would favor the retention of laminar flow.

GRAVITATIONAL ACCELERATION OF THE JET

When a jet emerges from a nozzle, the fluid velocity increases because of the effect of gravity. The jet diameter must therefore decrease. This effect must be considered when determining the exposure time and interfacial area.

It is assumed that the energy is conserved within a jet and that the kinetic energy flowing past any cross section of the jet can be calculated from the mean velocity at that cross section; a mechanical energy balance can be written as follows:

$$\bar{U}_0^2/2 + gh = \bar{U}_x^2/2 \quad (142)$$

where \bar{U}_0 is the average nozzle velocity and \bar{U}_x is the average velocity at any distance, h , downstream from the nozzle. The equation of continuity for this system is

$$D_0^2 \bar{U}_0 = D_x^2 \bar{U}_x \quad (143).$$

Combining Equations (142) and (143) gives

$$D_x = D_0 \left(1 + \frac{\pi^2 g D_0^4 h}{8 q^2} \right)^{-1/4} \quad (144)$$

where q equals the flow rate.

Spalding (18) and Scriven (31) have measured diameters of various jets and have found that they conform to Equation (144). These two studies validate the assumptions made.

BOUNDARY LAYER CONSIDERATIONS

The velocity at the surface of the jet at the nozzle exit is zero because of the boundary layer development by the viscous drag forces within the nozzle. As the fluid proceeds down the nozzle, the viscous forces within the jet accelerate the surface to the velocity of the core of the jet. This situation is shown in Fig. 26.

Thus, the time the jet surface is exposed to the absorbing gas is given by

$$t_e = \int_0^H dh/U_s \quad (145)$$

where U_s is the velocity of the surface. It is necessary to obtain an estimate of the surface velocity as a function of jet length.

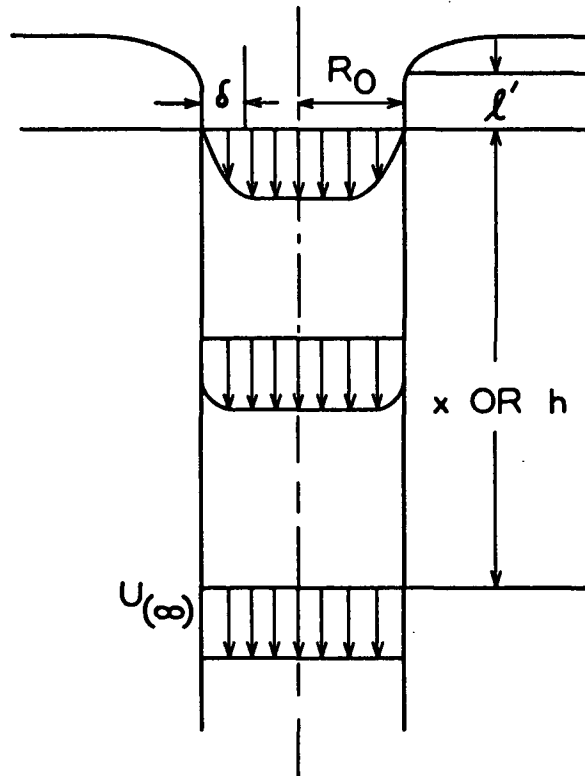


Figure 26. Velocity Distribution in the Jet

FLOW WITHIN THE NOZZLE

The first step is to determine the thickness of the boundary layer developed in the nozzle. Nikuradse (64) made some measurements on the velocity distribution in the inlet portion of a pipe. Spalding (18) analyzed these measurements and obtained the following empirical equation for the relative boundary layer thickness, b , as

$$b = \delta/R_0 = 2.42(\nu \ell'/R_0^2 \bar{U})^{0.391} \quad (146)$$

where δ is the boundary thickness, ℓ' is the length of pipe over which the boundary layer was formed, and ν is the kinematic viscosity.

Using the assumption of laminar flow established earlier, the boundary layer thickness at the nozzle can be calculated from Equation (146).

FLOW WITHIN THE JET

The boundary layer problem of flow within the jet is treated as a two-dimensional problem even though the actual apparatus is a cylindrical jet. This simplification can be made because the distance from the surface of the jet is small in comparison with the jet radius.

The boundary layer equation for two-dimensional motion without the pressure term is

$$U(\partial U/\partial x) + V(\partial U/\partial y) = \partial^2 U/\partial y^2 \quad (147)$$

where \underline{U} is the \underline{x} component of velocity and \underline{V} is the \underline{y} component. The boundary conditions for the case of the laminar jet can be shown to be (18)

$$y = 0; \quad \partial U/\partial y = 0, \quad V = 0 \quad (148)$$

$$Y = \infty; \quad U = U_{\infty}, \quad V = 0 \quad (149),$$

where U_{∞} is the velocity of the jet core.

The same equation and boundary conditions apply to the flow in the wake of a flat plate which has been solved by Goldstein (65). In his solution he used Blasius' solution for flow past a flat plate to describe the initial boundary layer.

Both Nikuradse's (64) measurements for the velocity distribution at the entrance of a pipe and Blasius' solution for the velocity distribution over a flat plate can be approximated by a parabolic velocity distribution. Therefore, the two cases should be enough alike to permit the use of Goldstein's solution

as an approximation to the flow in a jet. This analogy was also used by Scriven and Pigford (31) in the same manner as used here.

Blasius' solution relates boundary layer thickness and flatplate length by

$$\ell = (1/25)(U_{\infty}/\nu)\delta^2 \quad (150).$$

Thus, the equivalent flat plate length can be calculated by finding the boundary layer thickness from Equation (146) and substituting this into Equation (150).

The core velocity, U_{∞} , was obtained from the mean velocity, \bar{U} , by a material balance across the jet,

$$U_{\infty} = \bar{U}/(1 - 3b/4 - b^2/5) \quad (151).$$

Equation (151) is based upon Blasius' flat plate velocity distribution. The effect of gravity was superimposed over this by using mean diameters to calculate \bar{U} .

Spalding (18) then used Goldstein's solution and determined the velocity of the jet surface relative to the core velocity, U_s/U_{∞} , as a function of h/ℓ . A plot of the results is given in Fig. 27.

Thus, the exposure time can be calculated by obtaining the boundary layer thickness at the nozzle exit from Equation (146). One can then calculate the equivalent flat plate length and core velocity from Equations (150) and (151), respectively. One can then get the surface velocity as a function of jet length from Fig. 27. This function was placed in Equation (145) and the exposure time was calculated:

$$t_e = \int_0^H dh/U_s = \ell/U_{\infty} \int_0^{H/\ell} (U_{\infty}/U_s) d(H/\ell). \quad (152).$$

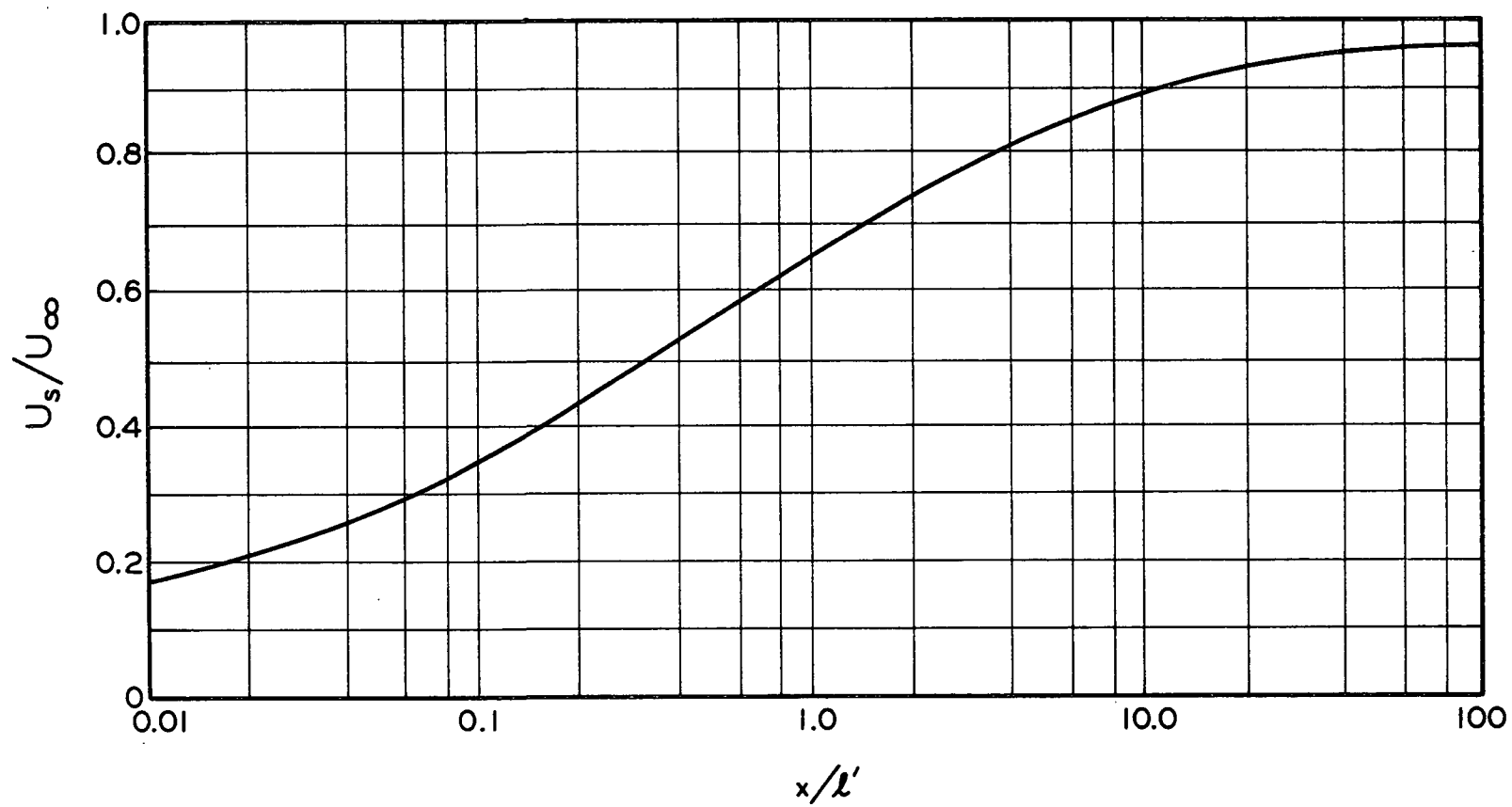


Figure 27. Surface Velocity of Jet as a Function of Jet Length — Goldstein's Solution (18)

The actual form used for Equation (152) was an empirical equation developed by Spalding (18). He fitted the curve in Fig. 27 to an empirical equation and integrated the results. The final form was

$$t_e = \ell/U_\infty [2.90 \{1 - \exp(-0.262H/\ell)\} - 1.061(H/\ell)] \quad (153).$$

A sample calculation appears in Appendix VIII.

The final results are quite insensitive to many of the assumptions made during their calculation. This is shown by the fact that the exposure times calculated from Goldstein's solution differ from those calculated by assuming an ideal jet by only a few per cent at most of the jet lengths used in this thesis. Also, if the boundary layer is arbitrarily halved, the resulting exposure times do not differ appreciably from those previously calculated except at very short jet lengths.

OTHER CONSIDERATIONS

EFFECT OF FINITE MEDIA AND CURVED SURFACES

The penetration theory and fluid flow equations were all derived for plane surfaces and a semi-infinite medium. Therefore, the equations would apply to this study only if the maximum depth of penetration were small in comparison with the radius of the jet. If the penetration depth is defined as the point where $\frac{C_A}{C_{A,e}} = 0.01$, then the depth of penetration at an exposure time of 0.05 second - calculated from Equation (109) - was only 4% of the jet radius. Since this was longer than the longest exposure time used in this study, it was concluded that the penetration theory and fluid flow equations can be used.

OTHER SOURCES OF ERROR

Various other possible sources of errors such as longitudinal diffusion (66), surface temperature (67), and radial movement of the absorbent (18) are discussed at length by other authors. The total of all these effects is estimated at about 2%, and this was assuming that all of the factors acted in the same direction. Therefore, it was concluded that these effects were negligible in this study.

APPENDIX III

DESCRIPTION OF ABSORPTION APPARATUS AND AUXILIARY EQUIPMENT

ABSORPTION APPARATUS

The general design of the absorption apparatus was taken from that used by Spalding (18). The basic considerations in the design of the apparatus are as follows:

1. To provide for a sudden termination of the jet without entrainment of any gas or loss of absorbent.
2. To provide a nonfluctuating flow through the nozzle.
3. To provide a means for obtaining an accurate sample of the liquid after absorption.

THE ABSORBENT SUPPLY SYSTEM

The absorbent supply system consists of (1) one storage tank, (2) a centrifugal pump, (3) two rotameters, (4) stainless steel needle valves, (5) a cooling coil, (6) a surge vessel, (7) a polyvinyl chloride standpipe, and (8) connecting pipe and tubing.

The storage tank was a 48-liter glass bottle.

The centrifugal pump was an Eastern model D-11, type 100, 316 stainless steel pump operated by a 1/8 h.p. motor at 3450 r.p.m.

The liquid rotameters were obtained from Fischer-Porter Co. (tube no. 2-F 1/4-20-5/36). They were equipped with stainless steel floats which gave them a flow range of 50 to 550 cc. of water per minute. These rotameters were used for adjustment purposes only.

The surge vessel consisted of a quart jar which was sealed at the top by a rubber stopper. The exit tube was inserted halfway down into the jar. This kept a layer of air in the top of the jar which would damp out small variations in flow rate.

The cooling coil was made of a 20-ft. length of 1/4-in. stainless steel tubing coiled into an 8-in. diameter.

The remainder of the connecting pipe and tubing was mostly glass with short sections of Tygon tubing for flexibility.

THE GAS SUPPLY AND EXHAUST SYSTEM

The gas supply system consisted of a gas cylinder, a cooling coil, a rotameter, a saturator, and a filter. The gas cylinders were 9-lb. hydrogen sulfide cylinders purchased from the Olin Mathieson Chemical Company. The flow of hydrogen sulfide was controlled by a Mathieson control valve attached to the cylinder.

The hydrogen sulfide gas was filtered by passing it through a tube filled with fiber glass. This filter removed any grease or oil which might be in the gas stream.

The gas was metered through a Fischer-Porter rotameter (tube no. 2-F 1/4-20-5/36) with a glass float. This gave a flow range of 1000 to 9000 cc. per minute metered at 14.7 p.s.i. and 70°F.

The gas was saturated with water vapor by bubbling the gas through two filter flasks in series. Gas dispersion tubes covered with fine sintered glass created small bubbles which helped achieve saturation.

The cooling coil was a 10-ft. section of stainless steel tubing wound into a 6-in. diameter coil.

The connecting tubing was made of glass which was joined to the various pieces of apparatus with short lengths of Tygon tubing.

After the hydrogen sulfide gas left the gas absorption chamber, it was bubbled through two successive bottles of sodium hydroxide. These bottles of sodium hydroxide provided a back pressure on the gas chamber and reduced the amount of hydrogen sulfide released to the atmosphere.

THE ABSORPTION CHAMBER, JET NOZZLE, TAKE-OFF TUBE, AND ALIGNING MECHANISM

The absorption chamber is shown in Fig. 28. It was constructed from pyrex glass by Norman Erway of Oregon, Wisconsin. The chamber was suspended in the constant-temperature bath by means of a clamp made from 1/2-in. brass plate. The chamber and clamp were isolated from the bath to prevent vibration from interfering with operation of the jet.

The jet nozzle was made of Lucite methyl methacrylate polymer which is chemically inert to solutions used in this study. The approach tube was constructed of 1-in. polyvinyl chloride Schedule 40 pipe which is also inert to the chemicals encountered.

The take-off tube was constructed by rotating the end of a 7-mm. glass tube in a very hot flame until the hole in the end of the tube became the correct size. The rounded end was ground flat with a piece of coarse and then fine emery paper. The glass tube was joined to a 10/30 ground-glass male joint. The top and inner surfaces were then coated with paraffin. This nonwetting surface aided the stability of the jet at the termination point.

The aligning mechanism was made by adapting a Bausch and Lomb microscope slide aligner to the nozzle tube holder. The nozzle tube holder was constructed

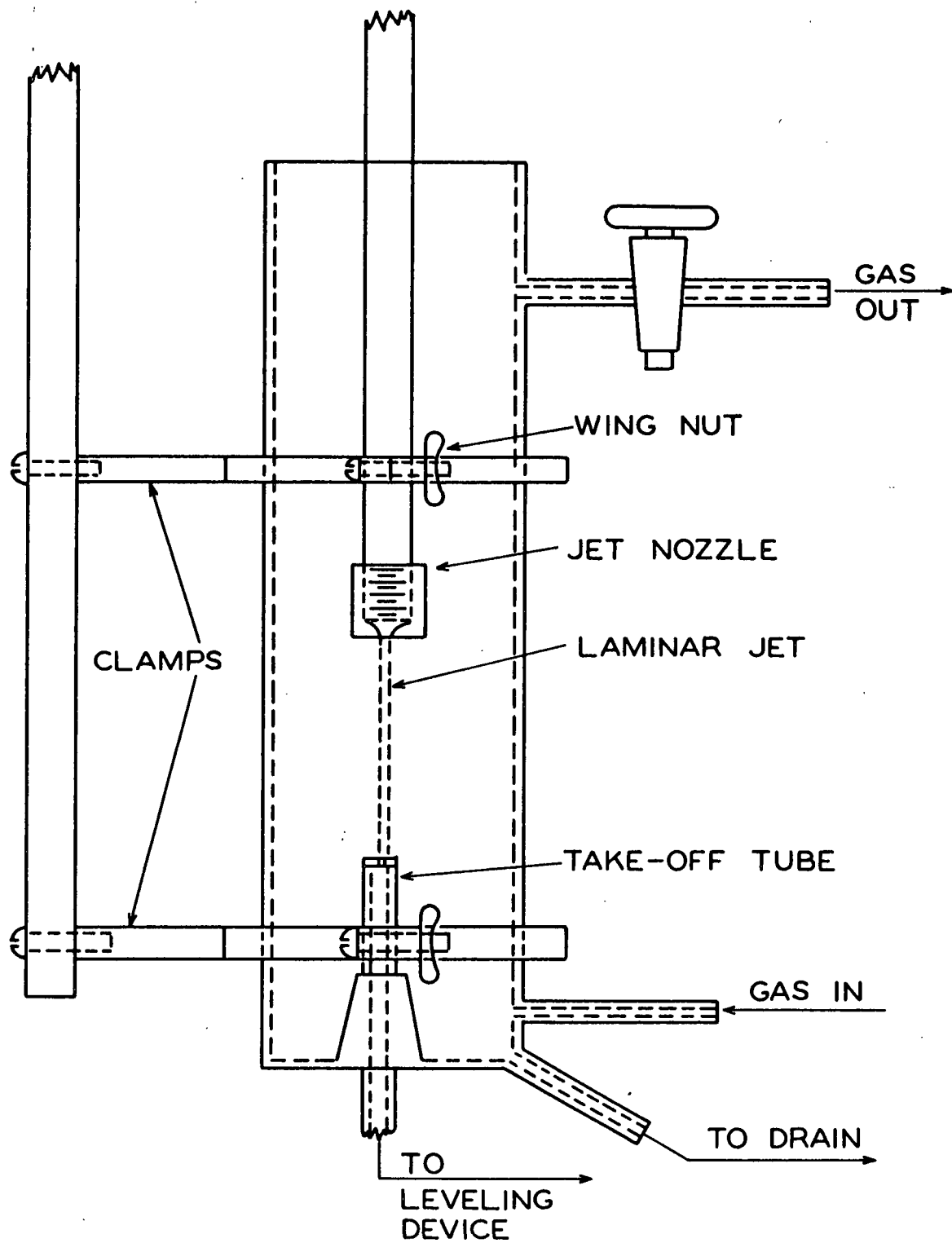


Figure 28. Absorption Chamber

of Lucite. The pieces were joined together using a 1,2 dichloroethene solution of the methyl methacrylate monomer as the bonding agent. The length of the jet could be varied by sliding the approach tube up and down through the nozzle tube holder.

THE LIQUID TAKE-OFF SYSTEM

The liquid take-off system was made up of a leveling device, a surge tube, and a sampling pipet.

The leveling device is shown in Fig. 29. Its function was to maintain a constant head on the take-off tube. The difference in absolute pressure between the absorption chamber and the leveling device had to be such as to cause the liquid flow rate away from the top of the take-off tube to be exactly equal to the flow rate of the laminar jet. The leveling device permitted this precise control. The sampling pipet, shown in Fig. 30, was constructed of pyrex glass by Norman Erway. The curved tube in the lower bulb was to prevent channeling and to insure complete mixing in the delivered sample. The pipet delivered 99.47 ml.

A surge tube was placed immediately after the absorption chamber to provide an escape for any bubbles of hydrogen sulfide which might be entrained during adjustment.

THE CONSTANT-TEMPERATURE BATH

The constant-temperature bath used in this study was a glass tank 15 in. by 24 in. The circulating pump was a Teel submersible pump capable of circulating 10 gal. per minute at zero head. The temperature was regulated by two 500-watt knife heaters. The thermoregulator was a Philadelphia Glass mercury column regulator with a sensitivity of 0.005°C . The regulator worked through a Precision

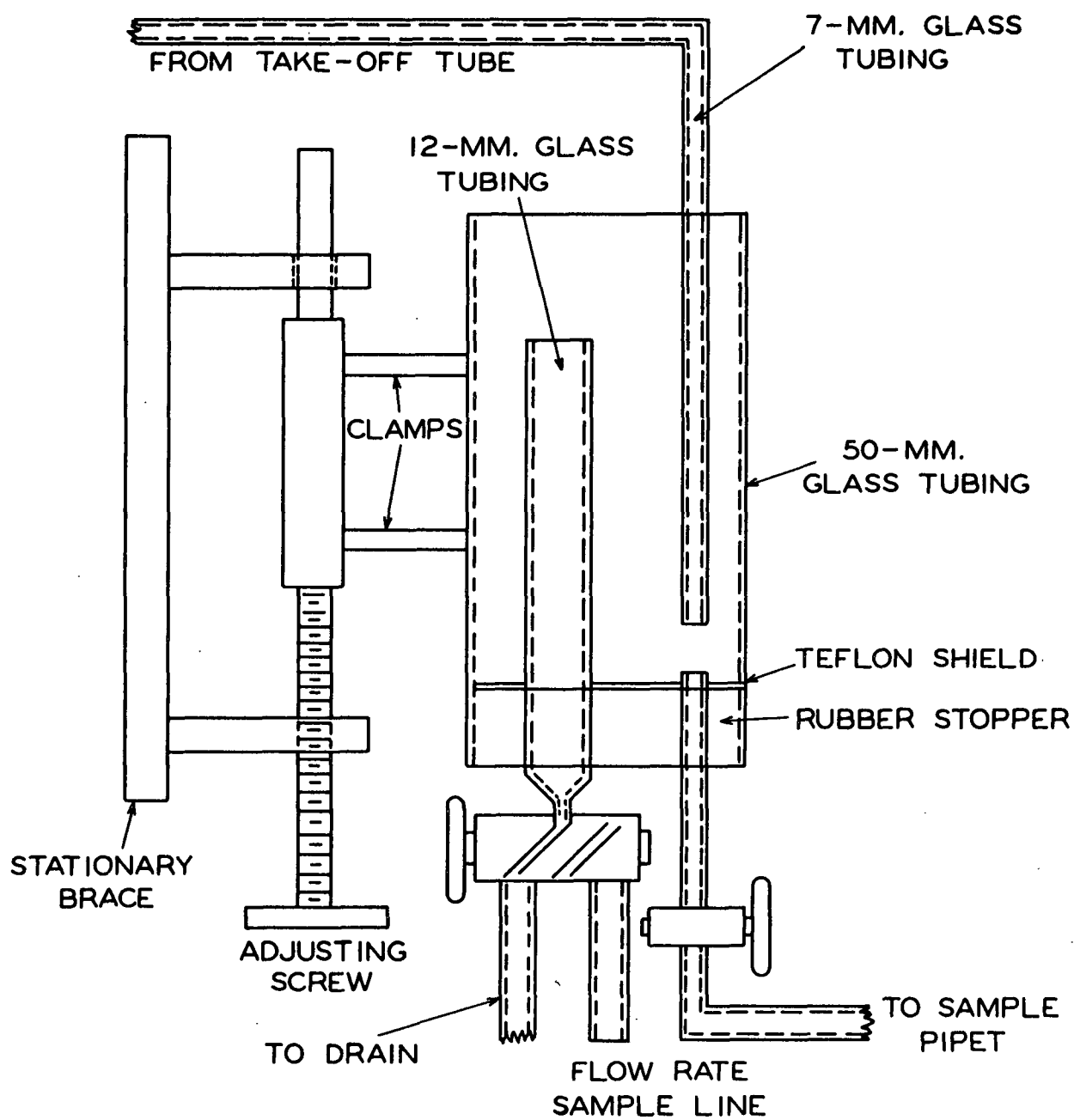


Figure 29.. Leveling Device

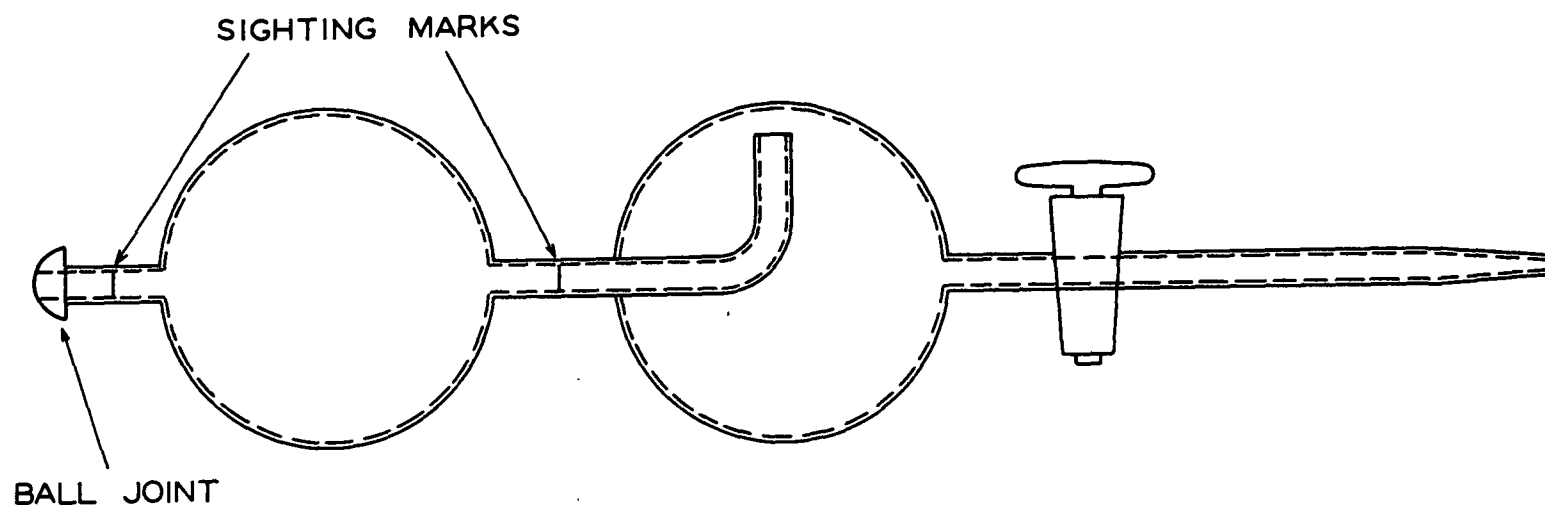


Figure 30. Sampling Pipet

Scientific electronic relay. The entire temperature bath could be controlled to within $\pm 0.01^{\circ}\text{C}$. and there were no detectable temperature gradients.

THE DEGASSING UNIT

The apparatus which was used to remove dissolved gases from the water prior to use in the absorption apparatus is shown in Fig. 31. The equipment consisted of a 50-liter, soft-glass carboy, a Graham condenser, a 12-liter round-bottom pyrex flask, and connecting piping and tubing.

To begin operation the steam and an aspirator were turned on. When live steam was flowing into the condenser and the vacuum had reached 15 in. of mercury, the valve between the carboy and the condenser was opened. The vacuum in the flask caused the water to flow from the carboy up through the condenser where it was heated to about 150°F . The water then flowed from the condenser through the nozzle where it was sprayed into the flask in fine droplets. After the flask was filled, the flow was shut off and the water was boiled for a few minutes. After boiling, the degassed water was siphoned into the absorption apparatus supply tank, where it was stored overnight before use.

Analytically distilled water was used for all the runs and a typical analysis of the water which came from the degassing unit is as follows:

pH	6.85
Solids, %	0.00
Dissolved oxygen	1.0 p.p.m.
Sp. resistance	300,000 ohms-cm.

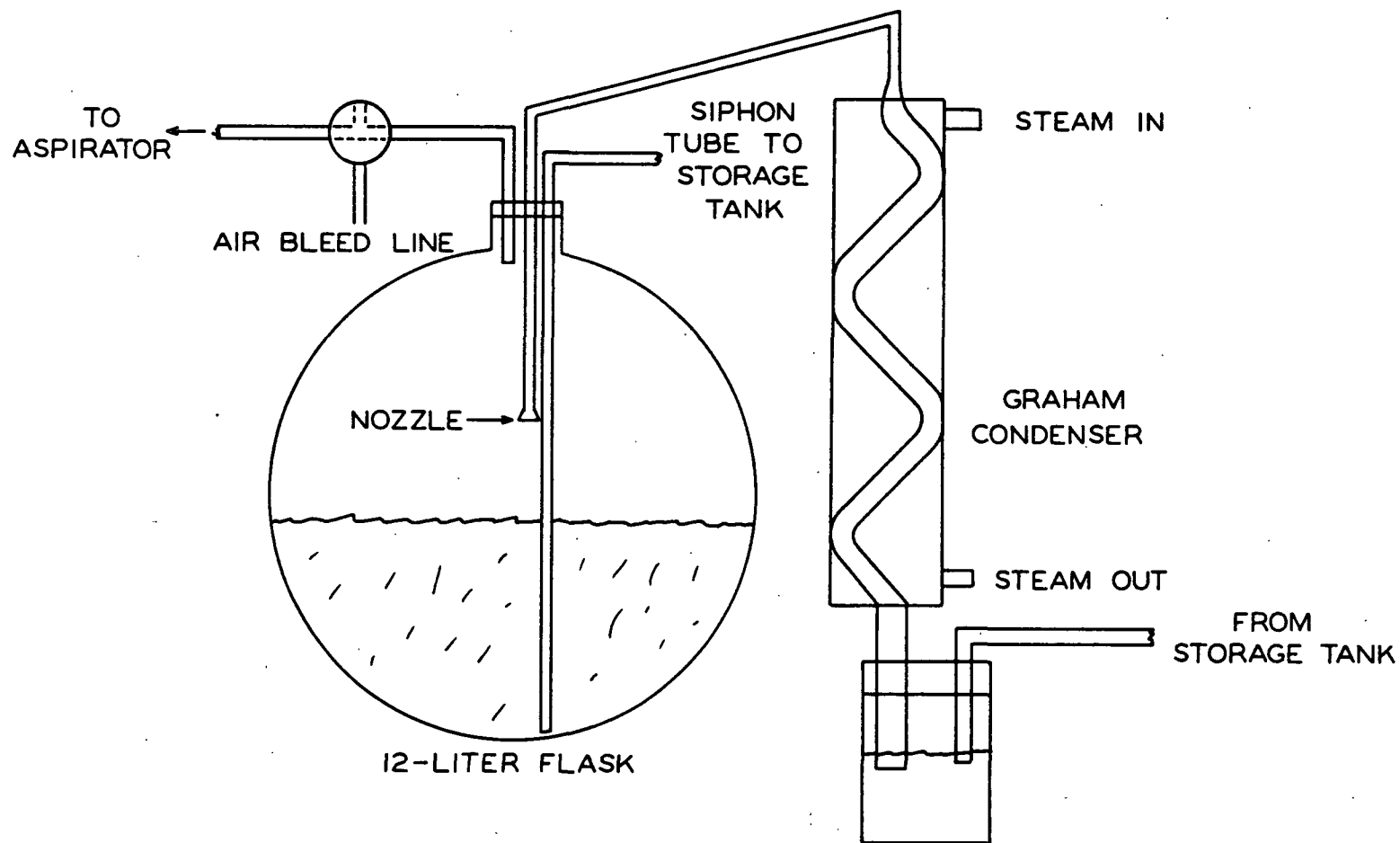


Figure 31. Degassing Unit

APPENDIX IV

ANALYTICAL PROCEDURES AND PREPARATION OF SOLUTIONS

PREPARATION AND STANDARDIZATION OF SOLUTIONS

Four standard solutions were necessary for the various analyses which were performed in this study. They are (1) 0.1 and 0.025N sodium thiosulfate, (2) 0.1N silver nitrate, (3) 0.1N sodium hydroxide, and (4) 0.1N hydrochloric acid.

SODIUM THIOSULFATE, 0.1 AND 0.025 NORMAL

The sodium thiosulfate was prepared by dissolving the necessary amount of anhydrous reagent-grade sodium thiosulfate in degassed, distilled water. Then 1 to 2 grams of sodium borate and 0.001 gram of mercuric iodide were added to each liter of the solution to act as a preservative agent against bacteriological action. The solution was then stored in a glass bottle which had been cleaned with dichromate cleaning solution and rinsed with hot, distilled water. The air above the solution was kept free from carbon dioxide by using an ascarite filter. Solutions prepared and stored in this manner were found to be very stable.

The sodium thiosulfate solutions were standardized using potassium iodate as the primary standard. An amount of reagent-grade potassium iodate which would consume 350 to 450 ml. of the thiosulfate solution was weighed to the nearest 0.1 mg. and dissolved in a 250-ml. volumetric flask. The flask was then filled to the mark with distilled water. Next, 2 grams of potassium iodide and 1 ml. of concentrated hydrochloric acid were dissolved in 50 ml. of water in a 500-ml. Erlenmeyer flask. A 25-ml. aliquot was then drawn from the potassium iodate solution and added to the flask. The iodine formed was then titrated with the sodium thiosulfate solution to the starch end point. The normality of

the thiosulfate solution was calculated from the known weight and purity of the potassium iodate and from the volume of thiosulfate solution that was required to reach the end point.

SILVER NITRATE, 0.1 NORMAL

The standard silver nitrate solution was prepared by placing approximately 17 grams of reagent-grade silver nitrate of known purity in a weighing bottle and drying it in an oven overnight at 105°C. The weighing bottle was then taken from the oven, cooled, and weighed to the nearest 0.1 mg. The contents were emptied into a 1000-ml. volumetric flask and the bottle was reweighed. The volumetric flask was then filled to the mark with degassed, distilled water. The normality of the silver nitrate solution was calculated from the weight and purity of the silver nitrate.

SODIUM HYDROXIDE, 0.1 NORMAL

The sodium hydroxide solution was prepared by dissolving 10 grams of reagent-grade sodium hydroxide in 10 ml. of water. This solution was then filtered through an asbestos filter which had been formed in a Gooch crucible. Four ml. of the filtered solution were placed in a 1000-ml. volumetric flask and diluted to the mark with degassed, distilled water.

The sodium hydroxide solution was standardized with potassium acid phthalate as the primary standard. First, 0.8 gram of potassium acid phthalate (weighed to the nearest 0.1 mg.) was dissolved in 50 ml. of distilled water. The resulting solution was then titrated to the phenolphthalein end point with the hydroxide solution. The normality was calculated from the weight and purity of the phthalate and the volume of sodium hydroxide required.

HYDROCHLORIC ACID, 0.1' NORMAL

Standard hydrochloric acid was prepared by diluting 8.5 ml. of concentrated (36%) reagent-grade hydrochloric acid to one liter.

The sodium carbonate method was used to standardize the hydrochloric acid solution. A 0.2-gram sample of sodium carbonate (weighed to the nearest 0.1 mg.) was dissolved in 50 ml. of distilled water and three drops of methyl red-bromocresol green mixed indicator were added. The solution was titrated to a faint pink color and an additional 0.5 ml. of acid was added. The solution was then heated to boiling to drive off the carbon dioxide. Standard base was then added to the solution until the color changed to green. Then the titration with the acid was continued to a sharp color change. The equivalents of standard base used were added to the equivalents of sodium carbonate to determine the normality of the hydrochloric acid.

PREPARATION AND INITIAL ANALYSIS OF ABSORBENT SOLUTIONS

The various solutions which were used as absorbents were prepared and analyzed prior to being used in the absorption system.

PREPARATION OF SOLUTIONS

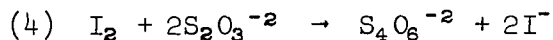
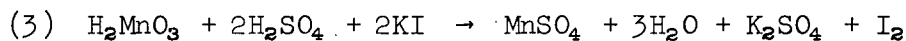
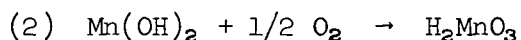
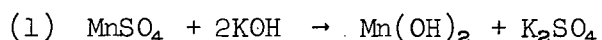
A stock solution of approximately 6 normal acid, base, or oxidizing agent was prepared and stored in 12-liter bottles. The hydrochloric acid solutions were prepared by diluting the proper amount of concentrated acid to 12 liters. The sodium hydroxide was made by dissolving the necessary amount of reagent-grade chemicals in 12 liters. The sodium hypochlorite solution was prepared by first dissolving sodium hydroxide in water and then bubbling chlorine gas through the solution until the pH was about 11.

As a particular absorbent was needed, an aliquot of the stock solution was withdrawn from the bottle and placed in the 48-liter storage tank. Distilled water was then passed through the degassing unit and into the storage tank. The absorbent was kept under a layer of n-heptane to prevent absorption of gases from the air. Since the solution was warm, the top of the tank was sealed off and allowed to stand overnight to cool.

ANALYSIS OF DISTILLED WATER

After filling the absorption system storage tank, a sample of the distilled water was taken and analyzed. Four different analyses were run: (1) dissolved oxygen, (2) pH, (3) percentage of solids, and (4) conductivity.

The dissolved oxygen was determined by the Winkler method (68). This method involves the oxidation of manganous hydroxide to manganic acid by the dissolved oxygen. The manganic acid then oxidizes iodide ions to iodine, which is then titrated with sodium thiosulfate. The reactions are:



The water sample was then taken in a clean, dry, glass-stoppered, 250-ml. Erlenmeyer flask. The flask was filled to the top and then stoppered to prevent absorption of oxygen from the air. Two ml. of each of the following reagents were added in order: (1) manganese sulfate solution - 363 grams of $\text{MnSO}_4 \cdot 5\text{H}_2\text{O}$ per liter, (2) alkaline-iodide solution - 700 grams of KOH and 150 grams of KI per liter, and (3) concentrated sulfuric acid. A 200-ml. sample was then withdrawn and titrated in a 500-ml. Erlenmeyer flask to a starch end point with standardized sodium thiosulfate.

The pH of the distilled water was determined with a Beckman Zeromatic pH meter.

The solids content was determined by placing a 100-ml. sample in a tared 150-ml. glass beaker, evaporating it to dryness in a 105°C. oven, and reweighing the beaker.

The conductivity was measured with a Dearborn Solu Bridge. The conductivity cell had a cell constant of 0.100/cm.

CONCENTRATION OF BASIC ABSORBENT SOLUTIONS

The concentration of the hydroxide ion in the basic solutions was determined by a standard neutralization technique. A sample of the solution was taken from the storage tank and transferred to an Erlenmeyer flask. Two or three drops of methyl red-bromocresol green mixed indicator were added and the sample was titrated to a faint pink color with the standardized acid. The sample size was selected so as to require between 10 and 50 ml. of acid to reach the end point.

CONCENTRATION OF ACIDIC ABSORBENT SOLUTIONS

The concentration of the acidic solutions was determined in exactly the same manner as the basic absorbents except that phenolphthalein was used as the indicator and standardized base was used as the titrating solution.

CONCENTRATION OF THE OXIDIZING ABSORBENT SOLUTIONS

The concentrations of the various components in the oxidizing solutions were determined by a system of material balances.

The concentration of the oxidizing agent was determined directly by an iodometric titration. A sample of the solution was taken and placed in a 500-ml. flask.

Excess potassium iodide was added and the solution was acidified with hydrochloric acid. The iodine which was formed was then titrated to the starch end point with standardized sodium thiosulfate. All of the oxidizing strength was assumed to be in the form of the hypochlorite ion (OCl^-).

Since the hypochlorite solutions were formed by bubbling chlorine gas through sodium hydroxide solutions, equal amounts of hypochlorite ions and chloride ions were formed.

The hydroxide ion concentration was calculated from the pH values for the solutions below pH 13. For the solutions whose pH was above 13, the hydroxide ion concentration was calculated from the amount of sodium hydroxide stock solution used in preparing the absorbent solution.

The sodium ion concentration was taken as being equal to the sum of the hypochlorite, chloride, and hydroxide ion concentrations.

The results of these determinations are given in Table XVII.

DETERMINATION OF HYDROGEN SULFIDE PICKUP

Three different methods of analysis were used to determine the amount of hydrogen sulfide which had been picked up by the absorbent solutions. An iodimetry technique was used to analyze all the acid and salt solutions and the basic solutions of pH 13 or lower. A silver nitrate technique was used to analyze the basic solutions with a pH greater than 13. An iodometric technique was used to determine the sulfide pickup by the hypochlorite solutions. The details of these techniques are as follows.

TABLE XVII
CHEMICAL COMPOSITION OF HYPOHALITE ABSORBENTS

Run No.	Oxidizing Agent	Concentration of Ionic Species, moles/liter			
		Na ⁺	OH ⁻	OX ⁻	X ⁻
121-122	NaOCl	0.101	--	0.050	0.050
123-124	NaOCl	0.124	0.02	0.052	0.052
125-126	NaOCl	0.171	0.07	0.050	0.050
127-129	NaOCl	1.10	1.0	0.051	0.051
130-135	NaOCl	0.60	0.5	0.052	0.052
136-138	NaOBr	0.60	0.5	0.054	0.054
145-147	NaOCl	0.30	0.2	0.051	0.051
148-150	NaOCl	0.099	--	0.049	0.049
151-153	NaOCl	0.082	--	0.041	0.041
154-159	NaOCl	0.100	--	0.050	0.050
160-162	NaOBr	0.104	--	0.052	0.052
163-165	NaOCl	0.100	--	0.050	0.050
166-169	NaOCl	0.100	--	0.050	0.050
170-172	NaOCl	0.290	--	0.145	0.145
173-175	NaOCl	0.052	--	0.026	0.026
176-178	NaOCl	0.200	--	0.100	0.100

THE POTASSIUM IODATE-IODIDE TECHNIQUE

It was originally intended to use a method of sulfide analysis suggested by Kolthoff and Elving (69) throughout this study. The suggested technique is first to precipitate the sulfide ions by adding ammoniacal cadmium chloride to the sample. An excess of standardized potassium iodate - iodide solution is then added and the mixture is quickly acidified with 6N hydrochloric acid. The excess iodine is then titrated to the starch end point with standardized sodium thiosulfate.

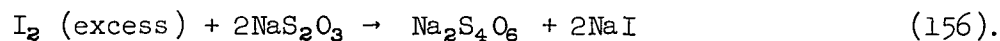
A number of absorption runs were actually made using this technique before it was found that the results were 10-15% high. A subsequent literature search revealed that similar findings had been obtained by Maurice (70) and Bethge (71). The reason for the high results obtained by this method is believed to be due to oxidation of some of the sulfide ions to sulfate ions during the acidification step. Maurice (70) and Bethge (71) then revised the order of addition of the various solutions and found that the new procedures gave accurate results. This revised method was then used in all subsequent absorption runs. The exact procedure is given below.

The solutions needed for this analysis were 0.025N sodium thiosulfate, approximately 0.04N potassium iodate - iodide, and 6N hydrochloric acid. The preparation and standardization of the thiosulfate has already been given. The potassium iodate - iodide solution was prepared by dissolving 1.4 grams of potassium iodate, 22 grams of potassium iodide, and 1-2 grams of sodium borate in one liter of water. The 6N hydrochloric acid was prepared by diluting 500 ml. of concentrated acid to one liter.

Before a run was begun, 25 ml. of the iodate - iodide solution were placed in a 500-ml. ground glass-stoppered Erlenmeyer flask and enough hydrochloric acid was added so that the final pH of the iodine solution plus the sample would be 3 or below. The absorption run was begun, and when a sample was taken, it was run into the iodine solution. Care was taken to keep the tip of the sampling pipet below the surface of the solution so as not to lose any of the dissolved gas to the atmosphere. After all the samples had been collected, the excess iodine was titrated to a starch end point with the 0.025N sodium thiosulfate.

A blank was made for each run by adding 100 ml. of the original absorbent to the iodine solution and titrating the resulting mixture.

The chemical equations which give the stoichiometry of the reactions are as follows:



THE SILVER NITRATE TECHNIQUE

The silver nitrate technique was used to determine the sulfide content of the strongly basic absorbents. The iodate-iodide technique was tried first, but the results were very scattered and appeared high. Again, it was suspected that oxidation to sulfate might be taking place. Therefore, it was decided to use a silver nitrate technique given by Borlew and Pascoe (72).

This titration was a potentiometric titration carried out in a very basic solution. The two solutions needed for this determination were a 0.1N silver nitrate solution and a 1N sodium hydroxide solution. The preparation and standardization of the silver nitrate has been given earlier. The sodium hydroxide solution was prepared by weighing out 40 grams of reagent-grade sodium hydroxide and dissolving it in one liter of water. Twenty-five ml. of ammonium hydroxide were added before the flask was filled to the mark. This prevented the precipitation of thiosulfate ions during the titration. The two electrodes used were a silver - silver sulfide electrode and a blue-tip glass reference electrode which had been conditioned in a 1N sodium hydroxide solution.

Before a run was begun, clean, dry, 125-ml., glass-stoppered Erlenmeyer flasks were set out. As the samples were collected, they were run into the flasks and stoppered. After all the samples had been collected, the titrations

were begun. First, 100 ml. of the 1N sodium hydroxide solution were placed in a 150-ml. beaker and a quantity of the absorbent which would require 3-9 ml. of the silver nitrate was added to the beaker. The titrations were carried out using a 10-ml. semimicro buret. As the equivalence point was reached, the silver nitrate was added in 0.05-ml. increments. The titration was run to the equivalence point and then two additional increments were added. A second-derivative method given by Lingane (73) was used to calculate the exact equivalence point.

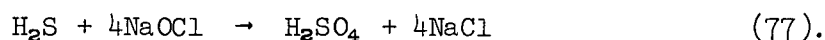
THE SODIUM HYPOCHLORITE TECHNIQUE

The sodium hypochlorite technique was used to determine the hydrogen sulfide pickup by the oxidizing absorbents. Four solutions were needed for this technique: (1) 0.1N sodium thiosulfate, (2) 10% potassium iodide, (3) 6N hydrochloric acid, and (4) 2N sodium hydroxide. The preparation and standardization of the sodium thiosulfate have been given earlier. The potassium iodide solution was prepared by dissolving 100 grams of reagent-grade KI in one liter of distilled water. The 6N hydrochloric acid was prepared by diluting 500 ml. of concentrated acid to one liter. The 2N sodium hydroxide was prepared by dissolving 80 grams of reagent-grade pellets in one liter of distilled water.

To prepare for a run, a number of clean, dry, 125-ml., glass-stoppered flasks were tared and set aside. A sample was taken by running part of the absorbent stream into a flask which was then stoppered and set aside until all the samples had been collected. The flasks and contents were reweighed to obtain the sample size.

A quantity of the 2N sodium hydroxide was then added to each sample to bring the hydroxide content up to at least 0.2N. The flasks were then placed on a hot plate and heated until the solutions became clear. Heating was continued for

5-10 more minutes. The contents of the 125-ml. flasks were then cooled and emptied into 500-ml. Erlenmeyer flasks. Fifteen ml. of the 10% potassium iodide were then added and the solutions were acidified with the 6N hydrochloric acid. The iodine which was formed was then titrated with the 0.1N sodium thiosulfate to a starch end point. Blank determinations were run in exactly the same manner using 25 ml. of the original sample. The amount of hydrogen sulfide picked up in the absorption chamber was determined by the difference between the blank and absorbent sample hypochlorite concentration. All of the oxidant consumed in passing through the absorption chamber was assumed to have reacted with hydrogen sulfide by



APPENDIX V

EQUILIBRIUM SOLUBILITY OF HYDROGEN SULFIDE IN AQUEOUS SOLUTIONS

A review of the literature showed that values for the equilibrium solubility of hydrogen sulfide in various solvents were not in agreement. Therefore, it was necessary to determine these values experimentally. The experimental details are given below. A discussion of the method used to estimate the equilibrium solubility in solvents which would react with hydrogen sulfide is also given.

EXPERIMENTAL PROCEDURES

Two methods were used to determine the equilibrium solubility of hydrogen sulfide in the various solvents - a static method and a dynamic method.

STATIC METHOD

The determinations by the static method were made by first placing 100-150 ml. of the desired solution in a 250-ml. gas washing bottle, and bubbling nitrogen through the solution for about 30 minutes to remove any dissolved oxygen. Hydrogen sulfide gas was then bubbled through the solution for 30 minutes. Next the gas washing bottle was placed in an ice bath, and the bubbling was continued for another 15 minutes. Both valves were then closed to seal the bottle from the atmosphere. The bottle was placed in a constant temperature bath at 25°C. for 2-3 hours. The pressure of hydrogen sulfide gas gradually built up inside the bottle and was relieved occasionally by opening the exit valve. The building up and relieving of pressure was continued until the level of the solution in the entrance tube did not change when the exit valve was opened. This indicated that the pressure inside the bottle was the same as atmospheric.

After attaining equilibrium, the bottle was removed from the bath and inverted. A delivery tube was attached to the exit valve, and 25-40 grams of the solution was run into a tared 500-ml. glass-stoppered flask which contained a known volume of standard iodine solution. The flask was then reweighed and the excess iodine was titrated with standard sodium thiosulfate. Care was taken to keep the end of the delivery tube below the surface of the iodine solution to prevent loss of hydrogen sulfide to the atmosphere.

The concentration of hydrogen sulfide was then calculated from the weight of the sample and the amount of iodine consumed. During the calculations, it was assumed that the absorption of hydrogen sulfide did not affect the density of the solution being used. The partial pressure of the hydrogen sulfide was determined by subtracting the vapor pressure of water at 25°C. from atmospheric pressure.

DYNAMIC METHOD

The dynamic method of determining the solubility was started by placing 100-150 ml. of the desired solution in a 250-ml. gas washing bottle. Nitrogen was bubbled through the solution for a period of 30 minutes to remove dissolved oxygen. The bottle was placed in a constant temperature bath at 25°C. for 2-3 hours. Hydrogen sulfide gas was then bubbled through the solution and exhausted to the atmosphere through an exhaust jar. After 40-60 minutes of passing gas through the bottle, it was removed from the bath and inverted, and the delivery tube was connected to the exit valve. From here on the procedure was identical with that of the static method except that the total pressure on the system was atmospheric pressure plus the slight amount of back pressure caused by the exhaust jar.

EQUILIBRIUM SOLUBILITY IN ACIDIC AND SALT SOLUTIONS

The results of the solubility experiments are shown in Table XVIII. The solubility of hydrogen sulfide at a partial pressure of 1 atm. was then calculated using Henry's Law and the results are shown in Table III.

TABLE XVIII

SOLUBILITY OF HYDROGEN SULFIDE IN AQUEOUS SOLUTIONS AT 25°C.

Solvent	Static Method		Dynamic Method	
	$\frac{P}{\text{H}_2\text{S}},$ atm.	Concn., g./l.	$\frac{P}{\text{H}_2\text{S}}$ atm.	Concn., g./l.
Water	0.949	3.38		
HCl				
0.2N	0.949	3.36		
0.4N	0.939	3.23		
0.6N	0.949	3.33		
0.8N	0.939	3.24		
1.0N	0.949	3.35		
NaCl				
50 g./l.	0.948	2.82	0.965	2.84
100 g./l.	0.948	2.44	0.965	2.47
150 g./l.	0.948	2.11	0.965	2.15
200 g./l.	0.948	1.88	0.965	1.88
NaSO ₄				
50 g./l.	0.944	2.54	0.964	2.62
100 g./l.	0.944	2.00	0.964	2.08
150 g./l.	0.944	1.65	0.964	1.66
200 g./l.	0.944	1.30	0.964	1.34

Note: The sodium chloride and sodium sulfate solutions were 0.1N in hydrochloric acid to prevent any hydrolysis of the hydrogen sulfide.

The values shown in Table II were then used to calculate the activity coefficient of hydrogen sulfide given by Equation (21). These values were then plotted as a function of ionic strength and are shown in Fig. 31.

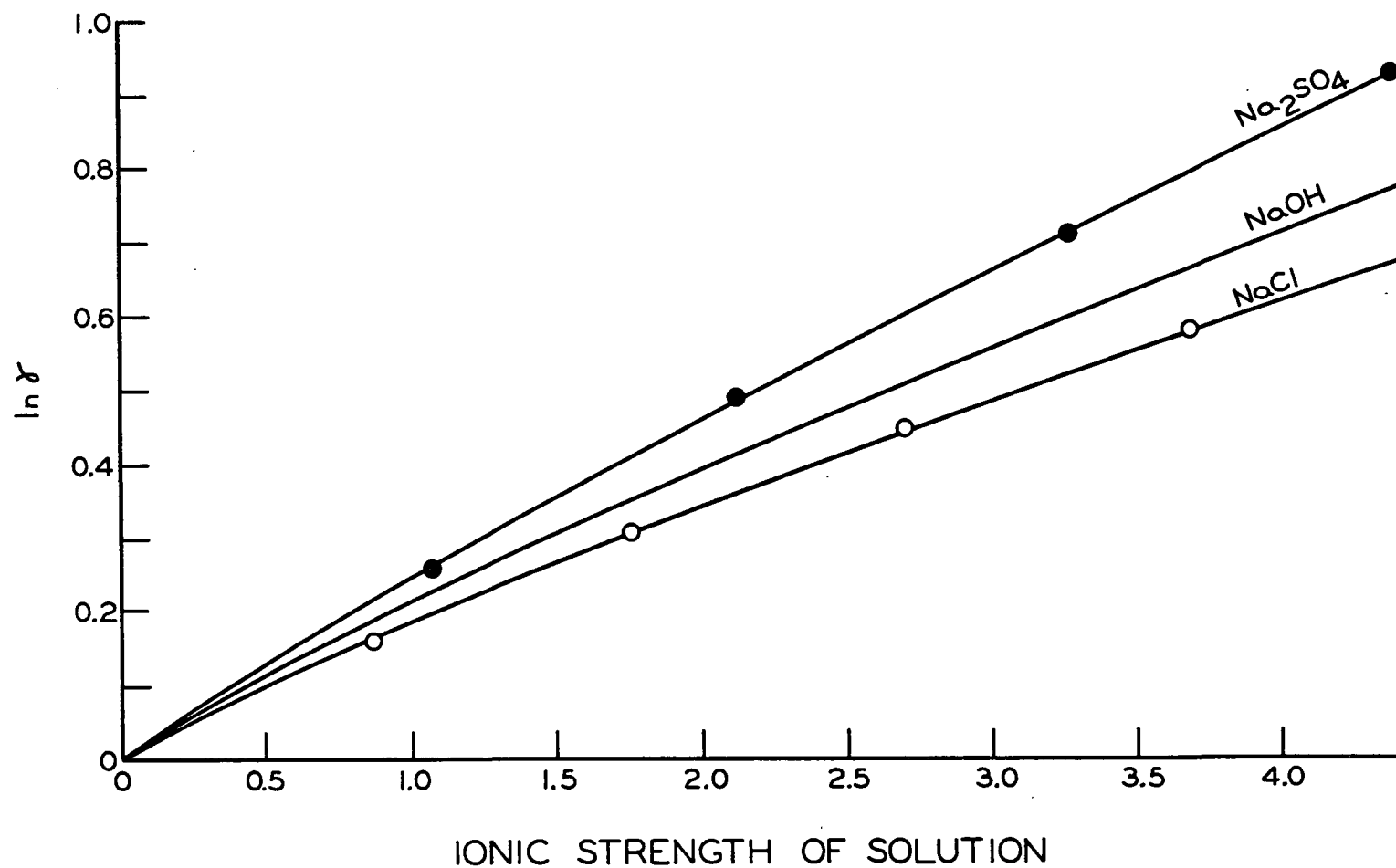


Figure 31. Activity Coefficients of Hydrogen Sulfide

SOLUBILITY IN BASIC AND OXIDIZING SOLUTIONS

The solubility of hydrogen sulfide in basic solutions and oxidizing solutions cannot be determined experimentally because of the reactions which would take place. Therefore, an estimate must be made of the solubility in these two types of solutions.

One method of calculating the activity coefficient of a neutral molecule in an ionic solution is the Debye-McAulay equation (74). The equation is

$$\ln \gamma = \ln(C_o/C_i) = \beta/2kTD_s \sum_{j=1}^N n_j e_j^2 / b_j \quad (157)$$

where

γ = activity coefficient of a neutral molecule

C_o = solubility of the neutral molecule in pure water

C_i = solubility of the neutral molecule in the salt solution

β = constant characteristic of the neutral molecule

k = Boltzmann's constant

T = temperature

D_s = dielectric constant of the solvent

n_j = number of ions of species j

e_j = total electric charge of ion of species j

b_j = radius of ion of species j

N = number of different ions present

Harned and Owen (75) state that this equation has the same form as that which is obtained empirically from experimental data — the log of the activity coefficient of a neutral molecule is proportional to the ionic strength of an electrolyte.

Equation (157), written for a 1-1 electrolyte, can be simplified by substituting the product of Avogadro's number times the molarity ($6.023 \times 10^{23} \underline{M}$) for $\underline{n_j}$ and making use of the fact that $\underline{e_j^2}$ is a constant. Performing the substitution and rearranging Equation (157) gives

$$\ln \gamma = (6.023 \times 10^{23} \underline{\rho_e^2} / 2k\underline{T}\underline{D}_s) \sum_1^N \underline{M_j} / \underline{b_j} \quad (158).$$

The group of terms ($6.023 \times 10^{23} \underline{\rho_e^2} / 2k\underline{T}\underline{D}_s$) is a constant which is independent of the salt, but is a function of the liquid and temperature.

The choice of the ionic radii of the various ions creates a problem when one uses the D - A equation. Stern and Amis (76) discussed methods of calculating ionic radii in solutions. The various methods gave different values for the same ion. The hydration theory was believed to be the one which most closely fit the conditions of this thesis and was used in this work.

The radii of the hydroxide ion and the hypochlorite ion had not been determined by the hydration theory. Therefore, the hydroxide ion radius was assumed to be equal to that of the fluoride ion. It was also noted that the chloride ion and the perchlorate ion had about the same radius. Therefore, the radius of the hypochlorite ion was assumed to be equal to that of the chloride ion. The radius of the bromide ion and hypobromite ion was also assumed to be equal to that of the chloride ion. The values of the ionic radii used are given on page 44.

Using the data for the hydrogen sulfide - sodium chloride system, the value of the group of constant terms, $\underline{K_D}$, in Equation (158) was calculated. This value is given on page 44.

Using the modified $\underline{D} - \underline{A}$ equation, the choice of the set of ionic radii values was not important. There are two reasons for this fact. The first is that a very large ionic radius error is needed to cause an appreciable error in the solubility. For a 0.2N solution, 100% ionic radius error will cause only a 0.2% solubility error. The second reason is that the results are consistent no matter which method is used to calculate the ionic radii.

APPENDIX VI

RESULTS OF STUDIES ON THE OXIDATION OF SODIUM AND HYDROGEN SULFIDE BY HYPOHALITE SOLUTIONS

PRESENT WORK

The stoichiometry of the reaction between sodium or hydrogen sulfide and sodium hypochlorite or hypobromite was determined by the procedure described earlier in the Apparatus and Procedures section. The results are given in Tables XIX and XX.

TABLE XIX

OXIDATION OF HYDROGEN SULFIDE

Sodium Hypochlorite		Sodium Hypobromite	
Initial pH	$\frac{\text{Moles NaOCl Consumed}}{\text{Moles H}_2\text{S Added}}$	Initial pH	$\frac{\text{Moles NaOCl Consumed}}{\text{Moles H}_2\text{S Added}}$
7.1	4.06	8.5	3.86
8.0	4.08	9.0	3.93
8.9	4.01	9.8	3.92
9.7	3.96	11.2	4.00
11.0	3.99	11.9	3.90
11.7	4.00	11.9	2.46
11.9	1.55	12.4	2.63
12.3	1.77	13.0	3.08
12.9	1.95	13.7 (0.5N NaOH)	3.72
13.7 (0.5N NaOH)	2.55	14.0 (1.0N NaOH)	3.98
14.0 (1.0N NaOH)	3.02	14.3 (2.0N NaOH)	3.95
14.3 (2.0N NaOH)	3.38	14.5 (3.0N NaOH)	3.92
14.5 (3.0N NaOH)	3.84	14.6 (4.0N NaOH)	3.99
14.6 (4.0N NaOH)	3.96	14.7 (5.0N NaOH)	3.95
14.7 (5.0N NaOH)	4.00		
14.8 (6.0N NaOH)	3.96		

TABLE XX

OXIDATION OF SODIUM SULFIDE

Sodium Hypochlorite		Sodium Hypobromite	
Initial pH	$\frac{\text{Moles NaOCl Consumed}}{\text{Moles H}_2\text{S Added}}$	Initial pH	$\frac{\text{Moles NaOCl Consumed}}{\text{Moles H}_2\text{S Added}}$
6.5	4.10	8.3	3.98
6.9	3.98	8.8	3.92
7.1	3.99	9.1	3.88
7.4	2.57	9.4	3.06
7.6	2.27	10.0	2.70
7.8	2.06	11.2	2.90
8.2	1.85	12.3	2.71
9.0	1.79	12.6	2.93
9.2	1.82	12.9	3.03
10.4	1.81	13.7 (0.5N NaOH)	3.76
12.5	2.03	14.0 (1.0N NaOH)	3.89
13.7 (0.5N NaOH)	2.72	14.3 (2.0N NaOH)	3.97
14.0 (1.0N NaOH)	3.02	14.5 (3.0N NaOH)	3.97
14.3 (2.0N NaOH)	3.61	14.6 (4.0N NaOH)	3.98
14.5 (3.0N NaOH)	3.92	14.7 (5.0N NaOH)	3.99
14.6 (4.0N NaOH)	3.95		
14.7 (5.0N NaOH)	4.00		
14.8 (6.0N NaOH)			

PREVIOUS WORK

WORK OF WILLARD AND CAKE

Willard and Cake (5) studied the effect of sodium hydroxide concentration on the stoichiometry of the oxidation of sodium sulfide by sodium hypochlorite and hypobromite solutions. They reported the data as milliliters of oxidant consumed by a given volume of a sulfide solution. The theoretical volume required to oxidize all of the sulfide to sulfate was 9.86 ml. Their results are given in Table XXI.

TABLE XXI

OXIDATION OF SODIUM SULFIDE BY HYPOCHLORITE AND HYPOBROMITE SOLUTIONS

Concn. of Sodium Hydroxide, moles/liter	NaOCl Consumed, ml.	NaOBr Consumed, ml.
1.0	7.05	8.11
2.0	9.45	9.50
3.0	9.68	9.82
4.0	9.78	9.82
5.0	9.83	9.86
6.0	9.85	9.86

WORK OF CHOPPIN AND FAULKENBERRY

Choppin and Faulkenberry (10) determined the effect of pH on the stoichiometry of the hypochlorite oxidation of sodium sulfide. Their results were reported as the ratio between the moles of sodium hypochlorite consumed per mole of sodium sulfide added, and are given in Table XXII.

TABLE XXII

EFFECT OF pH ON THE HYPOCHLORITE OXIDATION OF SODIUM SULFIDE

Initial pH	Buffer	Ratio NaOCl/Na ₂ S
14 (3.0N NaOH)	--	3.98
13.8 (1.5N NaOH)	--	3.71
13.4 (0.4N NaOH)	--	2.72
12.5	NaOH - NaCl Glycine	1.86
11.8	NaOH - H ₃ BO ₃	1.67
10.0	NaOH - H ₃ BO ₃	1.50
8.4	NaOH - H ₃ BO ₃	1.63
7.3	NaOH - KH ₂ PO ₄	1.85
5.4	NaOH - KHC ₈ H ₄ O ₄	3.00
3.3	NaOH - KHC ₈ H ₄ O ₄	3.74
2.0	HCl - KCl	4.01
1.0	HCl - KCl	4.01

WORK OF DUNICZ AND ROSENQVIST

Dunicz and Rosenqvist (12) studied the effect of pH and temperature on the stoichiometry of the reaction between hydrogen sulfide and sodium hypochlorite. Their results are presented in a figure where the initial pH is plotted against per cent conversion to sulfate. These results at a temperature of 20°C. were taken from the figure and are shown in Table XXIII.

TABLE XXIII

EFFECT OF pH ON THE STOICHIOMETRY OF THE OXIDATION
OF HYDROGEN SULFIDE BY SODIUM HYPOCHLORITE

Initial pH	Conversion to Sulfate, %	Initial pH	Conversion to Sulfate, %
8.1	100	12.4	61
9.7	100	12.8	73
10.8	96	13.1	90
11.3	91	13.5	96
11.7	70	14.1	92
11.9	62	14.3	100
12.0	93	14.6	100
12.1	58	15.0	92

WORK OF MURTHY AND RAO

Murthy and Rao (13) studied the effect of pH on the stoichiometry of the oxidation of hydrogen sulfide by chloramine-T. They also added compounds which were known stabilizers or decomposition catalysts for hydrogen peroxide. Their results were reported as the ratio of the amount of sulfide oxidized to the sulfate form to the amount of sulfide oxidized to sulfur. This means that a value of ∞ is quantitative oxidation to sulfate and 0 is quantitative oxidation to sulfur. Their results are given in Table XXIV.

TABLE XXIV

REACTION BETWEEN HYDROGEN SULFIDE AND CHLORAMINE-T

pH of Solution	Buffer	Ratio Sulfate/Sulfur	Other Compound Present
2N H_2SO_4	--	∞	--
0.65	Acetate	16.6	--
2.64	Acetate	10.9	--
4.76	Acetate	8.6	--
4.76	Acetate	12.0	Na_2MoO_4
7.0	Phosphate	1.6	--
7.0	Phosphate	1.0	Brucine
7.0	Phosphate	1.0	Osmic Acid
7.0	Phosphate	2.4	Na_2MoO_4
7.0	Phosphate	0.55	Na_2WO_4
9.2	Borax	0.85	--
12	Borate	0.02	--

APPENDIX VII

PERMANGANATE OXIDATION OF HYDROGEN SULFIDE

In an attempt to find an oxidizing agent which could be used in the absorption studies, the stoichiometry of the reaction between potassium permanganate and hydrogen sulfide was determined.

RESULTS OF VOLUMETRIC TECHNIQUES

The volumetric procedures used in this study were given in detail on page 29. A brief review is given below. First, a solution of potassium permanganate of the desired strength was prepared and a volume of aqueous hydrogen sulfide was added by means of a buret equipped with a side arm. An excess of potassium iodide was added and hydrochloric acid was used to acidify the solution. The iodine was then titrated with standardized sodium thiosulfate. Blanks were run in exactly the same manner except that no hydrogen sulfide was added. The concentration of the hydrogen sulfide solution was determined by running a given volume of hydrogen sulfide solution into an acidified iodine solution. It should be noted here that all permanganate solutions were approximately 0.1N in hydrochloric acid.

First, the effect of permanganate concentration was investigated. The results are shown in Fig. 32 where the equivalents of permanganate consumed per mole of hydrogen sulfide are plotted versus the amount of excess permanganate. During the experiments it was noted that a precipitate was formed which appeared to be manganese dioxide. Since manganese dioxide is known to catalyze the spontaneous decomposition of potassium permanganate, it was felt that the excessive consumption of permanganate was due to its decomposition.

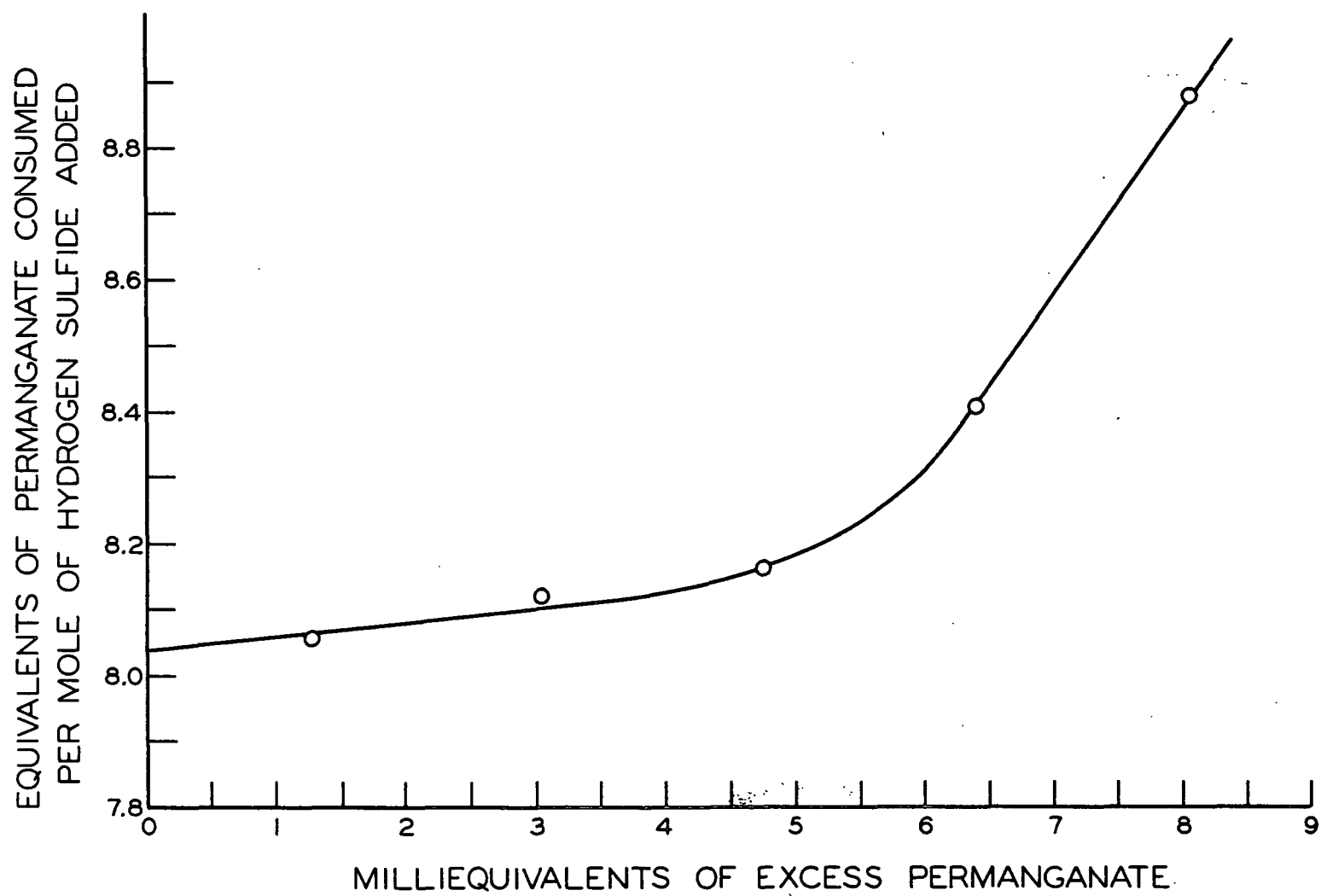


Figure 32. Amount of Permanganate Consumed by Hydrogen Sulfide

To verify this, constant volumes of hydrogen sulfide and permanganate solutions were mixed and allowed to stand for varying lengths of time before adding the potassium iodide. It was found that the consumption of permanganate rose from 8.2 to 9.1 equivalents per mole over a period of two hours.

RESULTS OF GRAVIMETRIC TECHNIQUES

The gravimetric technique used in this study was the common barium sulfate technique described in many textbooks on quantitative analysis (77). A slight modification was made prior to adding the barium chloride. After the hydrogen sulfide solution had been added to the permanganate solution, it was heated almost to boiling. Hydrogen peroxide was added to reduce all the manganese to the divalent state. Barium chloride was then added and the standard procedure was followed using Whatman's no. 42 filter paper and ashing the sample in a muffle furnace at 800°C. The theoretical yield of barium sulfate was determined from the volume and concentration of hydrogen sulfide solution.

The results of the gravimetric procedures are given in Table XXV where a comparison between the actual and theoretical yield of barium sulfate is made.

TABLE XXV

GRAVIMETRIC ANALYSIS RESULTS OF THE PERMANGANATE OXIDATION OF HYDROGEN SULFIDE

Initial pH	Theoretical Yield, mg.	Actual Yield, mg.
1.0	184	189.0
1.0	369	370.0
2.0	217	217.2
2.0	326	326.3
2.0	433	433.4

Note: Variation in determinations were ± 1 mg. from average.

Thus, it appears that potassium permanganate does quantitatively oxidize hydrogen sulfide to the sulfate form in acid solutions, with decomposition of permanganate giving high results when volumetric procedures are used.

COMPARISON WITH PREVIOUS WORK

Bethge (9) has made the only other study of the permanganate oxidation of sulfides. Using volumetric techniques, he found that alkaline permanganate would oxidize sulfides to sulfates as long as no more than 60% of the permanganate was consumed. Consuming more than this resulted in sulfur formation. He also found that the oxidation was not completely quantitative. Only 97% of the theoretically required amount of permanganate was consumed. No explanation for this low result was given.

SUMMARY AND CONCLUSIONS

It has been shown that potassium permanganate will oxidize hydrogen sulfide to the sulfate form in both acid and alkaline media. Volumetric techniques give high, nonreproducible results in acid systems and slightly low, reproducible results in alkaline systems. Gravimetric techniques give excellent results in acid systems.

The advantage of using permanganate as an oxidizing agent for the quantitative determination of sulfides would be that eight oxidizing equivalents are consumed per mole of sulfide as opposed to two equivalents per mole using iodimetric techniques. This would result in a much greater sensitivity and would provide an excellent tool for micro- or semimicroanalysis.

This sensitivity advantage is lost in acid systems because of the necessity of using a gravimetric technique which requires a fairly large sample size. The

sensitivity is also reduced in alkaline solutions because of the necessity for using a large excess of permanganate. Also the alkaline permanganate technique gives slightly low results.

APPENDIX VIII

SAMPLE CALCULATION AND SUMMARY OF ABSORPTION RUNS

CALCULATION OF EXPERIMENTAL ABSORPTION RATE

RUN NO. 155 DATA

Absorbent: 0.1N NaOCl, pH - 10.5
 $\rho = 1.0032 \text{ g./cm.}^3$
 $\eta = 1.0022$

Temperatures: Absorbent - - - 25.05°C.
 Hydrogen sulfide gas - - - 25.0°C.

Pressures: Atmospheric - - - 748.5 mm. Hg
 Jet chamber - - - 380.0 mm. H₂O

Absorbent Flow Rate: 4.84 cm.³/sec.

Nozzle Diameter: 0.1644 cm. = \underline{D}_0

Jet Length: 7.04 cm.

Titration of samples in 20% KI with 0.1103N sodium thiosulfate:

Sample	Sample Size, ml.	Thiosulfate, ml.
Blank	25.00	22.65
Blank	25.00	22.66
A	42.55	23.90
B	44.37	24.57

CALCULATIONS

a. Grams of H₂S absorbed/ml. of absorbent =

[normality of blank - average normality of the sample] x 34.08/8

$$\underline{W} = \left[\left(\frac{0.1103 \times 22.65}{25.00} \right) - \left(\frac{0.1103 \times 24.23}{43.96} \right) \right] \times 4.26 = 1.62 \times 10^{-4} \text{ g./ml.}$$

b. Rate of absorption = \underline{W} x absorbent flow rate

$$\underline{G} = 1.62 \times 10^{-5} \text{ g./ml.} \times 4.84 \text{ ml./sec.} = 7.94 \times 10^{-4} \text{ g./sec.}$$

c. Interfacial area = \bar{D} x jet length = \underline{A}

$$\text{where } \bar{D} = \frac{32q^2}{3\pi^2 g D_o^3} \left[\left(1 + \frac{\pi^2 g D_o^2 H}{8q^2} \right)^{3/4} - 1 \right] \quad (159)$$

$$\bar{D} = \frac{32 \times 4.84^2}{3 \times 3.14^2 \times 980 \times .1644^3 \times 7.04} \times \left[\left(1 + \frac{3.14^2 \times 980 \times .1644^4 \times 7.04}{8 \times 4.84^2} \right)^{3/4} - 1 \right]$$

$$\bar{D} = 0.826 \times 0.1930 = 0.1595 \text{ cm.}$$

$$A = 3.14 \times 0.1595 \times 7.04 = 3.52 \text{ cm.}^2$$

d. Average rate of absorption = $\underline{G}/\underline{A}$ =

$$7.94 \times 10^{-4} \text{ g./sec.} / 3.52 \text{ cm.}^2 = 22.5 \text{ g./cm.}^2 \text{ sec.}$$

e. Correction to $\underline{P}_{\text{H}_2\text{S}}$ = 1 atm.

Total pressure = atmospheric pressure + chamber pressure -
vapor pressure of water

$$748.5 + (380/13.56) - 23.8 = 753.5 \text{ mm. Hg}$$

$$\text{Rate of absorption at } \underline{P}_{\text{H}_2\text{S}} = 760 \text{ mm. Hg} = \underline{\bar{N}}_A$$

$$\underline{\bar{N}}_A = 22.5 \times 10^{-5} \text{ g./cm.}^2 \text{ sec.} \times (760/753.5) = 22.7 \times 10^{-5} \text{ g./cm.}^2 \text{ sec.}$$

CALCULATION OF EXPOSURE TIME

a. Average velocity of jet, $\underline{U} = 4q/\pi \bar{D}^2$

$$\text{where } \bar{D}^2 = \frac{16q^2}{\pi^2 g D_o^2} \left[\left(1 + \frac{\pi^2 g D_o^4 H}{8q^2} \right)^{1/2} - 1 \right] \quad (160)$$

$$\bar{D}^2 = \frac{16 \times 4.84^2}{3.14^2 \times 980 \times .1644 \times 7.04} \left[\left(1 + \frac{3.14^2 \times 980 \times .1644^2 \times 7.04}{8 \times 4.84^2} \right)^{1/2} - 1 \right]$$

$$\bar{D}^2 = 0.2036 \times 0.1252 = 0.02544 \text{ cm.}^2$$

$$\underline{U} = 4 \times 4.84 / 3.14 \times 0.02544 = 242 \text{ cm./sec.}$$

- b. Boundary layer thickness at nozzle exit, $\delta =$

$$2.42R_o(\eta l'/R_o^2 \bar{U}_o)^{0.391} \quad (146)$$

where \bar{U}_o is the velocity in the nozzle.

$$\bar{U}_o = 4q/\pi D_o^2 = (4 \times 4.84)/3.14^2 \times .1644^2 = 228 \text{ cm./sec.}$$

$$\delta = 2.42 \times 0.0822 \left(\frac{.009134 \times 0.0181}{0.0822^2 \times 228} \right)^{0.391}$$

$$\delta = 2.42 \times 0.0822 \times 0.2803 = 0.00557 \text{ cm.}$$

$$b = \delta/R_o = 0.0057/0.0822 = 0.0678$$

- c. Velocity at center of jet, U_∞

$$U_\infty = \bar{U}/[1 - (3b/4) - (b^2/5)] \quad (151)$$

$$U_\infty = 242/[1 - (3 \times .0678/4) - (.0678^2/5)] = 255 \text{ cm./sec.}$$

- d. Equivalent flat plate length, l ,

$$l = 1/25 (U_\infty/\eta)\delta^2 \quad (150)$$

$$l = (1/25) \times (255/0.009104) \times 0.00557^2 = 0.0349 \text{ cm.}$$

- e. Exposure time, t_e ,

$$t_e = \int_0^H \frac{dH}{U_s} = \frac{l}{U_\infty} \int_0^H \frac{U_\infty}{U_s} d\left(\frac{h}{l}\right) \quad (152)$$

U_s/U_∞ is given as a function of h/l in Fig. 27. The curve was fitted with an empirical equation and integrated in accordance with Equation (152). The result is

$$\int_0^H \frac{U_\infty}{U_s} d\left(\frac{h}{l}\right) = 2.90 \left\{ 1 - \exp \left[-0.262 \left(\frac{H}{l} \right) \right] \right\} + 1.061 \left(\frac{H}{l} \right) =$$

$$2.90 [1 - \exp(-0.262 \times 7.04/0.0349)] + 1.061(7.04/0.0349) =$$

$$3 + 214 = 217$$

$$t_e = (0.0349/255) \times 217 = 0.0296 \text{ sec.}$$

CALCULATION OF RATE OF ABSORPTION
WITHOUT CHEMICAL REACTION AND Φ

a. Equilibrium solubility, $\underline{C}_{A,e}$

$$\ln \gamma = K_D \sum_1^N M_j / b_j = \quad (56)$$

$$0.1818[(0.1/1.57) + (0.05/2.24) + (0.05/2.24)] = 0.0188$$

$$\gamma = 1.019$$

$$C_{A,e} = C_{A,o} / \gamma = 3.48 / 1.019 = 3.42 \text{ g./liter} = 3.42 \times 10^{-3} \text{ g./cm.}^3$$

b. Diffusion coefficient, \underline{D}_A

$$\underline{D}_A = D_{A,o} / \eta = 1.84 \times 10^{-5} \text{ cm.}^2/\text{sec.} / 1.022 = 1.82 \times 10^{-5} \text{ cm.}^2/\text{sec.}$$

c. Average rate of absorption without chemical reaction, \underline{N}_A^*

$$\underline{N}_A^* = 2 \underline{C}_{A,e} \sqrt{\underline{D}_A / \pi t_e} = 2 \times 3.42 \times 10^{-3} \sqrt{1.84 \times 10^{-5} / 3.14 \times .0296}$$

$$\underline{N}_A^* = 9.51 \times 10^{-5} \text{ g./cm.}^2 \text{ sec.}$$

$$\Phi = \underline{N}_A / \underline{N}_A^* = 22.7 \times 10^{-5} / 9.51 \times 10^{-5} = 2.39$$

CALCULATION OF FIRST-ORDER RATE CONSTANT

$$\underline{N}_A = C_{A,e} \sqrt{D_A k_1} \quad (78)$$

$$\therefore k = \underline{N}_A^2 / C_{A,e}^2 D_A = (22.7 \times 10^{-5})^2 / (3.42 \times 10^{-3})^2 \times 1.82 \times 10^{-5}$$

$$k_1 = 242 \text{ sec.}^{-1}$$

The product $(k_1 t_e)$ is larger than 4; therefore, the use of Equation (78) is valid.

CALCULATION OF THEORETICAL Φ WITH
"INFINITELY FAST" REACTION

$$\Phi = 1/\text{erf}(\alpha/\sqrt{D_A}) \quad (132)$$

where α is given by

$$\begin{aligned} n_B C_A, e^{\sqrt{D_A}} \exp(-\alpha^2/D_A) \text{erfc}(\alpha/\sqrt{D_B}) \\ n_A C_B, e^{\sqrt{D_B}} \exp(-\alpha^2/D_B) \text{erf}(\alpha/\sqrt{D_A}) \end{aligned} \quad (130)$$

Therefore,

$$\Phi = \frac{n_B C_B, e^{\sqrt{D_B}} \exp(-\alpha^2/D_B)}{n_A C_A, e^{\sqrt{D_A}} \exp(-\alpha^2/D_A) \text{erfc}(\alpha/\sqrt{D_B})} \quad (161)$$

Values of α were chosen until the Φ calculated from Equation (130) equaled the Φ calculated from Equation (161).

TABLE XXVI

SUMMARY OF ABSORPTION RUNS AT 25°C. AND A PARTIAL PRESSURE OF HYDROGEN SULFIDE OF 760 mm. Hg.

Run No.	Absorbent	pH	Rate of Absorption, g./cm. ² sec. x 10 ⁵	Exposure Time, sec.	Absorbent Flow Rate, ml./sec.	Jet Length, cm.
1A	0.1N HCl	1.0	10.08	0.0341	4.13	7.08
2A	"	1.0	10.89	0.0289	4.84	7.08
3A	"	1.0	11.36	0.0263	5.58	7.08
4A	0.26N NaOH	13.3	54.58	0.0341	4.13	7.09
5A	"	13.3	60.01	0.0298	4.84	7.09
6A	"	13.3	63.80	0.0267	5.48	7.09
1	0.1N HCl	1.1	8.00	0.0439	2.97	7.01
2	"	1.1	9.23	0.0336	4.16	7.01
3	"	1.1	11.69	0.0230	6.40	7.01
4	"	1.1	8.57	0.0393	3.43	7.01
5	"	1.1	9.88	0.0305	4.67	7.01
6	"	1.1	10.46	0.0261	5.58	7.01
7	"	1.1	7.10	0.0547	3.75	11.02
8	"	1.1	8.09	0.0437	4.99	11.02
9	"	1.1	7.02	0.0595	3.34	11.02
10	"	1.1	13.26	0.0160	4.06	3.08
11	"	1.1	14.51	0.0136	4.83	3.08
12	"	1.1	15.51	0.0119	5.60	3.08
13	"	1.1	8.90	0.0361	3.90	7.15
14	"	1.1	8.94	0.0361	3.90	7.15
15	"	1.1	8.95	0.0361	3.90	7.15
16	dil. HCl	3.1	8.87	0.0361	3.90	7.15
17	"	3.1	9.61	0.0310	4.67	7.15
18	"	3.1	10.51	0.0265	5.60	7.15
19	dil. HCl	5.4	9.20	0.0343	4.15	7.15
20	"	5.4	9.82	0.0303	4.80	7.15
21	"	5.4	10.63	0.0266	5.56	7.15

Note: Chlorine gas was the absorbate in Runs 1A through 6A.

TABLE XXVI (Continued)

SUMMARY OF ABSORPTION RUNS AT 25°C. AND A PARTIAL PRESSURE OF HYDROGEN SULFIDE OF 760 mm. Hg

Run No.	Absorbent	pH	Rate of Absorption, g./cm. ² sec. x 10 ⁵	Exposure Time, sec.	Absorbent Flow Rate, ml./sec.	Jet Length, cm.
22	Water	7.1	9.48	0.0338	4.22	7.15
23	"	7.1	9.82	0.0306	4.74	7.15
24	"	7.1	10.55	0.0268	5.51	7.15
25	dil. NaOH	8.3	9.09	0.0349	4.06	7.15
26	"	8.3	9.96	0.0302	4.82	7.15
27	"	8.3	10.67	0.0265	5.58	7.15
28	dil. NaOH	11.0	9.35	0.0343	4.14	7.15
29	"	11.0	9.92	0.0304	4.78	7.15
30	"	11.0	10.78	0.0264	5.62	7.15
31	0.1N NaOH	13.0	25.04	0.0350	4.05	7.15
32	"	13.0	27.55	0.0304	4.78	7.15
33	"	13.0	29.86	0.0265	5.58	7.15
34	dil. HCl	2.1	9.05	0.0353	4.03	7.19
35	"	2.1	9.70	0.0307	4.76	7.19
36	"	2.1	10.43	0.0264	5.65	7.19
37	dil. HCl	4.1	9.05	0.0355	4.00	7.19
38	"	4.1	9.74	0.0307	4.76	7.19
39	"	4.1	10.47	0.0264	5.64	7.19
40	dil. HCl	6.5	9.08	0.0359	3.95	7.19
41	"	6.5	9.85	0.0307	4.75	7.19
42	"	6.5	10.76	0.0265	5.63	7.19
43	dil. HCl	4.6	9.15	0.0351	4.06	7.19
44	"	4.6	9.72	0.0307	4.76	7.19
45	"	4.6	10.68	0.0266	5.59	7.19

Note: Runs no. 46-57 were not valid due to an incorrect choice of sulfide analysis procedure.

TABLE XXVI (Continued)

SUMMARY OF ABSORPTION RUNS AT 25°C. AND A PARTIAL PRESSURE OF HYDROGEN SULFIDE OF 760 mm. Hg

Run No.	Absorbent	pH	Rate of Absorption, g./cm. ² sec. x 10 ⁵	Exposure Time, sec.	Absorbent Flow Rate, ml./sec.	Jet Length, cm.
58	0.0421N NaOH	12.6	15.62	0.0312	4.13	6.42
59	"	12.6	16.47	0.0270	4.88	6.42
60	"	12.6	17.58	0.0236	5.67	6.42
61	dil. NaOH	12.0	10.75	0.0314	4.10	6.42
62	"	12.0	11.42	0.0274	4.80	6.42
63	"	12.0	12.29	0.0236	5.62	6.42
64	dil. NaOH	10.1	9.88	0.0308	4.19	6.42
65	"	10.1	10.48	0.0272	4.84	6.42
66	"	10.1	11.24	0.0238	5.62	6.42
67	dil. NaOH	8.0	9.37	0.0343	4.14	7.15
68	"	8.0	9.95	0.0299	4.87	7.15
69	"	8.0	10.76	0.0265	5.59	7.15
70	1.231N NaOH	14.1	454.7	0.0353	3.95	7.12
71	"	14.1	463.8	0.0312	4.59	7.12
72	"	14.1	473.9	0.0272	5.38	7.12
73	0.419N NaOH	13.6	93.78	0.0348	4.05	7.12
74	"	13.6	96.70	0.0305	4.73	7.12
75	"	13.6	100.2	0.0267	5.51	7.12
76	0.657N NaOH	13.8	185.02	0.0348	4.04	7.12
77	"	13.8	191.04	0.0366	4.71	7.12
78	"	13.8	193.51	0.0268	5.48	7.12
79	25 g./l. NaCl	2.2	7.85	0.0382	4.10	7.98
80	"	2.2	8.44	0.0335	4.80	7.98
81	"	2.2	8.98	0.0297	5.51	7.98
82	50 g./l. NaCl	2.2	7.16	0.0384	4.08	7.98
83	"	2.2	7.66	0.0333	4.83	7.98
84	"	2.2	8.14	0.0294	5.59	7.98

TABLE XXVI (Continued)

SUMMARY OF ABSORPTION RUNS AT 25°C. AND A PARTIAL PRESSURE OF HYDROGEN SULFIDE OF 760 mm. Hg

Run No.	Absorbent	pH	Rate of Absorption, g./cm. ² sec. x 10 ⁵	Exposure Time, sec.	Absorbent Flow Rate, ml./sec.	Jet Length, cm.
85	75 g./l. NaCl	2.1	6.36	0.0398	3.90	7.98
86	"	2.1	6.82	0.0345	4.64	7.98
87	"	2.1	7.35	0.0303	5.39	7.98
88	100 g./l. NaCl	2.1	5.84	0.0393	3.96	7.98
89	"	2.1	6.22	0.0346	4.61	7.98
90	"	2.1	6.63	0.0302	5.40	7.98
91	100 g./l. NaCl	2.0	7.37	0.0239	3.91	4.59
92	"	2.0	7.87	0.0206	4.62	4.59
93	"	2.0	8.58	0.0178	5.45	4.59
94	75 g./l. NaCl	2.2	8.18	0.0238	3.93	4.59
95	"	2.2	8.87	0.0203	4.70	4.59
96	"	2.2	9.39	0.0178	5.44	4.59
97	50 g./l. NaCl	2.2	9.04	0.0234	4.02	4.59
98	"	2.2	9.59	0.0294	4.68	4.59
99	"	2.2	10.37	0.0177	5.50	4.59
100	25 g./l. NaCl	2.2	9.99	0.0232	4.06	4.59
101	"	2.2	10.54	0.0205	4.66	4.59
102	"	2.2	11.56	0.0175	5.55	4.59
103	1.061N NaOH	14.0	335.0	0.0352	4.00	7.14
104	"	14.0	351.2	0.0309	4.67	7.14
105	"	14.0	353.5	0.0271	5.43	7.14
106	dil. HCl	2.1	11.17	0.0222	4.05	4.36
107	"	2.1	12.00	0.0191	4.79	4.36
108	"	2.1	13.08	0.0164	5.65	4.36
109	0.573N HCl	0.3	10.79	0.0222	4.04	4.36
110	"	0.3	12.02	0.0193	4.74	4.36
111	"	0.3	13.00	0.0163	5.73	4.36

TABLE XXVI (Continued)

SUMMARY OF ABSORPTION RUNS AT 25°C. AND A PARTIAL PRESSURE OF HYDROGEN SULFIDE OF 760 mm. Hg

Run No.	Absorbent	pH	Rate of Absorption, g./cm. ² sec. x 10 ⁵	Exposure Time, sec.	Absorbent Flow Rate, ml./sec.	Jet Length, cm.
112	0.270N HCl	0.6	11.06	0.0129	4.16	4.36
113	"	0.6	11.87	0.0190	4.81	4.36
114	"	0.6	12.97	0.0165	4.61	4.36
115	0.268N HCl	0.6	8.75	0.0364	4.07	7.51
116	"	0.6	9.32	0.0316	4.82	7.51
117	"	0.6	10.03	0.0274	5.67	7.51
118	0.564N HCl	0.3	8.81	0.0363	4.09	7.51
119	"	0.3	9.69	0.0315	4.83	7.51
120	"	0.3	10.15	0.0274	5.66	7.51
121	0.1006N NaOCl	11.6	27.08	0.0350	4.02	7.12
122	"	11.6	27.56	0.0295	4.92	7.12
123	0.1042N NaOCl	12.3	30.74	0.0367	3.80	7.12
124	"	12.3	26.32	0.0302	4.76	7.12
125	0.008N NaOCl	12.8	46.38	0.0354	3.97	7.12
126	"	12.8	40.41	0.0305	4.73	7.12
127	0.1019N NaOCl	14.0	371.4	0.0347	4.05	7.12
128	"	14.0	368.3	0.0308	4.69	7.12
129	"	14.0	372.5	0.0278	5.25	7.12
130	0.1040N NaOCl	13.7	227.3	0.0348	4.04	7.12
131	"	13.7	232.0	0.0301	4.80	7.12
132	"	13.7	231.3	0.0269	5.45	7.12
133	"	13.7	233.7	0.0314	3.95	4.12
134	"	13.7	230.0	0.0184	4.69	4.12
135	"	13.7	238.1	0.0160	5.48	4.12
136	0.1079N NaOBr	13.7	213.6	0.0351	3.97	7.08
137	"	13.7	213.5	0.0301	4.77	7.08
138	"	13.7	208.1	0.0264	5.53	7.08

TABLE XXVI (Continued)

SUMMARY OF ABSORPTION RUNS AT 25°C. AND A PARTIAL PRESSURE OF HYDROGEN SULFIDE OF 760 mm. Hg

Run No.	Absorbent	pH	Rate of Absorption, g./cm. ² sec. x 10 ⁵	Exposure Time, sec.	Absorbent Flow Rate, ml./sec.	Jet Length, cm.
139	0.206N NaOH	13.3	46.93	0.0346	4.05	7.08
140	"	13.3	50.26	0.0298	4.83	7.08
141	"	13.3	50.85	0.0264	5.54	7.08
142	"	13.3	51.58	0.0214	4.07	4.26
143	"	13.3	55.67	0.0183	4.86	4.23
144	"	13.3	59.51	0.0160	5.61	4.23
145	0.1019N NaOCl	13.3	98.12	0.0348	4.02	7.07
146	"	13.3	101.1	0.0299	4.81	7.07
147	"	13.3	102.7	0.0260	5.64	7.07
148	0.0987N NaOCl	8.1	31.85	0.0336	4.20	7.07
149	"	8.1	20.42	0.0290	4.99	7.07
150	"	8.1	19.38	0.0271	5.39	7.07
151	0.0810N NaOCl	7.1	35.35	0.0335	4.21	7.07
152	"	7.1	25.67	0.0295	4.89	7.07
153	"	7.1	10.27	0.0272	5.37	7.07
154	0.1000N NaOCl	10.5	23.52	0.0340	4.11	7.04
155	"	10.5	22.70	0.0296	4.84	7.04
156	"	10.5	22.05	0.0259	4.63	7.04
157	"	10.5	22.04	0.0214	4.08	4.23
158	"	10.5	22.41	0.0184	4.81	4.23
159	"	10.5	21.69	0.0161	5.58	4.23
160	0.1035N NaOBr	10.7	21.83	0.0336	4.21	7.09
161	"	10.7	20.77	0.0294	4.92	7.09
162	"	10.7	19.47	0.0261	5.63	7.09
163	0.1002N NaOCl	9.5	25.50	0.0344	4.09	7.09
164	"	9.5	22.59	0.0293	4.95	7.09
165	"	9.5	23.10	0.0262	5.62	7.09

TABLE XXVI (Continued)

SUMMARY OF ABSORPTION RUNS AT 25°C. AND A PARTIAL PRESSURE OF HYDROGEN SULFIDE OF 760 mm. Hg

Run No.	Absorbent	pH	Rate of Absorption, g./cm. ² sec. x 10 ³	Exposure Time, sec.	Absorbent Flow Rate, ml./sec.	Jet Length, cm.
166	0.0993N NaOCl	16.6	22.15	0.0102	5.58	2.61
167	"	16.6	22.76	0.0092	6.25	2.61
168	"	16.6	22.29	0.0413	4.21	8.89
169	"	16.6	22.33	0.0467	3.60	8.89
170	0.2902N NaOCl	10.9	65.80	0.0357	3.97	7.19
171	"	10.9	53.85	0.0313	4.64	7.19
172	"	10.9	58.82	0.0280	5.27	7.19
173	0.0516N NaOCl	10.6	16.02	0.0341	4.09	7.02
174	"	10.6	16.76	0.0297	4.82	7.02
175	"	10.6	17.36	0.0261	5.58	7.02
176	0.1998N NaOCl	10.6	36.53	0.0362	3.80	7.02
177	"	10.6	32.36	0.0304	4.69	7.02
178	"	10.6	31.73	0.0260	5.60	7.02